

**AMP-ACTIVATED PROTEIN KINASE IN THE
HEART: ROLE IN FATTY ACID DELIVERY,
FATTY ACID UTILIZATION AND CELL
DEATH**

by

GIRISH KEWALRAMANI

B.Pharmacy. Mumbai University, India 2002

M.Sc. University of Hertfordshire, United Kingdom 2004

**A THESIS SUBMITTED IN PARTIAL FULFILMENT OF
THE REQUIREMENTS FOR THE DEGREE OF
DOCTOR OF PHILOSOPHY**

in

**THE FACULTY OF GRADUATE STUDIES
(Pharmaceutical Sciences)**

**THE UNIVERSITY OF BRITISH COLUMBIA
(Vancouver)**

July 2009

© GIRISH KEWALRAMANI, 2009

ABSTRACT

Following hypoinsulinemia, glucose utilization is compromised and the myocardium switches to utilize fatty acids (FA). Previous studies have reported that PPAR- α promotes FA oxidation during chronic hypoinsulinemia. Whether the same modification also occurs in the heart during acute hypoinsulinemia and if AMP-activated protein kinase (AMPK) participates in the increase of cardiac fatty acid oxidation during this condition remains unclear. Using streptozotocin model of Type I diabetes, we report that in acute (4 days) diabetes AMPK by phosphorylating acetyl CoA carboxylase promotes cardiac fatty acid oxidation. Unexpectedly, in chronic diabetes (6 weeks), with the addition of augmented plasma and heart lipids, AMPK activation is prevented, and PPAR- α through its regulation of downstream targets controls myocardial FA oxidation. In addition to its role in FA utilization, AMPK has been implicated in controlling FA delivery through its regulation of the FA transporter, CD36. Given that LPL derived FA is the principal source of energy during insulin resistance, the question of interest was whether cardiac AMPK can regulate LPL translocation to the vascular lumen to increase the exogenous FA pool. Using dexamethasone (DEX) as an acute model of insulin resistance, my study demonstrates that, following a single dose of DEX, nongenomic phosphorylation of stress kinases such as AMPK together with insulin facilitate LPL translocation to the myocyte cell surface. Besides metabolism, AMPK has been implicated in modulating cell death. The production of tumor necrosis factor alpha (TNF- α) is reported to increase during obesity and diabetes and elevated plasma or endogenous cardiac TNF- α levels have shown to cause cardiomyocyte apoptosis. Using established AMPK activators like DEX or metformin (MET), my objective was to

determine if AMPK activation prevents TNF- α -induced apoptosis in cardiomyocytes. My data demonstrates that although DEX and MET are used as anti-inflammatory agents or insulin sensitizers, their common property to phosphorylate AMPK promotes cardiomyocyte survival through its regulation of Bad and the mitochondrial apoptotic mechanism.

TABLE OF CONTENTS

ABSTRACT.....	ii
TABLE OF CONTENTS	iv
LIST OF TABLES	viii
LIST OF FIGURES	ix
LIST OF ABBREVIATIONS	x
ACKNOWLEDGEMENTS	xii
DEDICATION.....	xiii
CO-AUTHORSHIP STATEMENT	xiv
1. INTRODUCTION.....	1
1.1 AMPK	1
1.1.1 Structure.....	1
1.1.2. Regulation.....	3
1.1.3 Downstream targets	14
1.1.4 Physiological roles of AMPK.....	16
1.1.5 Roles of AMPK in the heart.....	17
1.2 CARDIAC METABOLISM.....	18
1.2.1 Glucose metabolism.....	18
1.2.2 FA metabolism.....	19
1.2.3 Cardiac metabolism during insulin resistance and diabetes	20
1.3 AMPK AND CARDIAC METABOLISM	22
1.3.1 AMPK and glucose metabolism	22
a) GLUT4.....	22
b) Phosphofructokinase-1 (PFK-1)	24
1.3.2 AMPK and FA metabolism	25
1.3.2.1 AMPK and FA entry.....	25
a) FA transporters.....	25
b) Lipoprotein lipase (LPL).....	26
1.3.2.2 AMPK and FA oxidation.....	27
a) Acetyl CoA Carboxylase (ACC)	27
b) Peroxisome proliferator activated receptors (PPARs)	28
c) Malonyl CoA decarboxylase (MCD).....	29
d) Carnitine palmitoyl transferase (CPT).....	30
1.4 AMPK AND CARDIAC CELL DEATH	31
1.5 RATIONALE AND OBJECTIVES	32
1.6 FIGURES.....	34

1.7	BIBLIOGRAPHY	37
2.	AMPK CONTROL OF MYOCARDIAL FATTY ACID METABOLISM FLUCTUATES WITH THE INTENSITY OF INSULIN DEFICIENT DIABETES	55
2.1	INTRODUCTION	55
2.2	MATERIALS AND METHODS	57
2.2.1	Experimental animals.....	57
2.2.2	Cardiac glucose and fatty acid oxidation	58
2.2.3	Western blot analysis	59
2.2.4	Measurement of cardiac gene expression	59
2.2.5	Separation and characterization of cardiac lipids	60
2.2.6	Intralipid infusion.....	60
2.2.7	Plasma measurements	61
2.2.8	Statistical analysis.....	61
2.3	RESULTS	62
2.3.1	Control of cardiac substrate utilization in acute D55 (D55-A) diabetes.....	62
2.3.2	Control of cardiac substrate utilization in chronic (D55-C) diabetes	63
2.3.3	Changes in plasma and heart lipids in D55-A and D55-C diabetic hearts.....	63
2.3.4	Influence of lipids on AMPK activation.....	64
2.4	DISCUSSION	66
2.5	TABLES AND FIGURES	71
2.6	BIBLIOGRAPHY	80
3.	ACUTE DEXAMETHASONE-INDUCED INCREASE IN CARDIAC LIPOPROTEIN LIPASE REQUIRES ACTIVATION OF BOTH AKT AND STRESS KINASES	86
3.1	INTRODUCTION	86
3.2	MATERIALS AND METHODS	89
3.2.1	Experimental animals.....	89
3.2.2	Euglycemic hyperinsulinemic clamp.....	89
3.2.3	Tissue-specific response to insulin	89
3.2.4	LPL and AMPK gene expression	90
3.2.5	Heart tissue homogenization.....	90
3.2.6	Coronary lumen LPL activity	90
3.2.7	Western blotting.....	90
3.2.8	Isolated cardiac myocytes.....	91
3.2.9	Nuclear localization of p38 MAPK	92
3.2.10	Filamentous and globular actin.....	92
3.2.11	Immunoprecipitation.....	92
3.2.12	Silencing of p38 MAPK by siRNA	92
3.2.13	Plasma measurements	93
3.2.14	Materials	93
3.2.15	Statistical analysis.....	93
3.3.	RESULTS	94
3.3.1	General characteristics of experimental animals	94

3.3.2	Tissue-specific insulin resistance.....	94
3.3.3	Changes in LPL following DEX.....	94
3.3.4	Influence of DEX on cardiac AMPK and p38 MAPK	95
3.3.5	DEX stimulates cardiac actin polymerization.....	96
3.3.6	In vitro effects of DEX on isolated cardiomyocytes.....	96
3.3.7	Insulin mediates the in vitro effects of DEX on myocyte LPL activity.....	97
3.3.8	Silencing of p38 MAPK prevents cardiomyocyte LPL recruitment observed with DEX+Ins.....	98
3.4	DISCUSSION	99
3.5	TABLES AND FIGURES	105
3.6	BIBLIOGRAPHY	114
4	AMP-ACTIVATED PROTEIN KINASE CONFERS PROTECTION AGAINST TNF-ALPHA INDUCED CARDIAC CELL DEATH.....	121
4.1	INTRODUCTION	121
4.2	MATERIALS AND METHODS	124
4.2.1	Experimental animals.....	124
4.2.2	Isolation of cardiomyocytes.....	124
4.2.3	Administration of DEX to control rats.....	125
4.2.4	Estimation of cardiomyocyte intracellular free Ca ²⁺	125
4.2.5	Measurement of apoptosis	126
4.2.6	Separation of mitochondrial and cytosolic fractions	127
4.2.7	Western Blot	127
4.2.8	Immunoprecipitation.....	128
4.2.9	Cardiomyocyte AMPK gene expression.....	128
4.2.10	Materials	128
4.2.11	Statistical analysis.....	129
4.3	RESULTS	130
4.3.1	Influence of DEX on total and phosphorylated AMPK in isolated cardiac myocytes.....	130
4.3.2	Changes in cardiomyocyte intracellular Ca ²⁺ and CAMKI phosphorylation following DEX.....	130
4.3.3	Dual regulation of AMPK phosphorylation by DEX	131
4.3.4	TNF-alpha mediated effects on cardiomyocyte cell death	131
4.3.5	AMPK regulation of TNF-alpha mediated caspase-3 activation and cell death.....	132
4.3.6	DEX induced effects on Bad phosphorylation and cytochrome C Release	133
4.3.7	Consequence of AMPK inhibition on Bad phosphorylation and TNF alpha induced caspase-3 activation.....	134
4.3.8	Cardioprotective effects of MET against TNF-alpha induced caspase-3 activation.....	134
4.4	DISCUSSION	136
4.5	FIGURES	141
4.6	BIBLIOGRAPHY	152

5	CONCLUSIONS AND FUTURE DIRECTIONS.....	160
	APPENDIX.....	164
	Animal Care Certificate	164

LIST OF TABLES

- Table 2-1 General characteristics of the experimental animals
Table 2-2 Effects of diabetes on cardiac fatty acid composition
Table 3-1 General characteristics of experimental animals

LIST OF FIGURES

- Fig 1-1 Regulation of AMPK
- Fig 1-2 Glucose and FA delivery and utilization in cardiomyocytes
- Fig 2-1 Cardiac glucose and palmitate oxidation in STZ-treated hearts
- Fig 2-2 Cardiac AMPK and ACC phosphorylation in 4-day 55 mg/Kg STZ diabetic hearts
- Fig 2-3 Cardiac glucose and palmitate oxidation in chronic STZ-diabetic hearts
- Fig 2-4 Cardiac AMPK and ACC phosphorylation and plasma and cardiac lipids
- Fig 2-5 Cardiac AMPK and ACC phosphorylation and plasma and cardiac lipids in 4-day 100mg/kg STZ diabetic hearts
- Fig 2-6 Effects of intralipid on cardiac AMPK and ACC phosphorylation
- Fig 2-7 Effects of intralipid on cardiac AMPK phosphorylation in acute D55-A diabetic hearts
- Fig 3-1 Responses of skeletal muscle and heart to insulin (Ins)
- Fig 3-2 Lipoprotein lipase (LPL) gene expression and protein and activity measurements in hearts from control and DEX-treated animals
- Fig 3-3 Time-dependent changes in AMPK gene expression, phosphorylation of AMPK and p38 MAPK in hearts isolated from DEX-treated animals
- Fig 3-4 Phosphorylation of heat shock protein (HSP) 25 and actin polymerization following DEX
- Fig 3-5 Consequence of incubating cardiomyocytes with DEX in vitro
- Fig 3-6 Changes in cardiomyocyte heparin-releaseable (HR)-LPL activity with DEX and insulin
- Fig 3-7 Silencing of p38 MAPK by short interfering siRNA
- Fig 3-8 Schema of mechanisms that are likely involved in regulating the effects of DEX and insulin on cardiac LPL
- Fig 4-1 Time dependant changes in AMPK in control and DEX treated cardiomyocytes
- Fig 4-2 Effects of DEX on cardiomyocyte intracellular Ca^{2+} and CAMKI phosphorylation
- Fig 4-3 Inhibition of AMPK activation induced by DEX
- Fig 4-4 TNF-alpha induced cardiomyocyte apoptosis
- Fig 4-5 Effects of AMPK activation on TNF-alpha induced apoptosis
- Fig 4-6 DEX induced regulation of Bad phosphorylation and its association with BCL-xL
- Fig 4-7 Consequence of AMPK inhibition on TNF-alpha induced Bad phosphorylation and caspase-3 activity
- Fig 4-8 Graphic representation of the proposed mechanism mediating the protective effect of AMPK activation on TNF-alpha induced apoptosis in adult rat ventricular cardiomyocytes
- Fig 4-S1 TNF-alpha induced cardiomyocyte apoptosis
- Fig 4-S2 *In vivo* effects of DEX on TNF-alpha induced cell death in vitro
- Fig 4-S3 Metformin induced regulation of Bad phosphorylation, its association with Bcl-xL and its influence on caspase-3 activity.

LIST OF ABBREVIATIONS

ACC	Acetyl coenzyme A carboxylase
ACO	Acetyl coenzyme oxidase
ACS	Acetyl coenzyme synthase
ADP	Adenosine diphosphate
AICAR	5-aminoimidazole-4-carboxamide ribonucleoside
AMP	Adenosine monophosphate
AMPK	AMP activated protein kinase
AMPKK	AMP-activated protein kinase kinases
ANOVA	Analysis of variance
Ara-A	Adenine 9-beta-D-arabinofuraoside
AS160	Akt substrate of 160 kDa
ATP	Adenosine triphosphate
BSA	Bovine serum albumin
CaMKK	Ca ²⁺ /calmodulin dependant protein kinase kinase
CAMKI	Calmodulin-dependent protein kinases types I
CAMKIV	calmodulin-dependent protein kinases types IV
CBS	Cystothionine β synthase
CK	Creatine kinase
Comp C	Compound C
CPT1	Carnitine palmitoyl transferase1
DAG	Diacylglycerol
DEX	Dexamethasone
DNP	Dinitrophenol
eNOS	Endothelial nitric oxide synthase
FA	Fatty acid
FABPpm	Fatty acid binding protein plasma membrane
FAS	Fatty acid synthase
FATP	Fatty acid transport protein
F6P	Fructose 6 phosphate
F2,6BP	Fructose 2,6-bisphosphate
g	gram
GAPDH	Glyceraldehyde 3-phosphate dehydrogenase
GBD	Glycogen binding domain
GLUT	Glucose transporter
HMGR	HMG-CoA reductase
HPLC	High performance liquid chromatography
HR-LPL	Heparin releaseable-lipoprotein lipase
hr	hour
hsp-25	Heat shock protein-25
HSPG	Heparin sulphate proteoglycan
IL	Intralipid
Ins	Insulin
i.p.	Intraperitoneal

IRS	Insulin receptor substrate
i.v.	Intravenous
kg	Kilogram
LCAD	Long chain acyl-CoA dehydrogenase
LKB1	Tumor suppressor kinase 1
LPL	Lipoprotein lipase
M	Molar
MCD	Malonyl coenzyme A decarboxylase
MET	Metformin
mg	Milligram
min	Minute
ml	Milliliter
mm	Millimolar
mRNA	Messenger Ribonucleic acid
mTOR	Mammalian target of rapamycin
NAD/NADH	Nicotinamide adenine dinucleotide
nM	Nanomolar
P	Phosphorylated
PBS	Phosphate buffer saline
PDH	Pyruvate dehydrogenase
PDK	Pyruvate dehydrogenase kinase
PFK	Phosphofructokinase
PGC-1alpha	PPAR-gamma coactivator-1 alpha
PI3K	Phosphoinositide 3-kinases
PPAR	Peroxisome proliferator activated receptor
PP2A	Protein phosphatase 2A
PP2C	Protein phosphatase 2C
p38MAPK	p38 mitogen activated protein kinase
RT-PCR	Reverse transcription polymerase chain reaction
SEM	Standard error of mean
STZ	Streptozotocin
TAK1	Transforming growth factor- β -activated kinase 1
TAB	TAK-1 binding protein
TBS-T	Tris buffered saline-Tween
TGF β	Transforming growth factor- β
TG	Triglyceride
TNF-alpha	Tumor necrosis factor alpha
VLCAD	Very long chain acyl-CoA dehydrogenase
VLDL	Very low density lipoprotein
μ l	Microliter
μ M	Micromolar

ACKNOWLEDGEMENTS

First, I owe my most sincere gratitude to my supervisor, Dr. Brian Rodrigues who gave me the opportunity to work in his research laboratory. His wide knowledge, logical thinking, encouragement and instruction have been of great value for me. His guidance, support and his untiring help during difficult moments made it possible for me to achieve this degree.

During my Ph.D I have collaborated with my colleagues (Sanjoy, Thomas, Jeff, Dake, Prasanth, and Fang) for whom I have great regard and I wish to extend my warmest thanks to all of them. Their immense discussions around my work and interesting suggestions have been very helpful for all my studies. I warmly thank Ashraf Abrahani for his valuable technical advice and his friendly help. His kind support and guidance has been of great value in my studies.

A special thanks to my thesis committee members, Dr.Helen Burt, Dr. James D Johnson, Dr. Ismail Laher, Dr. Ujendra Kumar and Dr. Mike Allard for their valuable suggestions and insight during my doctoral training.

My deepest gratitude goes to my family for their love and support throughout my life, this thesis is simply impossible without them. I am indebted to my mother (Manisha Kewalramani), my father (Ramesh Kewalramani) and my brother (Avinash Kewalramani) for their care, love and support. Finally, I would like to thank my wonderful wife (Kanchan Makhija) with whom the most difficult tasks seem possible and appear easy.

The financial support of the University of British Columbia is gratefully acknowledged.

DEDICATION

*To my parents, my brother and my wife,
their support and understanding made this
possible*

CO-AUTHORSHIP STATEMENT

Dr. Ding An, a former Ph.D. student in Dr. Rodrigues's laboratory contributed to Chapter 2. His contributions included performing research and data analysis for Fig. 2-3A and Fig. 2-4B. He also assisted in revising the manuscript (Chapter 2) that has been published by the Journal of Molecular and Cellular Cardiology.

1. INTRODUCTION¹

1.1 AMP-activated protein kinase

AMP-activated protein kinase (AMPK) has emerged as a master sensor of cellular energy balance in mammalian cells. Prior to being coined as AMPK, this kinase was recognized as an upstream regulator of two key mediators of lipid metabolism, acetyl-CoA carboxylase and 3-hydroxy-3-methylglutaryl CoA reductase (1). Once identified, it was found to be a homolog of the metabolic stress sensing kinase, Snf1, a protein important for yeast survival during glucose starvation. Studies over the last ten years have linked AMPK in regulation of various cellular functions in almost every major tissue. This is particularly true for the untiring cardiac muscle, where AMPK has been implicated as a switch regulating energy metabolism and more recently, cell death.

1.1.1 Structure of AMPK

AMPK, a heterotrimeric enzyme complex is composed of a catalytic α (63kDa) subunit and two non-catalytic regulatory subunits (β ; 30 kDa and γ ; 38-63 kDa) (Fig. 1). Presence of all three subunits is crucial for AMPK function (2). Each of the three AMPK subunits expresses isoforms ($\alpha 1$, $\alpha 2$, $\beta 1$ and $\beta 2$, $\gamma 1$, $\gamma 2$ and $\gamma 3$) that are encoded by distinct genes. In skeletal and cardiac muscle, the $\alpha 2$ isoform of AMPK predominates, in pancreatic islet β -cells the $\alpha 1$ isoform prevails, and an equal distribution of both the $\alpha 1$ and $\alpha 2$ isoforms are found in the liver. $\gamma 1$ and $\gamma 2$ isoforms are both expressed in the heart, while $\gamma 3$ isoform is only found in the skeletal muscle. All three subunits (α , β and γ) of AMPK possess unique structural machinery that facilitate their varied roles in regulation of AMPK activity and its physiological functions in mammalian cells. The AMPK α

¹ "A version of this chapter has been submitted for publication. Kewalramani, G. and Rodrigues, B. (2009) AMP-activated protein kinase in the heart: role in cardiac glucose and fatty acid metabolism."

subunit possesses the highly conserved N-terminal catalytic domain that contains the activating phosphorylation site Thr172. In addition, it also incorporates an auto inhibitory domain and a C-terminal domain that forms a complex with the regulatory β and γ subunits (3). In addition to the previously characterized Thr172 site on AMPK α subunit, new phosphorylation sites (Thr 258, Ser 485 and Ser491) have been identified by mass spectrometry (4). As evaluation of the sequences adjoining Thr 258, Ser 485 and Ser491 have displayed similar consensus not found around Thr172, it is widely believed that Thr 258, Ser 485 and Ser491 could be phosphorylated by the same AMP-activated protein kinase kinases (AMPKK) dissimilar from the AMPKK that phosphorylates Thr172. Interestingly, the cellular localization of two AMPK α variants displays a distinct cellular distribution pattern in mammalian cells. AMPK α 1 isoform is localized in the non-nuclear fractions and AMPK α 2 displays its presence both in nuclear and non-nuclear portions of a cell. The AMPK β subunit was originally suggested to bind both α and γ subunits via its C-terminal sequence, rendering AMPK a stable heterotrimeric complex (5). A more recent study has challenged this finding and reported an absence of any direct binding between the β and γ subunit (Fig. 1) (6). β subunit targets AMPK to membranes via an N-terminal miristoyl group (Gly²), and to glycogen via a mid molecule glycogen binding domain (GBD) (7). Exclusion of GBD abolishes the association between AMPK and glycogen particles and hinders GBD mediated regulation of AMPK activity. Phosphorylation sites such as Ser24 and Ser25 on the AMPK β subunit govern the nuclear localization of AMPK. In support of this finding, AMPK β isoforms (β 1 and β 2) have been reported to exhibit their presence in both the nuclear and non-nuclear cellular fractions (8). Moreover, a Ser182 phosphorylation site on the β subunit has also

been indicated to regulate the very crucial AMPK catalytic activity (7). A distinct feature of the γ subunit is its N-terminal region followed by four highly conserved cystathionine- β -synthase (CBS) sequence motifs (9). Two CBS sequence motifs form two functional Bateman domains classified as Bateman domain 1 and Bateman domain 2. CBS domains bind to both ATP (at lower affinity than AMP) and AMP, with AMP binding being vital for AMPK activation (9). Of the three isoforms of AMPK γ subunit, the γ 1 isoform displays a preferential nuclear localization. Thus, in addition to controlling cytosolic and plasma membrane functions, the presence of specific AMPK isoforms (α 2, β 2 and γ 1) within the nucleus has suggested its role in modulating gene expression (10). Consistent with this theory, stimulation of cells by stress inducing agents has demonstrated a nuclear translocation of AMPK α 1/2 and β 1/2 subunits (11). Thus AMPK appears to maneuver its intracellular localization to meet the ever-changing necessities of the cell.

1.1.2 Regulation of AMPK

Phosphorylation on thr172 site within the catalytic α subunit activates AMPK. This phosphorylation and activation of AMPK was thought to occur primarily via an AMP mediated conformational change. Studies have now revealed a complex regulation of AMPK that engages multiple players (Fig. 1) such as AMPKK's, protein phosphatases, pharmacological activators and inhibitors, and physiological and pathophysiological stimuli. The section below will describe ways in which the above-mentioned players regulate AMPK activity.

Adenosine 5'-Monophosphate (5'-AMP)

The name AMPK originated due to studies that demonstrated that its activity was sensitive to 5'AMP (1). As discussed above, the γ subunit contains binding sites

(Bateman domains) that promote the interaction between AMP and the AMPK complex. Adenosine triphosphate (ATP) inhibits the binding between AMP and AMPK (12). In normoxic cells, very low AMP/ATP ratio keeps AMPK in an inactive state. In contrast, any energy imbalance increases the AMP/ATP ratio and allosterically activates AMPK. Minute changes in AMP concentrations indicate massive fluctuations in cellular energy status and these changes allosterically regulate AMPK activity to maintain cellular ATP levels.

AMPKK's

In addition to its allosteric regulation by AMP, AMPK can also be stimulated by upstream AMP-activated protein kinases kinases (AMPKK's) such as tumor suppressor kinase (LKB1), Ca²⁺/calmodulin dependant protein kinase kinase beta (CaMKK β) and transforming growth factor- β -activated kinase-1 (TAK1) (Fig. 1).

Tumor suppressor kinase (LKB1) The serine/threonine protein kinase LKB1 functions as a suppressor of cell proliferation and tumor formation. Thus, its mutation in the human disorder peutz-jeghers syndrome (PJS) leads to the development of tumors in various tissues (13). Researchers have found that LKB1 in a complex with two proteins (ste20-related adaptor protein; STRAD α/β and mouse protein-25; MO25 α/β) operates as an upstream activator of AMPK (14,15). Absence of MO25 and STRAD decreases LKB1 activity, suggesting the importance of these two accessories in LKB1 activation. In the heart, LKB1 is an recognized upstream kinase regulating AMPK and cardiac muscle lacking LKB1 displays a reduced basal AMPK α 2 activity and an ablated acetyl-CoA carboxylase (downstream substrate of AMPK) function (16). Under ischemic conditions, cardiac LKB1 has been suggested to play a crucial role in controlling

AMPK α 2 activation and acetyl-CoA carboxylase-2 phosphorylation (16). During myocardial ischemia, an increase in cellular AMP likely prevents phosphatase induced AMPK dephosphorylation. As LKB1 is constitutively active, inhibition of dephosphorylation leads to a rise in Thr172 phosphorylation and activation of AMPK (17; 18). Other studies utilizing perfused hearts subjected to ischemia have reported activation of AMPK with no change in LKB1 activity (19). Interestingly, in endothelial cells, hypoxia or metformin induced activation of AMPK requires PKC zeta to phosphorylate LKB1 at serine 428 (20; 21). Although this phosphorylation does not enhance LKB1 activity, it results in the association of LKB1 with AMPK and consequent AMPK Thr172 phosphorylation by LKB1 (21). These results could explain the absence of a change in LKB1 activity following ischemia. In addition to cardiac muscle, mouse liver lacking LKB1 displays reduced AMPK Thr172 phosphorylation, suggesting LKB1 as a key regulator of AMPK in the liver (22). Studies using LKB1 isolated from rat liver extracts have suggested that LKB1 can phosphorylate AMPK only if AMP enables tumor suppressor kinase access to the Thr172 phosphorylation site of AMPK (23). However, a recent study contradicted this finding and proposed that phosphatases were contaminating the LKB1 isolated from rat liver extracts and the AMP sensitivity for LKB1 dependant phosphorylation was due to the ability of AMP to inhibit phosphatases and hence prevent AMPK dephosphorylation (17).

Ca²⁺/calmodulin dependant protein kinase kinase (CaMKK) HeLa cells that lack LKB1 display some basal phosphorylation of Thr172 and AMPK activity (24). This finding suggests the presence of additional upstream AMPKK's that could modulate AMPK phosphorylation. The initial discovery came from the yeast system where Sak1

(Snf1 activating kinase 1), Elm1 (elongated morphology-1) and Tos3 (target of Sbf3) were identified as kinases that function upstream of the yeast homolog of AMPK, Snf1 (24; 26). Sequential and structural analysis of CaMKK revealed considerable homology with Snf1 kinase kinases, Elm1 and Tos3 and the mammalian AMPK kinase, LKB1. There are two distinct genes for CaMKK, CaMKK α and CaMKK β . Tissue distribution studies reveal the presence of both CaMKK isoforms in the neuronal tissue with CaMKK α being predominant in the skeletal muscle (27). CaMKK β is highly expressed in the brain with detectable levels found in thymus, testes, spleen, liver and lungs (27). Recent evidence also revealed the presence of both CaMKK β mRNA and protein in mouse and rat hearts and isolated rat cardiomyocytes (28). The activity of CaMKK isoforms is regulated by an increase in cytosolic calcium that facilitates a complex formation between Ca²⁺ and calmodulin. Ca²⁺/calmodulin complex associates itself with CaMKK that increases the activity of CaMKK α/β and the multifunctional calmodulin-dependent protein kinases types I and IV (CaMKI and CaMKIV) (29). Activation is achieved through selective phosphorylation of a Thr residue in the activation loop of CaMKI and CaMKIV, Thr177 and Thr196/Thr200 (30). Elevated cytosolic Ca²⁺ triggers cellular ATP-consumption by membrane driven pumps that drive out cytosolic calcium, and activation of proteins that control membrane traffic (31). Activation of AMPK by this upstream kinase could therefore be viewed as a mode to anticipate the excessive demand for energy that usually accompanies Ca²⁺ release. Studies utilizing CaMKK extracted from pig brain and AMPK isolated from liver have revealed an increased AMPK activity by CaMKK α/β (23). This increased AMPK activity was improved by the addition of AMP suggesting that CaMKK dependant activation of AMPK is sensitive to

changes in cellular AMP levels (23). A recent study however contradicted this finding and proposed that phosphatases were contaminating the CaMKK preparation and the AMP sensitivity for CaMKK dependant phosphorylation was due to the ability of AMP to inhibit phosphatases and prevent AMPK dephosphorylation (32). Thus, it is now clear that CaMKK's regulate AMPK function in a Ca^{2+} /calmodulin dependant manner that is independent of any mediation by AMP.

Transforming growth factor- β -activated kinase 1 (TAK1) A recent screen for kinases that activate the yeast homolog SNF1 yielded a further candidate, transforming growth factor- β (TGF β)-activated kinase-1 (TAK1). This member of MAPKKK family was initially thought to play a crucial role in TGF β signaling pathway, but recent evidence has emerged implicating TAK1 as an upstream kinase regulating AMPK function (33). TAK1 associates itself in a heterotrimeric complex with its adapter molecules TAK-1 binding protein-1 (TAB1), TAK-1 binding protein-2 (TAB2) and TAK-1 binding protein-3 (TAB3). Although the function of this newly discovered AMPKK is not completely understood, studies have indicated that the activation of TAK1 necessitates its association with the regulatory subunit TAB1. Once bound to TAK1, TAB1 by phosphorylating Thr184, Thr187 and Ser192 residues activates TAK1 (34). Similar to LKB1 and CaMKK, TAK1 activates AMPK by phosphorylating the Thr172 site within the catalytic α subunit. In addition, chemical agents (such as AICAR) that mimic an increase in cellular AMP content have been proposed to activate TAK1. Studies performed in cardiac muscle have demonstrated that loss of TAK1 activity prevents metformin-induced phosphorylation of AMPK (35). Consistent with the activation of TAK1 by

agents that alter or mimic cellular AMP:ATP ratios or directly phosphorylate the Thr172 AMPK residue, TAK1 has recently been implicated as an upstream AMPK kinase.

Protein phosphatases

AMPK is not only a better substrate for upstream kinases but also a poor substrate for protein phosphatases. Both protein phosphatase 2A (PP2A) and 2C (PP2C) dephosphorylate the Thr172 residue and reduce AMPK function (Fig. 1) (15). In ZDF *fa/fa* rat hearts, an increase in the expression of PP2C decreases AMPK activity and leads to a derangement of cardiac lipid metabolism (36). Phosphatase induced dephosphorylation of AMPK largely depends on cellular AMP levels. It has been demonstrated that AMP by allosterically inhibiting the access of protein phosphatases to the activating Thr172 site prevents AMPK dephosphorylation (37). This evidence confirmed that AMP rather than regulating phosphatase activity controls phosphatase access to the activating Thr172 AMPK residue.

Pharmacological activators and inhibitors

Understanding the physiological role of AMPK within various tissues has been greatly enhanced by the use of several AMPK activators and inhibitors.

AICAR (5-aminoimidazole-4-carboxamide 1- β -D-ribofuranoside) AICAR, an AMPK activator is transferred into the cell by the adenosine transporter and metabolized by adenosine kinase to 5-aminoimidazole-4-carboxamide 1- β -D-ribofuranosyl monophosphate (ZMP), an AMP analogue (38). Similar to AMP, ZMP then binds to the Bateman domains within the γ subunit and activates AMPK. Importantly, activation of AMPK by AICAR does not involve any fluctuations in the cellular AMP:ATP ratios. Thus, the AICAR metabolite ZMP by mimicking AMP serves as an AMPK activator.

Although widely used, AICAR is considered a poor activator of myocardial AMPK, requiring higher concentrations to demonstrate AMPK stimulation in the heart (39). Another drawback of using AICAR as an AMPK activator is its selectivity. AICAR can activate other AMP-responsive enzymes including fructose-1,6-bisphosphatase and glycogen phosphorylase (40). Hence, studies that utilize AICAR to evaluate AMPK function should be careful when interpreting data.

Metformin (N,N-dimethylimidodicarbonimidic diamide) Metformin, an oral anti-diabetic from the biguanide class, is the first line of drug for the treatment of Type 2 diabetes. This biguanide increases AMPK activity in various tissues but the mechanism behind this action remains unclear. A recent study by Xie et al revealed that loss of TAK1 protein abolished metformin-induced stimulation of cardiac AMPK, suggesting that TAK1 is crucial for the actions of metformin on AMPK (35). In non-cardiac cells such as hepatocytes, LKB1 knockout abolishes the effects of metformin to activate AMPK, suggesting that LKB1 is required by metformin for AMPK activation in the liver (22). Similarly, an additional study involving hepatocytes demonstrated that metformin by inhibiting the mitochondrial complex I (a key complex involved in mitochondrial ATP generation) alters cellular energy levels and elevates AMP to activate AMPK (41). In mouse skeletal muscle, studies have reported that phenformin (a metformin derivative) and not metformin increases intracellular AMP:ATP ratios suggesting that metformin-induced inhibition of mitochondrial complex may not be the only mechanism underlining its activation of AMPK in skeletal muscle. Thus, to what extent effects of metformin on AMPK could be mediated through alternative signaling pathways remains unknown and continues to be explored. Clinically metformin is used to improve insulin resistance (42),

but whether such treatment has any favorable impact on human cardiac metabolism is unclear. This is because the doses of metformin necessary to activate AMPK, increase glucose transport and alleviate insulin resistance in isolated tissues such as heart and muscle are usually higher than the therapeutic doses used to treat Type 2 diabetes (43).

Thiazolidinediones The class of thiazolidinedione (also referred as glitazones or TZDs) was introduced in the late 1990s as an additional therapy for Type 2 diabetes. Rosiglitazone and Pioglitazone are members of this class and are used to decrease blood glucose levels in humans with type 2 diabetes. TZDs are PPAR γ agonists known to activate AMPK. Researchers have demonstrated that TZDs increase the expression and stimulate the release of adiponectin (an adipocyte hormone) that activates AMPK in various tissues. TZDs also activate AMPK likely through inhibition of mitochondrial complex I and changes in cellular AMP/ATP ratio.

Mitochondrial toxins Dinitrophenol (DNP) and Rotenone are mitochondrial poisons used to activate AMPK in numerous tissues and cell types. Both these compounds activate AMPK by altering cellular AMP:ATP levels. DNP, a membrane permeable benzene based compound uncouples mitochondrial oxidation by transporting protons across the mitochondrial membrane. This leads to a rapid consumption of cellular ATP and activation of AMPK. In cardiomyocytes, DNP treatment duplicates hypoxic conditions and activates AMPK. Rotenone works by interfering with the electron transport chain within the mitochondria. It specifically prevents the movement of electrons from complex I to ubiquinone. This event largely reduces cellular ATP levels and stimulates AMPK. In isolated rodent skeletal muscle, a significant increase in AMPK activity in response to DNP and rotenone has been reported (44).

Oligomycin Oligomycin is commonly used in laboratory studies to activate AMPK. This compound by binding the F_0F_1 ATPase inhibits the mitochondrial proton pump, reduces mitochondrial respiration and depletes cellular ATP to elevate AMPK (45). In isolated perfused hearts and cardiomyocytes, oligomycin has been demonstrated to alter cellular AMP/ATP ratio and increase AMPK activity (46). In cardiomyocytes, oligomycin concentration up to 300 μ M has been used to activate AMPK (47). Besides cardiac cells, oligomycin is widely utilized as an AMPK activator in numerous tissues and cell types.

A-769662 A-769662, a novel chemical activator of AMPK, was first discovered in 2006 at Abbott Laboratories. This small molecule has been highlighted as a vital experimental tool to evaluate the downstream effects of AMPK activation in intact cells and *in vivo*. To activate AMPK, A-769662 duplicates two major effects of AMP on the AMPK system and includes allosteric regulation and inhibition of dephosphorylation. These effects of A-769662 are independent of any binding to the CBS sequence motifs of the γ subunit. Since the effects of A-769662 are independent of any upstream kinases (LKB1 and CaMKK β), this small molecule is considered to be a direct and specific activator of AMPK. In addition, when compared to AICAR, metformin or oligomycin, A-769662 is regarded as the most potent activator of AMPK available today (48).

Dexamethasone Dexamethasone (DEX), a potent member of the glucocorticoid class of steroid hormones is commonly used as an anti-inflammatory and immunosuppressive agent. Recently, DEX has emerged as an activator of AMPK in tissues such as liver and heart. DEX treatment increases AMPK α 1 and α 2 subunit protein contents and mRNA levels in rat and mice liver and AMPK α 1 protein expression, activity and

phosphorylation in hepatocytes (49). In addition, DEX has been shown to increase AMPK mRNA, protein expression and phosphorylation in intact rat hearts (50). Although, the mechanism responsible for this action of DEX is under investigation, recently published data from our laboratory utilizing cardiomyocytes demonstrated that DEX, by increasing cytosolic calcium, phosphorylates CaMKI (Thr177), an upstream regulator of AMPK (28).

Statins Statins are a class of drugs that prevent the formation of cholesterol in the liver by inhibiting HMG-CoA reductase, a rate-limiting enzyme involved in cholesterol synthesis (51). These agents, by increasing the synthesis of LDL receptors, accelerate the removal of LDL cholesterol from the blood stream (51). Recently, statins have been identified to positively regulate AMPK function, both in endothelial cells and myocardium (51). At a clinical dosage, atorvastatin has been reported to activate AMPK by phosphorylating the Thr172 residue and induce endothelial nitric oxide synthase to promote nitric oxide production (51).

Compound C (6-[4-(2-Piperidin-1-yl-ethoxy)-phenyl]-3-pyridin-4-yl-pyrazolo[1,5-a]-pyrimidine) Commonly used in research, Compound C is a cell-permeable pyrazolopyrimidine agent that acts as a potent ATP-competitive inhibitor of AMPK (52). Compound C inhibits AICAR induced activation of AMPK by inhibiting the adenosine transport system that facilitates uptake of AICAR into cells (53). However this agent fails to inhibit dinitrophenol induced augmentation in AMPK activity (53). Thus, whether Compound C will be effective against agents that activate AMPK by a pathway that does not include the adenosine transport system remains uncertain. Moreover, Compound C is not a selective inhibitor of AMPK and has been reported to inhibit

numerous proteins including CaMKK α and phosphorylase kinase (54). Thus, caution should be exercised in interpreting experimental data obtained with Compound C when investigating functions attributed to AMPK.

Ara-A (Adenine 9- β -D-arabinofuranoside) In cell-based studies, Ara-A is widely used as an AMPK inhibitor. Ara-A is taken up by the cells and converted to Ara-ATP, which acts as a competitive inhibitor of AMPK. In cardiomyocytes and hepatocytes, Ara-A is known to reduce AMPK activity. A study in skeletal muscle also revealed that AMPK α 1 isoform is resistant to Ara-A action and its effects are largely mediated by inhibiting AICAR stimulated AMPK α 2 activity (55).

Insulin Insulin has been shown to antagonize AMPK action in the heart through an ATP-independent mechanism (56). Overexpression of a constitutively active mutant form of Akt1 and Akt2 in cardiomyocytes has been demonstrated to suppress AMPK activity (57). It is likely that the ability of insulin to inhibit AMPK might be controlled via an Akt-dependant pathway. Conversely, in an *in vitro* model using insulin resistant cardiomyocytes, AMPK activators (metformin, phenformin and oligomycin), by phosphorylating AMPK, reinstated the sensitivity of glucose uptake to insulin by activating Akt via the PI3K dependant pathway. This finding emphasized the putative beneficial action of AMPK as an insulin-sensitizing agent (58). Under ischemic conditions, the ability of insulin to antagonize cardiac AMPK largely depends on the concentration of fatty acids (59). In mouse hearts subjected to global no-flow ischemia, insulin's ability to inhibit AMPK action is lost during reperfusion with fatty acids. Insulin's effect on myocardial glucose metabolism remains intact under these conditions (59).

Physiological and pathophysiological stimuli

During various physiological and pathophysiological conditions, cellular metabolism and energy balance is altered. Physiological stresses such as exercise and skeletal muscle contraction increase ATP consumption (in the absence of compromised ATP generation), alter cellular AMP/ATP ratios and activate AMPK. In the heart an increase in workload due to contraction stimulates glycolysis in the absence of any change in AMPK or AMP:ATP ratios. This finding implied that the normal heart adjusts its metabolism to additional energy demand without engaging AMPK (60). Moreover, in swine and isolated rat hearts, increasing cardiac work with agents such as dobutamine and adrenaline does not alter AMPK activity (61; 62). Pathophysiological conditions such as ischemia, hypoxia, hypertrophy, diabetes and glucose deprivation are all associated with a compromised ATP generation, which leads to a rise in AMP/ATP ratio and activation of AMPK (63). In addition, cytokines have also been implicated to regulate AMPK activity. Cytokines released by adipocytes (termed adipokines), such as leptin and adiponectin activate AMPK via AMP/ATP independent mechanisms and increase glucose uptake and fatty acid oxidation in skeletal muscle (64). Adiponectin also activates AMPK in liver, stimulating fatty acid oxidation and inhibiting glucose production (64). The specific mechanisms by which adipokines modulate AMPK activity remain unclear.

1.1.3 Downstream targets of AMPK

AMPK activation initiates signaling mechanisms that induce effects on cell metabolism, protein synthesis, and gene expression. These effects regulate numerous metabolic

events in the liver, adipose tissue, pancreas, skeletal muscle and heart. As AMPK the “fuel gauge” of the biological system is activated under conditions that deplete cellular ATP and elevate AMP levels, its phosphorylation inactivates a number of metabolic enzymes involved in ATP consuming pathways like fatty acid and cholesterol synthesis, and activates enzymes facilitating ATP generating mechanisms like fatty acid oxidation and glucose uptake. Acetyl CoA carboxylase (ACC) is a known downstream target of AMPK. In the heart and skeletal muscle, AMPK phosphorylates and inhibits both the isoforms of ACC (ACC1 and ACC2) (65; 67). This inhibition results in a drop in the cellular malonyl-CoA levels, which is an inhibitor of carnitine palmitoyl transferase (CPT1). A drop in the inhibition of CPT I promote fatty oxidation and increases ATP generation within the mitochondria. In adipose tissue and liver, AMPK mediated regulation of ACC and fatty acid synthase (FAS) is known to decrease fatty acid synthesis (68; 69). In cardiac tissue, skeletal muscle and adipocytes activation of AMPK leads to the induction of glucose transporter-4 (GLUT4) recruitment to the plasma membrane, promoting glucose uptake (63; 70-72). Moreover, the ability of AMPK to stimulate GLUT4 translocation to the plasma membrane occurs via a mechanism distinct from that stimulated by insulin. AMPK, by phosphorylating phosphofruktokinase (PFK2), is also known to promote glycolysis. In addition, AMPK has been shown to modulate the function of glycerol-3-phosphate acyltransferase, (GPAT) and HMG-CoA reductase, (HMGR) in the liver; malonyl-CoA decarboxylase, (MCD) in the liver, muscle and adipose tissue; creatine kinase, (CK) and glycogen synthase, (GS) in the skeletal muscle and hormone-sensitive lipase, (HSL) in the adipose tissue. Thus, the effects of AMPK activation are exerted not only on glucose and fatty

acid metabolism but also on the overall energy homeostasis including cholesterol, phosphocreatine and glycogen metabolism. Cardiac activation of AMPK has also been shown to regulate endothelial nitric oxide synthase (eNOS) activity promoting nitric oxide production (73). In addition to these acute effects, AMPK activation exerts distinct long-term effects on the expression of a number of glycolytic and lipogenic enzymes (74). AMPK activation reduces the hepatic SREBP transcription factor, a key modulator of the expression of various lipogenic enzymes. An additional transcription factor affected in response to AMPK activation is hepatocyte nuclear factor-4 α (HNF4 α). HNF4 α regulates the expression of genes residing in the liver and pancreatic β -cell. A newly recognized target of AMPK is the forkhead transcription factor, FKHR. AICAR, through its activation of AMPK has demonstrated to regulate hepatic FoxO1a (an FKHR substrate) protein expression (75). AMPK activation also phosphorylates hepatic translation elongation factor 2 (eEF2) thereby inhibition protein synthesis. Another mechanism by which AMPK can affect protein synthesis is through its inhibition of mammalian target of rapamycin (mTOR) pathway (76).

1.1.4 Physiological roles of AMPK

The classical view of AMPK, as described above, is as an intracellular energy gauge that modulates the energy balance within the cell. AMPK is known to regulate whole body energy metabolism through its effects on different tissues. In skeletal muscle and liver, activation of AMPK augments fatty acid oxidation and elevates glucose disposal to inhibit gluconeogenesis. As a paradox, AMPK inhibits lipolysis in adipocytes through its phosphorylation of HSL at Ser565 residue. In pancreatic β cells, AMPK stimulation decreases insulin secretion. Besides regulating energy expenditure in peripheral tissues,

AMPK also regulates food intake (77). AMPK acts on the hypothalamic neurons to regulate feeding. AMPK is expressed in several key hypothalamic nuclei (77). Fasting increases AMPK activity in multiple hypothalamic regions and refeeding inhibits it (78). Activation of AMPK in the hypothalamus increases feeding and body weight gain, whereas inhibition of hypothalamic AMPK activity promotes hypophagia and weight loss. A possible mechanism by which hypothalamic AMPK regulates food intake involves the ACC/malonyl CoA/CPT1 axis. High levels of glucose, leptin or insulin, by inhibiting hypothalamic AMPK, increase ACC activity, augment malonyl CoA and suppress food intake (77). Taken together, AMPK through its regulation of energy expenditure and food intake is believed to play a key role in controlling whole body energy balance.

1.1.5 Roles of AMPK in the heart

Although the role of AMPK in normal cardiac function, when cellular ATP levels are plentiful and the fuel gauge is inactive remains uncertain, a clearer role has emerged for its function during cardiac disease (79). Once activated, AMPK turns off energy consuming mechanisms such as protein synthesis, and turns on energy generating mechanisms such as glycolysis and FA oxidation. In the heart AMPK elevates glycolysis and glucose oxidation by targeting specific proteins and glucose transporters. In addition, AMPK facilitates the generation of ATP by promoting cardiac FA oxidation. Moreover, AMPK has also been implicated in regulating cardiac FA delivery through its control of specific enzymes and FA transporter proteins (47; 80; 81). An emerging role of AMPK also illustrates its ability to prevent cell death. In non-cardiac cells like endothelial cells or astrocytes, activation of AMPK has already been demonstrated to protect against

hyperglycemia or high fat induced apoptotic cell death (82; 83). Recently, in H9c2 rat cardiac muscle cell lines or adult cardiomyocytes, AMPK activation has been shown to protect against reactive oxygen species or palmitate induced cell death, likely through indirect mechanisms whereby excess substrate is directed towards oxidation (84; 85).

1.2 Cardiac metabolism

1.2.1 Glucose metabolism

To maintain continuous function the human heart needs to produce energy in the form of ATP. This process may consume various substrates such as fatty acids (FA), glucose, lactate and ketone bodies, of which glucose and FA are the major substrates utilized by the myocardium (86). In a normal heart 10-40% of ATP production is generated from glucose (86). Cardiac glucose metabolism involves multiple steps such as uptake, glycolysis and pyruvate decarboxylation (Fig. 2). Although, the myocardium contains endogenous glucose that is present in intracellular glycogen stores, the main source of glucose for ATP production comes from exogenous glucose that is taken up into the cardiac cell via two sarcolemmal glucose transporters, GLUT1 and GLUT4. Following its entry into the cardiac cell, glucose is broken down to pyruvate through glycolysis. Glycolysis is an anaerobic process and contributes to less than 10% of the total myocardial energy. Pyruvate generated via glycolysis has multiple fates. It can undergo carboxylation by pyruvate carboxylase to form oxaloacetate, it can be reduced to lactate or it can be decarboxylated to acetyl CoA. Pyruvate decarboxylation to acetyl CoA involves the coordinated action of several enzymes collectively called the pyruvate dehydrogenase (PDH) complex. Pyruvate dehydrogenase kinase (PDK) phosphorylates and inactivates PDH resulting in decreases in mitochondrial glucose oxidation (87).

Regulation of PDK is governed by pyruvate that inhibits PDK or high NADH/NAD(+) and acetyl-CoA/CoA ratios that activate PDK (87; 88). Eventually, acetyl CoA within the mitochondria enters the citric acid cycle and is oxidized to CO₂ and H₂O for ATP generation (Fig. 2).

1.2.2 Fatty acid metabolism

When compared to glucose, 60-90% of the ATP generation in the heart comes from the mitochondrial oxidation of FA (Fig. 2). FA are derived from three main sources, adipose tissue lipolysis that release fatty acids which enter the heart after associating with albumin, breakdown of endogenous cardiac TG stores and hydrolysis of circulating lipoproteins such as VLDL-TG and chylomicron-TG by lipoprotein lipase located at the endothelial surface of the coronary lumen (89). When compared, majority of the fatty acids utilized by the myocardium are derived from the breakdown of circulating lipoproteins. Over 99% of the FA in the plasma is bound to albumin. This binding limits the total content of free FA to levels that do not impair the cell membrane (90). It was long considered that FA (both free and albumin bound) could enter the cardiomyocyte via passive diffusion, dependant on metabolic rate and physicochemical properties of lipophilic substrates. However, the saturable nature of FA uptake and its susceptibility to competitive inhibition suggests the requirement of FA transporters (91). Although, the list of FA transporters is still growing, so far four proteins have been recognized to regulate myocardial FA uptake at both mRNA and protein levels (Fig. 2). These are the plasma membrane FA binding protein (FABPpm), the FA transporter CD36, and two members of the family of FA transport proteins (FATPs), FATP1 and FATP6. FABPs located at the cellular membrane or within the cytosolic compartment are regarded as the

intracellular counterpart of plasma albumin due to their role in the organized transport of FA (92). Once inside the cell, fatty acids are converted to acyl-CoA's which are transported into the mitochondria by a carnitine dependant transport system. Two key enzymes control this system of FA transport into the mitochondria, carnitine palmitoyl transferase 1 & 2 (CPT 1 & 2) localized in the mitochondrial membrane and the matrix. Another key regulator of cardiac fatty acid oxidation is malonyl CoA. Large increases in cytosolic malonyl CoA levels inhibit CPT-1 activity thereby limiting FA entry and utilization (93; 94). Conversely, a drop in cytosolic malonyl CoA removes CPT-1 inhibition and elevates FA entry and oxidation (95). Carboxylation of acetyl CoA by ACC yields malonyl CoA. This formation of malonyl CoA from acetyl CoA is reversible and is governed by malonyl CoA decarboxylase (MCD). Phosphorylation of AMPK has been demonstrated to inhibit ACC activity, reduce cytosolic malonyl CoA and promote FA oxidation. Eventually, once within the mitochondria, acetyl CoA undergoes β -oxidation to generate energy (Fig. 2).

1.2.3 Cardiac energy metabolism during insulin resistance and diabetes

Insulin resistance alone is known to increase the risk of coronary heart disease and can directly contribute to cardiac dysfunction (96). Alteration in cardiac energy metabolism has been demonstrated during insulin resistance and primarily includes an elevated fatty acid and decreased glucose utilization. Clinically, insulin resistance in young women has been related to increased myocardial fatty acid uptake and oxidation as measured by positron emission tomography (97). Rodent studies utilizing DEX as a model of insulin resistance have demonstrated an alteration in myocardial energy metabolism (50). Specifically, acute DEX treatment in adult male Wistar rats produces whole body insulin

resistance, which was likely accounted for by changes in the responses of skeletal muscle to insulin (50). In the heart, although no changes were observed in insulin signaling, significant alteration in myocardial glucose and fatty acid oxidation was evident (50). The ultimate metabolic manifestation of long-term insulin resistance is diabetes. During diabetes, remarkable changes in plasma substrate levels induce changes in cardiac metabolism. An elevation in circulating plasma levels of both glucose and fatty acids is evident during diabetes. Increased hepatic glucose production coupled with a decreased glucose clearance contributes to a rise in plasma glucose levels. In addition, elevated adipocyte lipolysis and hepatic lipoprotein production contributes to the rise in circulating fatty acids. Although, the circulating levels of both glucose and fatty acids are high during diabetes, their uptake into the cardiomyocyte dictates their utilization. Insulin is known to regulate glucose uptake by mobilizing GLUT4 vesicles to the sarcolemmal membrane (98). A decreased cardiac glucose uptake is an established event in diabetes. However, whether the reduction in glucose uptake during Type 1 diabetes is due to cardiac specific insulin resistance is still unclear (99; 100). A reduction in cardiac glucose uptake renders fatty acids the substrate of choice during diabetes. Studies using streptozotocin (STZ) induced animal model of Type 1 diabetes have shown an elevation in the level of cardiac FA transporters (due to their increased expression) facilitating FA uptake and increased intracellular FA levels (101). In Type 2 diabetes, altered glucose uptake does not appear to be a result of insulin resistance but rather an outcome of increased fatty acid levels inhibiting GLUT4 mRNA expression. Numerous studies have established that augmented rates of FA oxidation influence the rate of glycolysis and glucose oxidation. Although a reduction in substrate availability during diabetes is the

primary cause of decreased myocardial glycolysis, inhibition of phosphofructokinase-1 (PFK-1) by cytosolic citrate (that builds up with excessive mitochondrial fatty acid oxidation) also influences the rate of glycolysis. Additionally, excess FA delivery to the myocyte induces the expression of genes (like PPAR- α) involved in FA oxidation. This increase in PPAR- α expression activates PDK4 that further inhibits PDH activity and prevents glucose oxidation (102). Elevated fatty acid oxidation also leads to the mitochondrial accumulation of acetyl-CoA and NADH thereby decreasing cardiac glucose oxidation. In diabetes, although fatty acid is an efficient substrate for the heart, its excess supply and utilization can be detrimental. An increase in cardiac fatty acid utilization can generate reactive oxygen species that are known to induce significant myocardial damage. Another outcome of this switch in myocardial substrate is for the FA supply to surpass the myocardial oxidative capacity. In addition, accumulated unoxidized FA due to excess delivery can be transformed to intracellular lipid intermediates that pose the risk of cardiac lipotoxicity, a condition that is associated with cellular dysfunction and cell death (103).

1.3 AMPK and cardiac metabolism

1.3.1 AMPK and glucose metabolism

In the heart, AMPK activation has been shown to elevate glucose transport by transferring glucose transporters from the intracellular stores to the sarcolemma and augment glycolysis by modulating the function of the enzyme phosphofructokinase-1 (PFK1).

a) GLUT4 The inability of hydrophilic compounds to bypass phospholipid bilayers renders glucose uptake a protein mediated process. Members of the GLUT family that

belong to a large family of twelve transmembrane segment transporters regulate this process. Two major isoforms of the GLUT family that have been identified to reside in the myocardium are GLUT1 and GLUT4 (104). GLUT1 controls basal glucose uptake and its actions are independent of insulin. GLUT4, the principal glucose transporter in the heart is localized in the intracellular pool that translocates to the cell surface by both insulin and non-insulin dependent stimulation. Insulin treatment of cardiomyocytes activates the PI3K/Akt pathway that phosphorylates the component proteins of GLUT4 containing vesicles promoting GLUT4 translocation. AMPK has been demonstrated to induce cardiac GLUT4 translocation by an insulin independent mechanism (Fig. 2) (105; 106). AMPK was first shown to stimulate cardiac GLUT4 in isolated rat heart papillary muscles treated with AICAR (70). Although, transgenic mice expressing inactive AMPK have demonstrated normal GLUT4 expression and intact basal and insulin stimulated glucose uptake, a decreased glucose uptake and glycolysis has been reported in these mice during ischemia (107). AMPK also mediates GLUT4 transport to the plasma membrane during physiological conditions such as exercise (108). However, whether AMPK has a vital role in this response to exercise still remains unknown. Cardiac AMPK regulates GLUT4 translocation partly by targeting proteins such as protein kinase C, endothelial nitric oxide synthase (eNOS), p38 mitogen-activated protein kinase and transforming growth factor β -activated protein kinase 1-binding protein 1 (TAB1) complex (109; 110). Recently, studies utilizing DEX as a model of whole body insulin resistance have demonstrated that in the presence of normal cardiac insulin signaling, AMPK-mediated phosphorylation of Akt substrate of 160 kDa (AS160) is the predominant factor that controls cardiac GLUT4 movement (80). Although multiple

mechanisms by which AMPK mediates cardiac GLUT4 transport are still being explored, possible targets include proteins involved in the cytoplasmic retention of GLUT4 vesicles and/or mechanisms involved in the docking or fusion of these vesicles at the plasma membranes. A reduction in GLUT4 endocytosis can also increase glucose uptake (43). A recent study utilizing cardiomyocytes demonstrated that metformin leads to a longer retention time of GLUT4 at the plasma membrane due to an AMPK mediated decline in GLUT4 endocytosis (43). As endocytosis is an energy consuming process, blocking this process would conserve energy that follows from signaling via the AMPK pathway.

b) Phosphofruktokinase-1 Following its entry into the cardiac cell, glucose is broken down to pyruvate through glycolysis. Glycolysis is an anaerobic process and contributes to less than 10% of the total myocardial energy (111). Phosphofruktokinase-1 (PFK-1) is a rate-limiting enzyme that irreversibly converts fructose 6 phosphate (F6P) to fructose 1,6 bisphosphate (F1,6BP) and controls glycolysis. PFK-1 is activated by AMP, ADP and fructose-2,6-bisphosphate (F2,6BP) and inhibited by ATP, citrate, low pH and F1,6BP. Phosphofruktokinase-2 (PFK-2) catalyses the formation of F2,6BP from F6P. AMPK by activating phosphofruktokinases has been demonstrated to stimulate cardiac glycolysis (112). AMPK phosphorylates PFK-2 and increases the formation of F2,6BP, a positive regulator of the important glycolytic enzyme PFK-1 (Fig. 2) (106). Thus the capacity of AMPK to activate PFK and increase glycolysis makes it a central component in inducing cellular response to stress conditions like anaerobic exercise, anoxia and ischemia.

1.3.2 AMPK and FA metabolism

Complete FA metabolism involves two major processes, (a) entry of long chain FA into the cardiomyocyte and (b) subsequent utilization of FA within the mitochondria for ATP generation.

1.3.2.1 AMPK and FA entry

a) FA transporters It was long considered that FA could enter a cell via passive diffusion, dependant on metabolic rate and physicochemical properties of lipophilic substrates. However, the saturable nature of FA uptake and its responsiveness to competitive inhibition suggests the requirement of FA transporters (113). Although, the list of FA transporters is still growing, so far four proteins have been recognized to regulate myocardial FA uptake at both mRNA and protein levels. In the heart, these transporters are localized at the sarcolemma and facilitate FA uptake. The importance of these FA transporters in the myocardium is established by studies that divulge a 55-80% drop of myocardial FA transport by transport inhibitors (114). In addition, overexpression of myocardial FATPs or CD36 augments FA uptake and metabolism. Both transcriptional and post-translational regulation of FA transporters govern FA uptake (115; 116). Contraction induced cardiac AMPK activation or acute stimulation of AMPK by AICAR augments FA uptake through translocation of CD36 from an intracellular pool to the sarcolemma membrane (47; 115). Conversely, in perfused hearts and isolated cardiomyocytes prolonged myocardial AMPK activation by AICAR augments both protein expression and plasmalemma content of fatty acid transporters CD36 and FABPpm (116). Importantly, these AICAR induced effects on fatty acid uptake are prevented when the AMPK signaling pathway is blocked. Moreover,

contraction mimicking stimuli like oligomycin also stimulates cardiac FA uptake by activating AMPK induced CD36 pathway (47). A recent study demonstrated that AMPK mediated increase in FA uptake critically depends on the transporter CD36 and its deficiency completely abolishes cardiac FA uptake (81). This effect has been suggested to be a result of activation of a signaling axis made up of LKB1 and AMPK α 2 (117). Although the effect of AMPK on the FA transporter CD36 has been studied extensively, its precise role in regulating other FA carriers still remains unclear.

b) Lipoprotein lipase The limited capacity of the heart to synthesize or store triglycerides (TG) renders it to depend heavily on exogenous supply. Albumin bound FA and circulating TG-rich lipoproteins are the two main exogenous sources of FA serving the myocardium. The concentration of FA in lipoprotein TG is ~10 fold higher than that found in FA bound to albumin and the former is known to be the principal source of FA supplied to the myocardium (118). Lipoproteins in the blood are hydrolyzed by lipoprotein lipase (LPL) an enzyme that is synthesized in the cardiomyocyte and is transported to the heparin sulphate proteoglycan binding (HSPG) sites located at the myocyte cell surface (119). From here, LPL is then transported to HSPG binding sites located on the endothelial cells of the coronary blood vessel. At these sites LPL hydrolyzes the circulating TG-rich lipoproteins, such as very low density lipoproteins (VLDL) or chylomicrons to release FA that are utilized by the myocardium. It has been established that LPL plays a crucial role in regulating myocardial FA delivery and any alteration in LPL function impacts myocardial FA delivery and oxidation. Indeed, an augmentation in myocardial LPL gene expression elevates FA uptake and tissue specific knock-out of cardiac LPL switches the cardiac substrate preference to glucose (120).

Recently, AMPK has also been reported to control FA delivery through its regulation of LPL (46). In adult male Wistar rats, fasting activates cardiac AMPK and increases coronary luminal LPL activity. This increase in LPL activity was independent of any change in LPL mRNA or alterations in protein and activity, suggesting that the LPL increase at the coronary lumen was via posttranslational mechanisms (46). Importantly, the AMPK induced increases in luminal LPL activity was prevented when cardiomyocytes were incubated with an AMPK inhibitor. In addition, during conditions of increased cardiac workload and excessive energy expenditure, the β -agonist isoproterenol by activating AMPK has been shown to increase cardiac luminal LPL activity (121). During acute diabetes, when cardiac glucose utilization is compromised, AMPK recruitment of LPL to the cardiomyocyte surface has been stated to represent an immediate compensatory response by the heart to guarantee fatty acid supply (39). Thus in addition to regulating CD36, a novel mechanism by which AMPK facilitates myocardial FA delivery is through its control of LPL.

1.3.2.2 AMPK and FA oxidation

a) Acetyl CoA Carboxylase (ACC) ACC is commonly known to regulate FA biosynthesis in liver and adipose tissue. Despite the limited capacity of the myocardium for FA biosynthesis, ACC is also expressed within the heart (122). Till date, two major isoforms of ACC have been typified in rodents and humans. ACC1 is strongly expressed in liver and adipose tissue, whereas ACC2 predominates in the heart and skeletal muscle. ACC1 resides in the cytosol whereas ACC2 is associated with the mitochondria. Intracellular localization of each isoform has revealed that ACC2 generates malonyl CoA that is responsible for inhibiting fatty acid oxidation (123). Consistent with this theory,

ACC2 deficient mice are leaner when compared to their wild type counterparts, likely due to increased FA utilization in the cardiac and skeletal muscle (124). In the heart, phosphorylation reactions regulate ACC activity. Both *in vivo* and *in vitro* phosphorylation of AMPK has been reported to inactivate ACC and reduce malonyl CoA levels to promote FA oxidation (68). AICAR by activating AMPK inactivates ACC and promotes cardiac fatty acid utilization (68). During ischemia reperfusion, AMPK activation has been stated to inactivate ACC and increase cardiac FA oxidation (107). Studies utilizing DEX as a model of whole body insulin resistance have reported that acute DEX treatment by phosphorylating AMPK inhibits ACC and augments cardiac fatty acid oxidation (50). Conversely, AMPK inhibitors such as insulin and Ara-A activate ACC and inhibit cardiac FA utilization. The above evidences clearly suggest that AMPK by regulating ACC plays a crucial role in controlling cardiac FA oxidation.

b) Peroxisome proliferator activated receptors (PPARs) Belonging to the superfamily of nuclear receptors, PPAR's are a group of ligand-activated transcriptional factors that can be activated by pharmacological and natural ligands such as FA (125). Upon activation, PPAR's heterodimerize with retinoid X receptors and transcriptionally activate genes responsible for fatty acid oxidation. Till date, three isoforms of PPARs have been identified: PPAR- α , PPAR- β (also known as PPAR- δ) and PPAR- γ . PPAR- α and β are highly expressed in the heart and are considered to be the principal regulators of FA metabolism within the cardiac tissue (126). Upon activation by intracellular FA, both PPAR- α and β augment the expression of genes controlling cardiac FA metabolism at various steps such as FA entry (CD36, LPL and FABPpm), FA esterification (acyl CoA synthase) and FA oxidation (CPT1, LCAD, VLCAD and ACO). Overexpression of

cardiac PPAR- α and β has demonstrated to augment FA uptake and oxidation (127). In addition, cardiac specific knockout of PPAR- α and β reduces the FA oxidative gene expression and FA oxidation (128). PPAR- γ , the third isoform of the PPAR family is expressed abundantly in the adipose tissue and is detected at lower levels in the heart suggesting a limited role for this isoform in regulating cardiac FA metabolism (129). AMPK, in addition to its acute regulation, also displays long term effects to control fatty acid oxidation. In non-cardiac tissues, AMPK by activating PPAR- α and peroxisome proliferator-activated receptor gamma co-activator (PGC-1 α) promotes mitochondrial fatty acid oxidation. In addition, metformin and AICAR by activating AMPK α 1 have been proposed to stimulate mitochondrial proliferation that likely elevates mitochondrial biogenesis (130). In white adipocytes, prolonged AICAR induced AMPK activation has been shown to elevate FA oxidation likely through up-regulation of PGC-1 and PPAR- α mRNA levels (131). In the heart, whether AMPK directly regulates PPAR-alpha to promote fatty acid oxidation is unclear and not yet established. In contrast, some studies have also suggested that prolonged AMPK activation might result in a decrease of the enzymes that would be crucial to cardiac fatty acid oxidation (132).

c) Malonyl CoA decarboxylase (MCD) Cardiac malonyl CoA levels tightly regulate fatty acid oxidation by inhibiting CPT1, a rate-limiting enzyme that controls FA entry into the mitochondria (133). Large increases in cytosolic malonyl CoA inhibits CPT1, and reduce mitochondrial FA uptake and oxidation. In the heart, malonyl CoA levels are controlled by its rate of synthesis and degradation. Malonyl CoA is synthesized from acetyl CoA and can be degraded back to acetyl CoA by MCD. The enzyme MCD has been suggested to strongly dictate cardiac FA oxidation by altering malonyl CoA levels.

Research has revealed that elevated MCD activity in the presence of a reduced ACC activity decreases malonyl CoA levels and increases FA oxidation in post-natal and ischemia reperfused heart (134). In streptozotocin induced diabetes, high fat feeding and fasting, an augmentation in MCD mRNA expression has been proposed to regulate cardiac fatty acid oxidation (62; 134). AMPK modulates cardiac fatty acid metabolism largely by regulating two key enzymes, ACC and MCD. As mentioned earlier, AMPK activation phosphorylates and inactivates ACC, reducing malonyl CoA and promoting cardiac FA oxidation. As AMPK is indirectly involved in the production of malonyl CoA, several researchers have investigated whether MCD is a direct target of AMPK. In non-cardiac tissues such as longus muscle, AICAR by activating AMPK significantly elevates MCD activity by two fold (135). In addition, muscle contraction induced activation of AMPK has been suggested to increase both MCD phosphorylation and activity (135). To further corroborate this direct role of AMPK, Park et al demonstrated that exercise induced activation of AMPK increased MCD activity in liver and muscle, and this effect was reversed by the addition of PP2A (136). In H9c2 cardiac ventricular cell line, Lopaschuk's group has demonstrated that increasing AMPK activity by overexpression of constitutively active AMPK increases cytosolic MCD expression and mitochondrial MCD expression and activity (137). However, whether MCD acts as a direct substrate for cardiac AMPK in vivo is unknown and needs further investigation.

d) Carnitine palmitoyl transferase (CPT) The uptake of cytosolic FA within the mitochondria is tightly regulated by a carnitine transport system. As long chain acyl-CoA's are not readily permeable through the mitochondrial matrix, first CPT1 catalyses the conversion of cytosolic acyl CoA's to acyl carnitine in the compartment localized

between the inner and outer mitochondrial membrane (86). Next, CPT2 converts acyl carnitine back to acyl CoA in the mitochondrial matrix (86). Ideally, CPT-1 is considered as the primary regulator of FA uptake into the mitochondria. Two isoforms of CPT1 have been identified, CPT-1 α that is highly expressed in the liver and CPT1 β that predominates in the myocardium. It has been demonstrated that CPT1 β is approximately thirty times more sensitive to inhibition by malonyl CoA as compared to CPT1 α . As mentioned earlier, malonyl CoA is a key regulator of fatty acid oxidation in the heart. A rise in its level inhibits CPT1 function and reduces mitochondrial FA uptake and oxidation. AMPK through its regulation of ACC reduces malonyl CoA levels and indirectly influences CPT1 activity to promote cardiac FA uptake and oxidation.

1.4 AMPK and cardiac cell death

Cardiomyocyte cell death is increased during heart disease and is one of the key factors causing heart failure. Stimulation of cardiac AMPK has the potential to increase energy production or pathways that can inhibit apoptosis thereby protecting the heart during stress stimuli. However, the exact role of AMPK in apoptosis is not clear, with studies reporting both pro and anti-apoptotic actions. AMPK by influencing the jun kinase pathway, the pro-apoptotic protein p53 and caspase-3 activity induces apoptosis in non-cardiac cells like vascular smooth muscle and pancreatic cells (138; 139). In cardiac cells, majority of the studies suggest that AMPK activation is protective. AMPK stimulation has been demonstrated to protect against high fat induced apoptosis in both neonatal and adult rat cardiomyocytes (85; 140). During ischemia reperfusion, AMPK α 2 knock-out mice display left ventricular dysfunction and increased apoptosis, implicating AMPK as an important mediator of the anti-apoptotic pathway (107). Adiponectin

through its regulation of AMPK also protects against myocardial ischemia reperfusion injury with adiponectin deficient mice displaying increased infarct size and apoptosis (141). In addition, treatment of neonatal rat cardiomyocytes with adiponectin confers protection against hypoxia induced apoptosis and inclusion of the dominant negative mutant of AMPK abolishes these protective effects (142). Taken together, the above studies clearly indicate that AMPK activation can protect the heart against apoptosis.

1.5 Rationale and objectives

Following hypoinsulinemia, glucose utilization is compromised and the myocardium switches to utilize FA. Previous studies have reported that PPAR- α promotes FA oxidation during chronic hypoinsulinemia (182). Whether the same modification also occurs in the heart during acute hypoinsulinemia and if AMPK participates in the increase of cardiac fatty acid oxidation remains unclear. In addition to its role in FA oxidation, AMPK has been implicated in controlling FA delivery through its regulation of the FA transporter, CD36 (97). Given that LPL derived FA is the principal source of energy during insulin resistance, the question of interest was whether cardiac AMPK can regulate LPL translocation to the vascular lumen to increase the exogenous FA pool. Finally, besides its role in metabolism, AMPK has been suggested to modulate cell death. In non-cardiac cells such as endothelial cells and astrocytes, activation of AMPK has been shown to protect against hyperglycemia or high fat induced cell death (98; 99). In H9c2 cardiac muscle cell line or in adult cardiomyocytes, AMPK activation has been shown to protect against reactive oxygen species and palmitate induced cell death (100; 101). The production of TNF- α is widely reported to increase during obesity, diabetes and ischemia reperfusion and elevated plasma or endogenous cardiac TNF- α levels have

been shown to cause cardiac myocyte apoptosis (204; 205). Given the emerging role of AMPK in preventing cell death, it is unclear whether AMPK could protect cardiomyocytes against TNF- α induced apoptosis. Taken together, the overall hypothesis for my Ph.D. project is:

“Cardiac AMPK regulates fatty acid oxidation and delivery during diabetes and confers protection against cytokine induced cardiac cell death”

Specific Aims

1. To determine the regulation of cardiac FA oxidation by AMPK following acute and chronic hypoinsulinemia.
2. To investigate whether activation of AMPK augments cardiac LPL at the coronary lumen to facilitate FA delivery.
3. To investigate whether AMPK activation prevents TNF- α -induced apoptosis in adult rat ventricular cardiomyocytes.

1.6 Figures

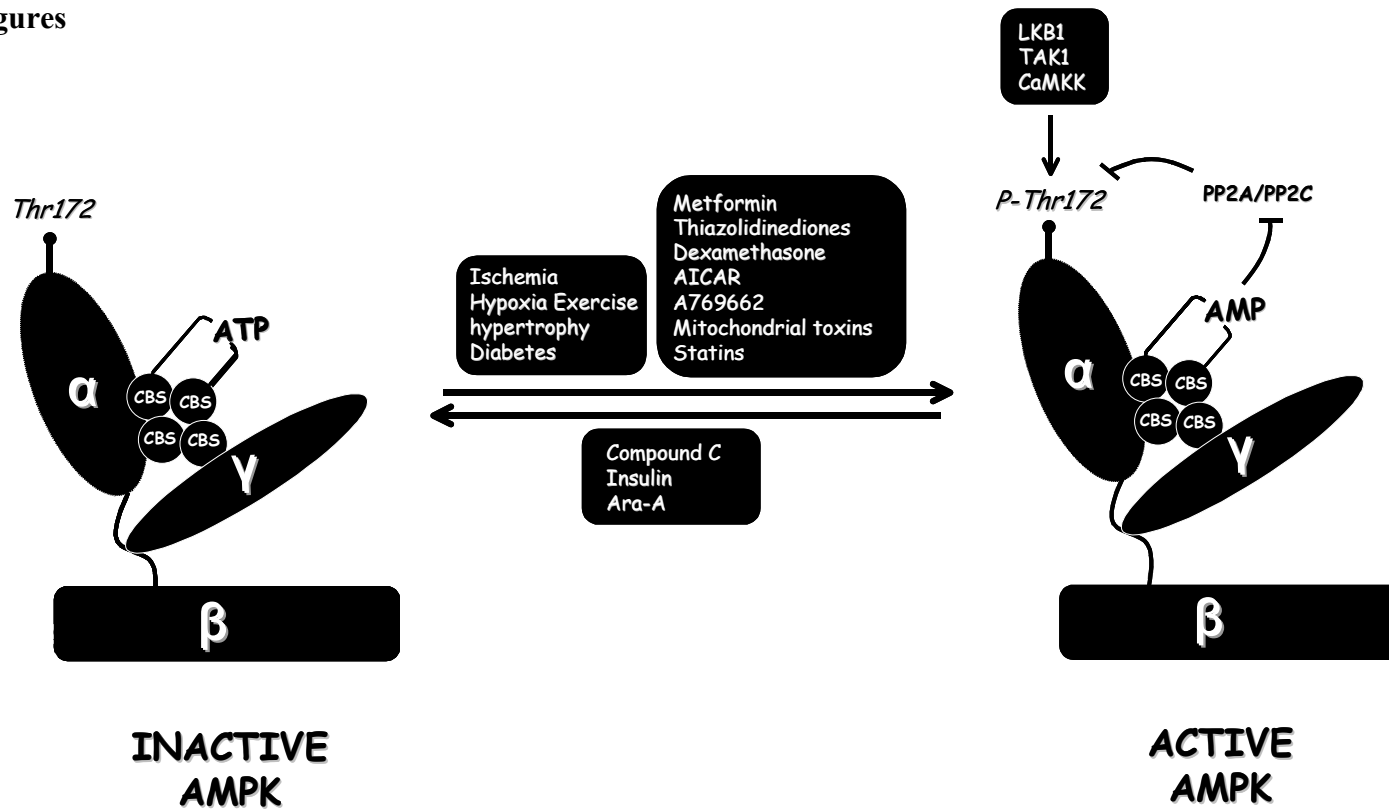


Fig. 1-1 Regulation of AMPK. Major mechanisms that transform AMPK from an inactive state to an active phosphorylated state include allosteric regulation by AMP, phosphorylation by the tumor suppressor kinase LKB1, stimulation by the Ca^{2+} calmodulin dependant protein kinase kinase (CaMKK) and phosphorylation by the serine/threonine protein kinase transforming growth factor-1 β -activated kinase 1 (TAK1). Protein phosphatases 2A and 2C by dephosphorylating AMPK transform this kinase back to its inactive quiescent state. Furthermore, AMPK function can be regulated under pathophysiological conditions, by various drugs and pharmacological activators and inhibitors.

Fig. 1-2 Glucose and FA delivery and utilization in cardiomyocytes. Glucose entry into the cardiac cell is facilitated through GLUT1 and GLUT4 transporters. Once within the cell, glucose is broken down to glucose-6-phosphate, which is either stored as glycogen or converted to phosphofructokinase-1 (PFK1), a rate limiting enzyme that regulates glycolysis. PFK2 through its action on 2,6-bisphosphate can positively regulate PFK1. Following glycolysis, pyruvate dehydrogenase complex (PDH) promotes pyruvate entry into the mitochondria to form acetyl CoA. Phosphorylation by pyruvate dehydrogenase kinase (PDK) inactivates PDH complex. Eventually, acetyl CoA enters the citric acid cycle and is broken down to H₂O and CO₂ for ATP production. Majority of the fatty acids utilized by the myocardium are derived from the breakdown of circulating lipoproteins such as very low density lipoprotein triglycerides (VLDL-TG) or chylomicron triglycerides (Chy-TG). These TG-rich lipoproteins upon hydrolysis by lipoprotein lipase (LPL), are transported into the cardiomyocyte by three FA transporters (CD36, fatty acid transporter protein (FATP) and fatty acid binding protein plasma membrane (FABPpm)). Once within the cell, FA are converted to fatty acyl CoA that is transported into the mitochondria through a carnitine mediated transport system. Within the mitochondria, fatty acyl CoA undergo β -oxidation to generate energy. Oxidation of FA is governed by multiple mechanisms. By directly activating PPAR- α , FA can turn on genes responsible for FA oxidation. The stress sensing kinase AMPK modulates both glucose and FA metabolism. AMPK by recruiting GLUT4 at the plasma membrane and by phosphorylating PFK2 promotes glucose entry and glycolysis. AMPK also inhibits ACC and reduces malonyl CoA levels to promote fatty acid oxidation.

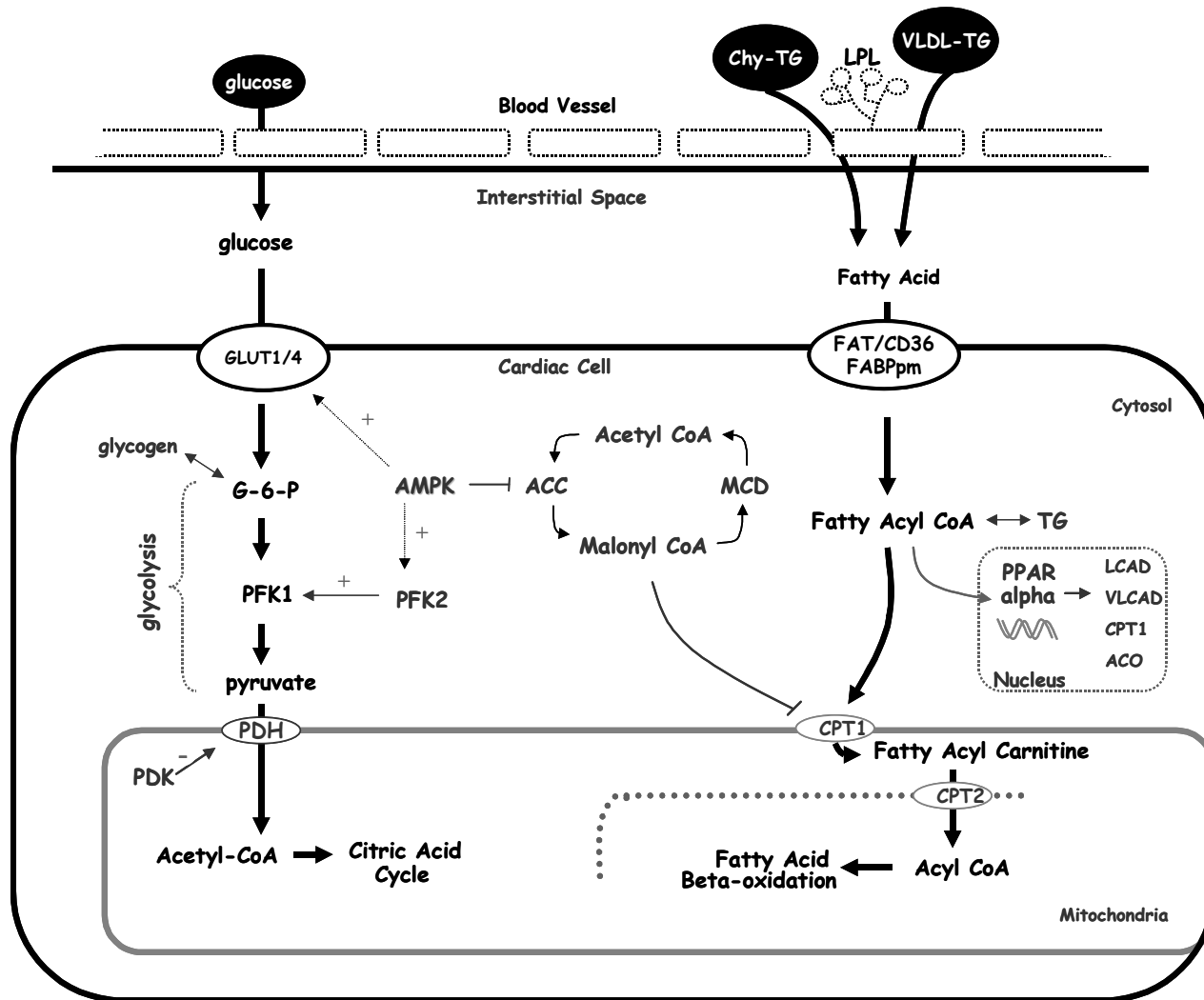


Fig. 1-2 Glucose and FA delivery and utilization in cardiomyocytes

1.7 Bibliography

1. Carling D, Zammit VA, Hardie DG. A common bicyclic protein kinase cascade inactivates the regulatory enzymes of fatty acid and cholesterol biosynthesis. *FEBS Lett.* 1987;223:217-222.
2. Woods A, Cheung PC, Smith FC et al. Characterization of AMP-activated protein kinase beta and gamma subunits. Assembly of the heterotrimeric complex in vitro. *J Biol Chem.* 1996;271:10282-10290.
3. Pang T, Xiong B, Li JY et al. Conserved alpha-helix acts as autoinhibitory sequence in AMP-activated protein kinase alpha subunits. *J Biol Chem.* 2007;282:495-506.
4. Woods A, Vertommen D, Neumann D et al. Identification of phosphorylation sites in AMP-activated protein kinase (AMPK) for upstream AMPK kinases and study of their roles by site-directed mutagenesis. *J Biol Chem.* 2003;278:28434-28442.
5. Mitchelhill KI, Mitchell BJ, House CM et al. Posttranslational modifications of the 5'-AMP-activated protein kinase beta1 subunit. *J Biol Chem.* 1997;272:24475-24479.
6. Wong KA, Lodish HF. A revised model for AMP-activated protein kinase structure: The alpha-subunit binds to both the beta- and gamma-subunits although there is no direct binding between the beta- and gamma-subunits. *J Biol Chem.* 2006;281:36434-36442.
7. Warden SM, Richardson C, O'Donnell J, Jr. et al. Post-translational modifications of the beta-1 subunit of AMP-activated protein kinase affect enzyme activity and cellular localization. *Biochem J.* 2001;354:275-283.
8. Salt I, Celler JW, Hawley SA et al. AMP-activated protein kinase. greater AMP dependence, and preferential nuclear localization, of complexes containing the alpha2 isoform. *Biochem J.* 1998;334(Pt 1):177-187.

9. Kemp BE. Bateman domains and adenosine derivatives form a binding contract. *J Clin Invest.* 2004;113:182-184.
10. Witczak CA, Sharoff CG, Goodyear LJ. AMP-activated protein kinase in skeletal muscle: from structure and localization to its role as a master regulator of cellular metabolism. *Cell Mol Life Sci.* 2008;65:3737-3755.
11. Kodiha M, Rassi JG, Brown CM, Stochaj U. Localization of AMP kinase is regulated by stress, cell density, and signaling through the MEK-->ERK1/2 pathway. *Am J Physiol Cell Physiol.* 2007;293:C1427-1436.
12. Scott JW, Hawley SA, Green KA et al. CBS domains form energy-sensing modules whose binding of adenosine ligands is disrupted by disease mutations. *J Clin Invest.* 2004;113:274-284.
13. Kyriakis JM: At the crossroads. AMP-activated kinase and the LKB1 tumor suppressor link cell proliferation to metabolic regulation. *J Biol.* 2003;2:26.
14. Baas AF, Boudeau J, Sapkota GP et al. Activation of the tumour suppressor kinase LKB1 by the STE20-like pseudokinase STRAD. *Embo J.* 2003;22:3062-3072.
15. Kim AS, Miller EJ, Young LH. AMP-activated protein kinase: a core signalling pathway in the heart. *Acta Physiol (Oxf).* 2009;196:37-53.
16. Sakamoto K, Zarrinpashneh E, Budas GR et al. Deficiency of LKB1 in heart prevents ischemia-mediated activation of AMPKalpha2 but not AMPKalpha1. *Am J Physiol Endocrinol Metab.* 2006;290:E780-788.
17. Sanders MJ, Grondin PO, Hegarty BD, Snowden MA, Carling D. Investigating the mechanism for AMP activation of the AMP-activated protein kinase cascade. *Biochem J.* 2007;403:139-148.

18. Hardie DG. Role of AMP-activated protein kinase in the metabolic syndrome and in heart disease. *FEBS Lett.* 2008;582:81-89.
19. Altarejos JY, Taniguchi M, Clanachan AS, Lopaschuk GD. Myocardial ischemia differentially regulates LKB1 and an alternate 5'-AMP-activated protein kinase kinase. *J Biol Chem.* 2005;280:183-190.
20. Xie Z, Dong Y, Scholz R, Neumann D, Zou MH. Phosphorylation of LKB1 at serine 428 by protein kinase C-zeta is required for metformin-enhanced activation of the AMP-activated protein kinase in endothelial cells. *Circulation.* 2008;117:952-962.
21. Xie Z, Dong Y, Zhang M et al. Activation of protein kinase C zeta by peroxynitrite regulates LKB1-dependent AMP-activated protein kinase in cultured endothelial cells. *J Biol Chem.* 2006;281:6366-6375.
22. Shaw RJ, Lamia KA, Vasquez D et al. The kinase LKB1 mediates glucose homeostasis in liver and therapeutic effects of metformin. *Science.* 2005;310:1642-1646.
23. Hawley SA, Selbert MA, Goldstein EG et al. 5'-AMP activates the AMP-activated protein kinase cascade, and Ca²⁺/calmodulin activates the calmodulin-dependent protein kinase I cascade, via three independent mechanisms. *J Biol Chem.* 1995;270:27186-27191.
24. Hawley SA, Boudeau J, Reid JL et al. Complexes between the LKB1 tumor suppressor, STRAD alpha/beta and MO25 alpha/beta are upstream kinases in the AMP-activated protein kinase cascade. *J Biol.* 2003;2:28.
25. Nath N, McCartney RR, Schmidt MC. Yeast Pak1 kinase associates with and activates Snf1. *Mol Cell Biol.* 2003;23:3909-3917.

26. Sutherland CM, Hawley SA, McCartney RR. Elm1p is one of three upstream kinases for the *Saccharomyces cerevisiae* SNF1 complex. *Curr Biol.* 2003;13:1299-1305.
27. Jensen TE, Rose AJ, Jorgensen SB et al. Possible CaMKK-dependent regulation of AMPK phosphorylation and glucose uptake at the onset of mild tetanic skeletal muscle contraction. *Am J Physiol Endocrinol Metab.* 2007;292:E1308-1317.
28. Kewalramani G, Puthanveetil P, Wang F et al. AMP-activated protein kinase confers protection against TNF- α -induced cardiac cell death. *Cardiovasc Res.* (2009).
29. Soderling TR: The Ca-calmodulin-dependent protein kinase cascade. *Trends Biochem Sci.* 1999;24:232-236.
30. Anderson KA, Means RL, Huang QH et al. Components of a calmodulin-dependent protein kinase cascade. Molecular cloning, functional characterization and cellular localization of Ca²⁺/calmodulin-dependent protein kinase kinase beta. *J Biol Chem.* 1998;273:31880-31889.
31. Towler MC, Hardie DG. AMP-activated protein kinase in metabolic control and insulin signaling. *Circ Res.* 2007;100:328-341.
32. Wu Y, Song P, Xu J, Zhang M, Zou MH. Activation of protein phosphatase 2A by palmitate inhibits AMP-activated protein kinase. *J Biol Chem.* (2007);282:9777-9788.
33. Momcilovic M, Hong SP, Carlson M. Mammalian TAK1 activates Snf1 protein kinase in yeast and phosphorylates AMP-activated protein kinase in vitro. *J Biol Chem.* (2006);281:25336-25343.
34. Kishimoto K, Matsumoto K, Ninomiya-Tsuji J. TAK1 mitogen-activated protein kinase kinase kinase is activated by autophosphorylation within its activation loop. *J Biol Chem.* 2000;275:7359-7364.

35. Xie M, Zhang D, Dyck JR et al. A pivotal role for endogenous TGF-beta-activated kinase-1 in the LKB1/AMP-activated protein kinase energy-sensor pathway. *Proc Natl Acad Sci U S A*. 2006;103:17378-17383.
36. Wang MY, Unger RH. Role of PP2C in cardiac lipid accumulation in obese rodents and its prevention by troglitazone. *Am J Physiol Endocrinol Metab*. 2005;288:E216-221.
37. Davies SP, Helps NR, Cohen PT, Hardie DG. 5'-AMP inhibits dephosphorylation, as well as promoting phosphorylation, of the AMP-activated protein kinase. Studies using bacterially expressed human protein phosphatase-2C alpha and native bovine protein phosphatase-2AC. *FEBS Lett*. 1995;377:421-425.
38. Corton JM, Gillespie JG, Hawley SA, Hardie DG. 5-aminoimidazole-4-carboxamide ribonucleoside. A specific method for activating AMP-activated protein kinase in intact cells? *Eur J Biochem*. 1995;229:558-565.
39. Kim MS, Kewalramani G, Puthanveetil P et al. Acute diabetes moderates trafficking of cardiac lipoprotein lipase through p38 mitogen-activated protein kinase-dependent actin cytoskeleton organization. *Diabetes*. 2008;57:64-76.
40. Vincent MF, Erion MD, Gruber HE, Van den Berghe G. Hypoglycaemic effect of AICArifoside in mice. *Diabetologia*. 1996;39:1148-1155.
41. Owen MR, Doran E, Halestrap AP. Evidence that metformin exerts its anti-diabetic effects through inhibition of complex 1 of the mitochondrial respiratory chain. *Biochem J*. 2000;348 Pt 3:607-614.
42. Davidson MB, Peters AL: An overview of metformin in the treatment of type 2 diabetes mellitus. *Am J Med*. 1997;102:99-110.

43. Yang J, Holman GD. Long-term metformin treatment stimulates cardiomyocyte glucose transport through an AMP-activated protein kinase-dependent reduction in GLUT4 endocytosis. *Endocrinology*. 2006;147:2728-2736.
44. Fujii N, Hirshman MF, Kane EM et al. AMP-activated protein kinase alpha2 activity is not essential for contraction- and hyperosmolarity-induced glucose transport in skeletal muscle. *J Biol Chem*. 2005;280:39033-39041.
45. Korystov YN, Kublik LN, Kudryavtsev AA et al. Opposite effects of low oligomycin concentrations on the apoptosis of normal and tumor cells. *Dokl Biol Sci*. 2003;392:475-477.
46. An D, Pulinilkunil T, Qi D et al. The metabolic "switch" AMPK regulates cardiac heparin-releasable lipoprotein lipase. *Am J Physiol Endocrinol Metab*. 2005;288:E246-253.
47. Luiken JJ, Coort SL, Willems J et al. Contraction-induced fatty acid translocase/CD36 translocation in rat cardiac myocytes is mediated through AMP-activated protein kinase signaling. *Diabetes*. 2003;52:1627-1634.
48. Goransson O, McBride A, Hawley SA et al. Mechanism of action of A-769662, a valuable tool for activation of AMP-activated protein kinase. *J Biol Chem*. 2007;282:32549-32560.
49. Viana AY, Sakoda H, Anai M et al. Role of hepatic AMPK activation in glucose metabolism and dexamethasone-induced regulation of AMPK expression. *Diabetes Res Clin Pract*. 2006;73:135-142.

50. Qi D, An D, Kewalramani G et al. Altered cardiac fatty acid composition and utilization following dexamethasone-induced insulin resistance. *Am J Physiol Endocrinol Metab.* 291, E420-427 (2006).
51. Sun W, Lee TS, Zhu M et al. Statins activate AMP-activated protein kinase in vitro and in vivo. *Circulation.* 2006;114:2655-2662.
52. Zhou G, Myers R, Li Y et al. Role of AMP-activated protein kinase in mechanism of metformin action. *J Clin Invest.* 2001;108:1167-1174.
53. Fryer LG, Parbu-Patel A, Carling D. Protein kinase inhibitors block the stimulation of the AMP-activated protein kinase by 5-amino-4-imidazolecarboxamide riboside. *FEBS Lett.* 2002;531:189-192.
54. Bain J, Plater L, Elliott M et al. The selectivity of protein kinase inhibitors: a further update. *Biochem J.* 2007;408:297-315.
55. Musi N, Hayashi T, Fujii N et al. AMP-activated protein kinase activity and glucose uptake in rat skeletal muscle. *Am J Physiol Endocrinol Metab.* 2001;280:E677-684.
56. Horman S, Vertommen D, Heath R et al. Insulin antagonizes ischemia-induced Thr172 phosphorylation of AMP-activated protein kinase alpha-subunits in heart via hierarchical phosphorylation of Ser485/491. *J Biol Chem.* 2006;281:5335-5340.
57. Kovacic S, Soltys CL, Barr AJ et al. Akt activity negatively regulates phosphorylation of AMP-activated protein kinase in the heart. *J Biol Chem.* 2003;278:39422-39427.
58. Bertrand L, Ginion A, Beauloye C et al. AMPK activation restores the stimulation of glucose uptake in an in vitro model of insulin-resistant cardiomyocytes via the activation of protein kinase B. *Am J Physiol Heart Circ Physiol.* 2006;291:H239-250.

59. Folmes CD, Clanachan AS, Lopaschuk GD: Fatty acids attenuate insulin regulation of 5'-AMP-activated protein kinase and insulin cardioprotection after ischemia. *Circ Res.* 2006;99:61-68.
60. Beauloye C, Marsin AS, Bertrand L et al. The stimulation of heart glycolysis by increased workload does not require AMP-activated protein kinase but a wortmannin-sensitive mechanism. *FEBS Lett.* 531, 324-328 (2002).
61. Hall JL, Lopaschuk GD, Barr A et al. Increased cardiac fatty acid uptake with dobutamine infusion in swine is accompanied by a decrease in malonyl CoA levels. *Cardiovasc Res.* 1996;32:879-885.
62. Goodwin GW, Taegtmeyer H. Regulation of fatty acid oxidation of the heart by MCD and ACC during contractile stimulation. *Am J Physiol.* 1999;277:E772-777.
63. Kahn BB, Alquier T, Carling D, Hardie DG. AMP-activated protein kinase: ancient energy gauge provides clues to modern understanding of metabolism. *Cell Metab.* 2005;1:15-25.
64. Yamauchi T, Kamon J, Minokoshi Y et al. Adiponectin stimulates glucose utilization and fatty-acid oxidation by activating AMP-activated protein kinase. *Nat Med.* 2002;8:1288-1295.
65. Jager S, Handschin C, St-Pierre J, Spiegelman BM. AMP-activated protein kinase (AMPK) action in skeletal muscle via direct phosphorylation of PGC-1alpha. *Proc Natl Acad Sci U S A.* 2007;104:12017-12022.
66. Kewalramani G, An D, Kim MS et al. AMPK control of myocardial fatty acid metabolism fluctuates with the intensity of insulin-deficient diabetes. *J Mol Cell Cardiol.* 2007;42:333-342.

67. Brownsey RW, Boone AN, Elliott JE, Kulpa JE, Lee WM. Regulation of acetyl-CoA carboxylase. *Biochem Soc Trans.* 2006;34:223-227.
68. Hardie DG: The AMP-activated protein kinase pathway--new players upstream and downstream. *J Cell Sci.* 2004;117:5479-5487.
69. Ruderman NB, Park H, Kaushik VK et al. AMPK as a metabolic switch in rat muscle, liver and adipose tissue after exercise. *Acta Physiol Scand.* 2003;178:435-442.
70. Russell RR, 3rd, Bergeron R, Shulman GI, Young LH. Translocation of myocardial GLUT-4 and increased glucose uptake through activation of AMPK by AICAR. *Am J Physiol.* 1999;277:H643-649.
71. Ojuka EO, Jones TE, Nolte LA et al. Regulation of GLUT4 biogenesis in muscle: evidence for involvement of AMPK and Ca(2+). *Am J Physiol Endocrinol Metab.* 2002;282:E1008-1013.
72. Daval M, Fougere F, Ferre P. Functions of AMP-activated protein kinase in adipose tissue. *J Physiol.* 2006;574:55-62.
73. Chen ZP, Mitchelhill KI, Michell BJ et al. AMP-activated protein kinase phosphorylation of endothelial NO synthase. *FEBS Lett.* 1999;443:285-289.
74. Viollet B, Ailhaud Y, Mounier R et al. AMPK: Lessons from transgenic and knockout animals. *Front Biosci.* 2009;14:19-44.
75. Hong YH, Varanasi US, Yang W, Leff T. AMP-activated protein kinase regulates HNF4alpha transcriptional activity by inhibiting dimer formation and decreasing protein stability. *J Biol Chem.* 2003;278:27495-27501.

76. Bolster DR, Crozier SJ, Kimball SR, Jefferson LS. AMP-activated protein kinase suppresses protein synthesis in rat skeletal muscle through down-regulated mammalian target of rapamycin (mTOR) signaling. *J Biol Chem.* 2002;277:23977-23980.
77. Lage R, Dieguez C, Vidal-Puig A, Lopez M: AMPK. a metabolic gauge regulating whole-body energy homeostasis. *Trends Mol Med.* 2008;14:539-549.
78. Minokoshi Y, Kim YB, Peroni OD et al. Leptin stimulates fatty-acid oxidation by activating AMP-activated protein kinase. *Nature.* 2002;415:339-343.
79. Dolinsky VW, Dyck JR. Role of AMP-activated protein kinase in healthy and diseased hearts. *Am J Physiol Heart Circ Physiol.* 2006;291:H2557-2569.
80. Puthanveetil P, Wang F, Kewalramani G et al. Cardiac glycogen accumulation after dexamethasone is regulated by AMPK. *Am J Physiol Heart Circ Physiol.* 2008;295:H1753-1762.
81. Habets DD, Coumans WA, Voshol PJ et al. AMPK-mediated increase in myocardial long-chain fatty acid uptake critically depends on sarcolemmal CD36. *Biochem Biophys Res Commun.* 2007;355:204-210.
82. Blazquez C, Geelen MJ, Velasco G, Guzman M. The AMP-activated protein kinase prevents ceramide synthesis de novo and apoptosis in astrocytes. *FEBS Lett.* 2001;489:149-153.
83. Ido Y, Carling D, Ruderman N. Hyperglycemia-induced apoptosis in human umbilical vein endothelial cells: inhibition by the AMP-activated protein kinase activation. *Diabetes.* 2002;51:159-167.
84. Hwang JT, Kwon DY, Park OJ, Kim MS. Resveratrol protects ROS-induced cell death by activating AMPK in H9c2 cardiac muscle cells. *Genes Nutr.* 2008;2:323-326.

85. An D, Kewalramani G, Chan JK et al. Metformin influences cardiomyocyte cell death by pathways that are dependent and independent of caspase-3. *Diabetologia*. 2006;49:2174-2184.
86. Stanley WC, Recchia FA, Lopaschuk GD. Myocardial substrate metabolism in the normal and failing heart. *Physiol Rev*. 2005;85:1093-1129.
87. Houten SM, Chegary M, Te Brinke H et al. Pyruvate dehydrogenase kinase 4 expression is synergistically induced by AMP-activated protein kinase and fatty acids. *Cell Mol Life Sci*. 2009;66:1283-1294.
88. Holness MJ, Sugden MC. Regulation of pyruvate dehydrogenase complex activity by reversible phosphorylation. *Biochem Soc Trans*. 2003;31:1143-1151.
89. Pulinilkunnil T, Rodrigues B. Cardiac lipoprotein lipase: metabolic basis for diabetic heart disease. *Cardiovasc Res*. 2006;69:329-340.
90. Barta E, Sideman S, Bassingthwaite JB. Facilitated diffusion and membrane permeation of fatty acid in albumin solutions. *Ann Biomed Eng*. 2000;28:331-345.
91. Bonen A, Chabowski A, Luiken JJ, Glatz JF. Is membrane transport of FFA mediated by lipid, protein, or both? Mechanisms and regulation of protein-mediated cellular fatty acid uptake: molecular, biochemical, and physiological evidence. *Physiology (Bethesda)*. 2007;22:15-29.
92. Glatz JF, van Nieuwenhoven FA, Luiken JJ, Schaap FG, van der Vusse GJ. Role of membrane-associated and cytoplasmic fatty acid-binding proteins in cellular fatty acid metabolism. *Prostaglandins Leukot Essent Fatty Acids*. 1997;57:373-378.

93. Zammit VA, Fraser F, Orstorphine CG. Regulation of mitochondrial outer-membrane carnitine palmitoyltransferase (CPT I): role of membrane-topology. *Adv Enzyme Regul.* 1997;37:295-317.
94. Ussher JR, Lopaschuk GD. The malonyl CoA axis as a potential target for treating ischaemic heart disease. *Cardiovasc Res.* 2008;79:259-268.
95. Cuthbert KD, Dyck JR. Malonyl-CoA decarboxylase is a major regulator of myocardial fatty acid oxidation. *Curr Hypertens Rep.* 2005;7:407-411.
96. Rodrigues B, Cam MC, McNeill JH. Myocardial substrate metabolism: implications for diabetic cardiomyopathy. *J Mol Cell Cardiol.* 1995;27:169-179.
97. Peterson LR, Herrero P, Schechtman KB et al. Effect of obesity and insulin resistance on myocardial substrate metabolism and efficiency in young women. *Circulation.* 2004;109:2191-2196.
98. Schwenk RW, Luiken JJ, Bonen A, Glatz JF. Regulation of sarcolemmal glucose and fatty acid transporters in cardiac disease. *Cardiovasc Res.* 2008;79:249-258.
99. Avogaro A, Nosadini R, Doria A et al. Myocardial metabolism in insulin-deficient diabetic humans without coronary artery disease. *Am J Physiol.* 1990;258:E606-618.
100. Nuutila P, Knuuti J, Ruotsalainen U et al. Insulin resistance is localized to skeletal but not heart muscle in type 1 diabetes. *Am J Physiol.* 1993;264:E756-762.
101. Luiken JJ, Arumugam Y, Bell RC et al. Changes in fatty acid transport and transporters are related to the severity of insulin deficiency. *Am J Physiol Endocrinol Metab.* 2002;283:E612-621.

102. Gottlicher M, Widmark E, Li Q, Gustafsson JA. Fatty acids activate a chimera of the clofibrilic acid-activated receptor and the glucocorticoid receptor. *Proc Natl Acad Sci U S A*. 1992;89:4653-4657.
103. Sharma S, Adroque JV, Golfman L et al. Intramyocardial lipid accumulation in the failing human heart resembles the lipotoxic rat heart. *Faseb J*. 2004;18:1692-1700.
104. Kraegen EW, Sowden JA, Halstead MB et al. Glucose transporters and in vivo glucose uptake in skeletal and cardiac muscle: fasting, insulin stimulation and immunoisolation studies of GLUT1 and GLUT4. *Biochem J*. 1993;295(Pt 1):287-293.
105. Yang J, Holman GD. Insulin and contraction stimulate exocytosis, but increased AMP-activated protein kinase activity resulting from oxidative metabolism stress slows endocytosis of GLUT4 in cardiomyocytes. *J Biol Chem*. 2005;280:4070-4078.
106. Arad M, Seidman CE, Seidman JG. AMP-activated protein kinase in the heart: role during health and disease. *Circ Res*. 2007;100:474-488.
107. Russell RR, 3rd, Li J, Coven DL et al. AMP-activated protein kinase mediates ischemic glucose uptake and prevents postischemic cardiac dysfunction, apoptosis, and injury. *J Clin Invest*. 2004;114:495-503.
108. Coven DL, Hu X, Cong L et al. Physiological role of AMP-activated protein kinase in the heart: graded activation during exercise. *Am J Physiol Endocrinol Metab*. 2003;285:E629-636.
109. Li J, Miller EJ, Ninomiya-Tsuji J, Russell RR, 3rd, Young LH. AMP-activated protein kinase activates p38 mitogen-activated protein kinase by increasing recruitment of p38 MAPK to TAB1 in the ischemic heart. *Circ Res*. 2005;97:872-879.

110. Pelletier A, Joly E, Prentki M, Coderre L. Adenosine 5'-monophosphate-activated protein kinase and p38 mitogen-activated protein kinase participate in the stimulation of glucose uptake by dinitrophenol in adult cardiomyocytes. *Endocrinology*. 2005;146:2285-2294.
111. Lopaschuk GD. AMP-activated protein kinase control of energy metabolism in the ischemic heart. *Int J Obes (Lond)*. 2008;32:Suppl 4, S29-35.
112. Marsin AS, Bertrand L, Rider MH et al. Phosphorylation and activation of heart PFK-2 by AMPK has a role in the stimulation of glycolysis during ischaemia. *Curr Biol*. 2000;10:1247-1255.
113. Stremmel W. Fatty acid uptake by isolated rat heart myocytes represents a carrier-mediated transport process. *J Clin Invest*. 1988;81:844-852.
114. Koonen DP, Glatz JF, Bonen A, Luiken JJ. Long-chain fatty acid uptake and FAT/CD36 translocation in heart and skeletal muscle. *Biochim Biophys Acta*. 2005;1736:163-180.
115. Chabowski A, Coort SL, Calles-Escandon J et al. The subcellular compartmentation of fatty acid transporters is regulated differently by insulin and by AICAR. *FEBS Lett*. 2005;579:2428-2432.
116. Chabowski A, Momken I, Coort SL et al. Prolonged AMPK activation increases the expression of fatty acid transporters in cardiac myocytes and perfused hearts. *Mol Cell Biochem*. 2006;288:201-212.
117. Habets DD, Coumans WA, El Hasnaoui M et al. Crucial role for LKB1 to AMPKalpha2 axis in the regulation of CD36-mediated long-chain fatty acid uptake into cardiomyocytes. *Biochim Biophys Acta*. 2009;1791:212-219.

118. Merkel M, Eckel RH, Goldberg IJ. Lipoprotein lipase: genetics, lipid uptake, and regulation. *J Lipid Res.* 2002;43:1997-2006.
119. Camps L, Reina M, Llobera M, Vilaro S, Olivecrona T. Lipoprotein lipase: cellular origin and functional distribution. *Am J Physiol.* 1990;258:C673-681.
120. Augustus AS, Buchanan J, Park TS et al. Loss of lipoprotein lipase-derived fatty acids leads to increased cardiac glucose metabolism and heart dysfunction. *J Biol Chem.* 281, 8716-8723 (2006).
121. An D, Kewalramani G, Qi D et al. beta-Agonist stimulation produces changes in cardiac AMPK and coronary lumen LPL only during increased workload. *Am J Physiol Endocrinol Metab.* 288, E1120-1127.
122. Hardie DG. Regulation of fatty acid and cholesterol metabolism by the AMP-activated protein kinase. *Biochim Biophys Acta.* 1992;1123:231-238.
123. Abu-Elheiga L, Brinkley WR, Zhong L et al. The subcellular localization of acetyl-CoA carboxylase 2. *Proc Natl Acad Sci U S A.* 2000;97:1444-1449.
124. Abu-Elheiga L, Matzuk MM, Abo-Hashema KA, Wakil SJ. Continuous fatty acid oxidation and reduced fat storage in mice lacking acetyl-CoA carboxylase 2. *Science.* 2001;291:2613-2616.
125. Forman BM, Chen J, Evans RM. Hypolipidemic drugs, polyunsaturated fatty acids, and eicosanoids are ligands for peroxisome proliferator-activated receptors alpha and delta. *Proc Natl Acad Sci U S A.* 1997;94:4312-4317.
126. Barger PM, Kelly DP. PPAR signaling in the control of cardiac energy metabolism. *Trends Cardiovasc Med.* 2000;10:238-245.

127. Finck BN, Han X, Courtois M et al. A critical role for PPARalpha-mediated lipotoxicity in the pathogenesis of diabetic cardiomyopathy: modulation by dietary fat content. *Proc Natl Acad Sci U S A*. 2003;100:1226-1231.
128. Cheng L, Ding G, Qin Q et al. Cardiomyocyte-restricted peroxisome proliferator-activated receptor-delta deletion perturbs myocardial fatty acid oxidation and leads to cardiomyopathy. *Nat Med*. 2004;10:1245-1250.
129. Vidal-Puig AJ, Considine RV, Jimenez-Linan M et al. Peroxisome proliferator-activated receptor gene expression in human tissues. Effects of obesity, weight loss, and regulation by insulin and glucocorticoids. *J Clin Invest*. 1997;99:2416-2422.
130. Kukidome D, Nishikawa T, Sonoda K et al. Activation of AMP-activated protein kinase reduces hyperglycemia-induced mitochondrial reactive oxygen species production and promotes mitochondrial biogenesis in human umbilical vein endothelial cells. *Diabetes*. 2006;55:120-127.
131. Gaidhu MP, Fediuc S, Anthony NM et al. Prolonged AICAR-induced AMP-kinase activation promotes energy dissipation in white adipocytes: novel mechanisms integrating HSL and ATGL. *J Lipid Res*. 2009;50:704-715.
132. Hongo M, Ishizaka N, Furuta K et al. Administration of angiotensin II, but not catecholamines, induces accumulation of lipids in the rat heart. *Eur J Pharmacol*. 2009;604:87-92.
133. Kudo N, Barr AJ, Barr RL, Desai S, Lopaschuk GD. High rates of fatty acid oxidation during reperfusion of ischemic hearts are associated with a decrease in malonyl-CoA levels due to an increase in 5'-AMP-activated protein kinase inhibition of acetyl-CoA carboxylase. *J Biol Chem*. 1995;270:17513-17520.

134. Sakamoto J, Barr RL, Kavanagh KM, Lopaschuk GD. Contribution of malonyl-CoA decarboxylase to the high fatty acid oxidation rates seen in the diabetic heart. *Am J Physiol Heart Circ Physiol.* 2000;278:H1196-1204.
135. Saha AK, Schwarsin AJ, Roduit R et al. Activation of malonyl-CoA decarboxylase in rat skeletal muscle by contraction and the AMP-activated protein kinase activator 5-aminoimidazole-4-carboxamide-1-beta -D-ribofuranoside. *J Biol Chem.* 2000;275:24279-24283.
136. Park H, Kaushik VK, Constant S et al. Coordinate regulation of malonyl-CoA decarboxylase, sn-glycerol-3-phosphate acyltransferase, and acetyl-CoA carboxylase by AMP-activated protein kinase in rat tissues in response to exercise. *J Biol Chem.* 2002;277:32571-32577.
137. Sambandam N, Steinmetz M, Chu A et al. Malonyl-CoA decarboxylase (MCD) is differentially regulated in subcellular compartments by 5'AMP-activated protein kinase (AMPK). Studies using H9c2 cells overexpressing MCD and AMPK by adenoviral gene transfer technique. *Eur J Biochem.* 2004;271:2831-2840.
138. Igata M, Motoshima H, Tsuruzoe K et al. Adenosine monophosphate-activated protein kinase suppresses vascular smooth muscle cell proliferation through the inhibition of cell cycle progression. *Circ Res.* 2005;97:837-844.
139. Kefas BA, Cai Y, Ling Z et al. AMP-activated protein kinase can induce apoptosis of insulin-producing MIN6 cells through stimulation of c-Jun-N-terminal kinase. *J Mol Endocrinol.* 2003;30:151-161.

140. Hickson-Bick DL, Buja LM, McMillin JB. Palmitate-mediated alterations in the fatty acid metabolism of rat neonatal cardiac myocytes. *J Mol Cell Cardiol.* 2000;32:511-519.
141. Shibata R, Sato K, Pimentel DR et al. Adiponectin protects against myocardial ischemia-reperfusion injury through AMPK- and COX-2-dependent mechanisms. *Nat Med.* 2005;11:1096-1103.
142. Terai K, Hiramoto Y, Masaki M et al. AMP-activated protein kinase protects cardiomyocytes against hypoxic injury through attenuation of endoplasmic reticulum stress. *Mol Cell Biol.* 2005;25:9554-9575.

2. AMPK CONTROL OF MYOCARDIAL FATTY ACID METABOLISM FLUCTUATES WITH THE INTENSITY OF INSULIN-DEFICIENT DIABETES²

2.1 INTRODUCTION

Dependent on their availability, cardiac tissue is characterized by its ability to obtain its energy via oxidation of various substrates like fatty acid (FA), glucose, lactate and ketone bodies (1; 2). This flexibility in substrate selection is essential for the heart to maintain production of energy and contractile function. Metabolic flexibility occurs through multiple mechanisms including regulation via a nuclear receptor, peroxisome proliferator-activated receptor- α (PPAR- α) (3). Following activation, PPAR- α regulates the expression of genes such as fatty acyl CoA synthase (4), CPT-1 (5), and acyl-CoA oxidase (ACO) (6), which are involved in FA utilization. Recent studies have also shown that AMP activated protein kinase (AMPK) also plays a key role in the regulation of cardiac metabolism. Once activated, AMPK switches off energy consuming processes like protein synthesis, whereas ATP generating mechanisms, such as FA oxidation and glycolysis, are turned on (7; 8). In heart and skeletal muscle, AMPK stimulates glucose uptake (9) and subsequent glycolysis through the activation of 6-phosphofructo-2-kinase (10). AMPK also facilitates FA utilization through its control of acetyl-CoA carboxylase (ACC) (11; 12). As ACC catalyzes the conversion of acetyl-CoA to malonyl-CoA, AMPK by inhibiting ACC is able to decrease malonyl-CoA and minimize its inhibition of CPT-1, the rate limiting enzyme controlling FA oxidation. AMPK has also been

² "A version of this chapter has been published. Kewalramani, G. An, D. Kim, MS. Ghosh, S. Qi, D. Abrahani, A. Pulinilkunnil, T. Sharma, V. Wambolt, RB. Allard, MF. Innis, SM. Rodrigues, B. (2007) AMPK control of myocardial fatty acid metabolism fluctuates with the intensity of insulin deficient diabetes. *J Mol Cell Cardiol.* 42:333-342."

implicated in FA delivery to cardiomyocytes through its regulation of the FA transporter, CD36 (13). Additionally, results from our laboratory have demonstrated a strong correlation between activation of whole heart AMPK and increases in coronary lumen lipoprotein lipase activity (14).

During ischemia, hypoxia, or exercise, AMPK is activated and regulates cardiac metabolism (15-17). It is unclear whether the same modification also occurs in the heart following hypoinsulinemia. In the current study, we examined changes in cardiac AMPK and metabolism in both acute and chronic diabetes and the underlying mechanisms that may contribute to these changes. Our data for the first time demonstrate that in the absence of hyperlipidemia, hearts from STZ induced diabetic rats exhibit AMPK activation, which likely contributes to augmented FA oxidation. This activation of AMPK is abolished with increasing intensity of diabetes and the availability of both circulating and endogenous fatty acids.

2.2 MATERIALS AND METHODS

2.2.1 Experimental animals

The investigation conforms to the guide for the care and use of laboratory animals published by the US National Institutes of Health and the University of British Columbia (Animal Care Certificate # A04-1009). Adult male Wistar rats (280-300g) were obtained from the UBC Animal Care Unit and supplied with a standard laboratory diet (PMI Feeds, Richmond, VA), and water ad libitum. Streptozotocin (STZ) [2-deoxy-2-(3-methyl-3-nitrosourea) 1-D-glucopyranose] is a broad spectrum glycoside antibiotic. Selective β -cell death and the ensuing diabetic state can be produced after a single intravenous dose of STZ. A dose-dependent increase in severity of diabetes is produced by 25-100 mg/kg STZ. After an i.v. injection of 55 mg/kg STZ, stable hyperglycemia develops within 24-48 hrs and remains 2-3 times higher than normal in concert with a \approx 50% reduction in plasma insulin levels. Although these animals are insulin deficient, they do not require insulin supplementation for survival and do not develop ketoacidosis (18). These animals were kept for 4 days (acute diabetes; D55-A) or 6 weeks (chronic diabetes; D55-C), prior to termination. The rationale for using two different durations of diabetes was the absence of changes in plasma and cardiac lipids in D55-A diabetes, alterations that are apparent following extension of the length of diabetes to 6 weeks. To determine if the increase in cardiac AMPK and ACC in D55-A could be reversed, some D55-A rats were injected with a rapid acting insulin (8 U, Humulin R, Eli Lilly Canada Inc.) into the tail vein. After 3 hrs (time required for establishment of sustained euglycemia), hearts from these animals were removed for subsequent assays.

100 mg/kg dose of STZ causes intense β -cell necrosis, 98% loss of pancreatic insulin stores, and severely reduced plasma insulin compared to control. Comparable to chronic D55-C diabetic rats, these D100 animals also show remarkable elevation of plasma glucose and lipids, but within acute 4 days of STZ injection. These animals die of diabetic ketoacidosis if not supplemented with exogenous insulin. Halothane-anesthetized rats were injected with 100 mg/kg STZ (IV, Sigma Chemical Co.) or an equivalent volume (1 mL/kg) of saline, and kept for 4 days after STZ injection (D100-A). Hyperglycemia was tested at 24 hours after STZ injection with a glucometer. At the indicated intervals, rats were anesthetized with sodium pentobarbital (65 mg/kg, i.p.), the thoracic cavity opened, and hearts removed.

2.2.2 Cardiac glucose and fatty acid oxidation

To measure glucose oxidation, isolated hearts were perfused for 30 min with Krebs-Henseleit buffer in the working mode at a preload of 11.5 mmHg and an afterload of 80 mmHg, as previously described (19). Rates of glucose oxidation were quantitatively measured by collection of $^{14}\text{CO}_2$ liberated from [U- ^{14}C] glucose at the pyruvate dehydrogenase reaction and in the citric acid cycle. To measure cardiac palmitate oxidation, hearts were perfused in the working mode with modified Krebs-Henseleit buffer (including 0.8-1.0 mM [9,10- ^3H] palmitate prebound to 3% BSA, 5.5 mM glucose, 2.0 mM calcium, and 100 U/L insulin) at a preload of 11.5 mmHg, as described previously (19). An afterload of 80 mmHg was maintained, and samples of perfusate and hyamine hydroxide were taken every 10 min for measurement of fatty acid oxidation.

2.2.3 Western blot analysis

On immediate removal of hearts from the various groups, 50 mg of ventricular tissue was ground under liquid nitrogen and homogenized. Western blot was carried out as described previously (14). Briefly, after centrifugation at 5,000 g for 20 min, the protein content of the supernatant was quantified using a Bradford protein assay. Samples were diluted, boiled with sample loading dye, and 50 µg used in SDS-polyacrylamide gel electrophoresis. After transfer, membranes were blocked in 5% skim milk in Tris-buffered saline containing 0.1% Tween-20. Membranes were incubated either with rabbit AMPK- α , phospho-AMPK (Thr172), or phospho-ACC (Ser79) antibody (Cell Signaling), and subsequently with secondary goat anti-rabbit HRP-conjugated antibody, and visualized using an ECL detection kit.

2.2.4 Measurement of cardiac gene expression

Gene expression was measured in the indicated groups using RT-PCR. Briefly, total RNA from hearts (100 mg) was extracted using Trizol (Invitrogen). After spectrophotometric quantification and resolving of RNA integrity using a formaldehyde agarose gel, reverse transcription was carried out using an oligo (dT) primer and superscript II RT (Invitrogen). cDNA of PPAR- α , CPT-1, ACO, malonyl-CoA decarboxylase (MCD) and CD36 were amplified using specific primers: 5'-GACAAGGCCTCAGGATACCA-3' (left) and 5'-AAACGGATTGCATTGTGTGA-3' (right) for PPAR- α ; 5'-TATGTGAGGATGCTGCT TCC-3' (left) and 5'-CTCGGAGAGCTAAGCTTGTC-3' (right) for CPT-1; 5'-GCCCTCAGCTATGGTATTAC-3' (left) and 5'-AGGAACTGCTCTCA CAATGC-3' (right) for ACO; 5'-GCCTGGTACCTTTACGGTGA-3' (left) and 5'-

GCTACCAGGCTGAG GATCTG-3' (right) for MCD; 5'-CTCTGACATTTGCAGGTCCA-3' (left) and 5'-CACAGGCTTTCCTTCTTTGC-3' (right) for CD36. The β -actin gene was amplified as an internal control using 5'-CGTAAAGACCTCTATGCCAA-3' (left) and 5'-AGCCATGCCAAATGTCTCAT-3' (right). The linear range was found to be between 15-40 cycles. The amplification parameters were set at: 94°C for 1 min, 56-58°C for 1 min and 72°C for 1 min, for a total of 28-35 cycles. The PCR products were electrophoresed on a 1.7% agarose gel containing ethidium bromide. Expression levels were represented as the ratio of signal intensity of the respective genes relative to β -actin.

2.2.5 Separation and characterization of cardiac lipids

Total cardiac lipids were extracted and solubilized in chloroform:methanol:acetone:hexane (4:6:1:1v/v/v/v). Separation of triglycerides and FA was achieved using HPLC (Waters 2690 Alliance HPLC, Milford, MA) equipped with an auto-sampler and column heater. FA were quantified as their respective methyl esters using heptadecaenoic acid (17:0) as the internal standard with a Varian 3400 GLC equipped with a flame ionization detector, a Varian Star data system, and a SP-2330 capillary column (30 m x 0.25 mm PA). Value of cardiac FA and triglycerides were expressed as μg lipid/mg protein.

2.2.6 Intralipid infusion

To determine the direct and acute effect of FA on AMPK activation, animals were anaesthetized with sodium pentobarbital (Somnotol; 65 mg/kg), and the left jugular vein cannulated. Intralipid (IL 1% and 5%; 1.2 ml/kg/h) or vehicle (saline) was then infused over a period of 4h, following which hearts were removed for determination of AMPK.

Intralipid was chosen as its principal component, Soy Oil, contains 40-60% linoleic acid, 20-30% oleic acid, and 5-15% palmitic acid. All of these FA's showed a robust increase in D55-C and D100-A rat hearts (Table 2). At each 30 min intervals, blood samples were obtained from the tail vein for analysis of plasma FA levels.

2.2.7 Plasma measurements

At termination, blood samples were obtained from the tail vein in heparinized glass capillary tubes. Blood samples were immediately centrifuged and plasma was collected and stored at -20°C until assayed. Diagnostic kits were used to measure glucose, triglyceride (Sigma), non-esterified fatty acid (NEFA, Wako), and insulin (Linco).

2.2.8 Statistical analysis

Values are means \pm SE. Wherever appropriate, one-way or two-way ANOVA followed by the Tukey or Bonferroni tests or the unpaired and paired Student's t-test was used to determine differences between group mean values (as indicated in the specific figure legends). The level of statistical significance was set at $P < 0.05$.

2.3 RESULTS

2.3.1 Control of cardiac substrate utilization in acute D55 (D55-A) diabetes

Four days following injection of 55 (D55-A) mg/kg STZ, diabetic rats showed the characteristic decline in weight gain (Table 2-1). This dose of STZ also precipitated a loss of circulating insulin, and overt hyperglycemia (Table 2-1).

Glucose metabolism is regulated through multiple steps, including uptake, glycolysis, and pyruvate decarboxylation, and insulin is known to influence all of these events (20). Myocardial glucose metabolism in control and diabetic hearts is summarized in Fig. 2-1A. Mean steady state rates of glucose oxidation were determined from data obtained during the initial portion of the heart perfusion. Compared to control, the rate of cardiac glucose oxidation in D55-A was significantly decreased (Fig. 2-1A, top panel). In contrast to glucose, FA is the preferred substrate, and accounts for approximately 70% of ATP generated in an aerobic heart. With the occurrence of a decrease in glucose utilization, D55-A hearts demonstrated an increase in cardiac palmitate oxidation (Fig. 2-1A, lower panel).

In tissues with high FA metabolism like the heart, PPAR- α is highly expressed. Once activated, PPAR- α promotes expression of genes that regulate FA oxidation at various steps (21). Interestingly, in spite of the increase in FA oxidation, no significant change in cardiac PPAR- α , CPT-1, ACO, MCD, or CD36 gene expression was observed in D55-A hearts (Fig. 2-1B). AMP activated protein kinase (AMPK) also plays a key role in the regulation of FA utilization. In the heart, AMPK facilitates FA utilization through its control of acetyl-CoA carboxylase (ACC). As ACC catalyzes the conversion of acetyl-CoA to malonyl-CoA, AMPK by inhibiting ACC is able to decrease malonyl-CoA and

minimize its inhibition of FA oxidation. Measurement of AMPK and ACC revealed that both AMPK (Fig. 2-2A) and ACC (Fig. 2-2B) phosphorylation were significantly higher in D55-A hearts. As extracellular hormones such as insulin are known to inhibit AMPK, this activation of AMPK was not surprising. Indeed, injection of insulin into D55-A animals reversed both AMPK and ACC phosphorylation (Fig. 2-2A and 2-2B). Reversal of AMPK and ACC phosphorylation by insulin also suggests that these observed changes are a consequence of diabetes, and not the direct effects of STZ on the heart.

2.3.2 Control of cardiac substrate utilization in chronic (D55-C) diabetes

Extending the duration of diabetes to 6 weeks sustained weight loss (control 494 ± 7 , D55-C 440 ± 8 g; $P < 0.05$) and hyperglycemia (control 5.7 ± 0.3 , D55-C 26 ± 1 mM; $P < 0.05$). Unexpectedly, AMPK and ACC (Fig. 2-3A) phosphorylation were comparable in control and D55-C hearts. In the absence of AMPK and ACC activation, these chronic diabetic hearts exhibit an increased palmitate oxidation rate along with a reduction in glucose oxidation (Fig. 2-4A). To determine the mechanisms that may be responsible for this altered cardiac metabolism, we measured gene expression of PPAR- α and its downstream targets. Although no change was observed in PPAR- α , downstream targets of this nuclear receptor like CPT-1, MCD, CD36 and ACO all showed increased gene expression (Fig. 2-4B).

2.3.3 Changes in plasma and heart lipids in D55-A and D55-C diabetic rats

FA has been reported to influence AMPK activation (22). During diabetes, excessive lipolysis and loss of adipose tissue mass results in increases in both serum FA and TG. Indeed, both plasma FA and TG levels were elevated in D55-C animals (Fig. 2-3B). Similar to changes in plasma lipids, D55-C rats also demonstrated an increase in total

cardiac FA and TG (Fig. 2-3B), indicating a cardiac lipid overload in these animals. Interestingly, measurement of these parameters in D55-A plasma and heart showed no significant difference when compared to control (Fig. 2-3B). We also determined the individual FA composition in hearts from D55-A and D55-C animals. Linoleic, oleic, palmitic and arachidonic acid levels were significantly higher, only in the hearts from chronic 6-week diabetic rats (Table 2-2), and could potentially be responsible for the absence of AMPK activation in these hearts.

2.3.4 Influence of lipids on AMPK activation

Given the probable relationship between lipids and AMPK activation, we used two strategies to validate this association. In the first experiment, we induced severe diabetes by injecting animals with 100 mg/kg STZ, and terminated the animals after 4 days of diabetes. Our goal was to provoke both hyperglycemia and hyperlipidemia in these diabetic animals. Compared to D55-A, D100-A animals had the lowest body weight at the time of death (Table 2-1). D100-A rats also displayed a greater loss of insulin, and higher plasma glucose when compared to D55-A (Table 2-1). In addition, these acute diabetic animals were characterized by amplification in both plasma and cardiac FA and TG (Table 2-2 and Fig. 2-5B), results similar to those observed with chronic D55-C rats. In D100-A, oxidation of exogenous glucose was almost obliterated (control 542 ± 36 , D100-A 22 ± 7 nmol/min/g dry wt; $P < 0.05$), whereas palmitate oxidation increased further (control 923 ± 115 , D100-A 2692 ± 192 nmol/min/g dry wt; $P < 0.05$). To determine whether this increase in FA oxidation is regulated by AMPK activation, cardiac AMPK and ACC phosphorylation was also measured in D100-A diabetic hearts. Similar to the observations in D55-C, there was no difference in cardiac AMPK and ACC

phosphorylation in D100-A rats compared to control (Fig. 2-5A). This lack of AMPK activation in D100-A correlated well with augmented plasma and cardiac FA and TG in these animals.

An alternate strategy used the infusion of IL to control rats to enlarge circulating FA. 1% and 5% IL increased plasma FA to levels similar to those observed with D55-C and D100-A rats (Fig. 2-6A). Measurement of AMPK and ACC phosphorylation revealed that their phosphorylation was inhibited by acute intralipid infusion (Fig. 2-6B). To examine if IL per se is capable of reducing AMPK activation observed in D55-A hearts, some animals from this group were infused with 1% IL. Interestingly, with the rise in plasma FA and TG in these animals (Fig. 2-7A), cardiac AMPK phosphorylation was lowered (Fig. 2-7B).

2.4. DISCUSSION

In the present study, our data for the first time revealed activation of AMPK (as evidenced by elevated AMPK and ACC phosphorylation) in hearts from acute D55-A diabetic rats. AMPK can be activated by both ATP dependent and independent mechanisms (23). At present, the contribution of ATP in modulating AMPK in these hearts is unresolved. Regarding ATP independent mechanisms, insulin is known to inhibit cardiac AMPK, and in vitro perfusion of hearts in the absence of insulin showed higher AMPK phosphorylation than perfusion in the presence of this hormone (24; 25). Given that the level of insulin declines within 24 hours of STZ administration (18), and that a single injection of this hormone to D55-A diabetic rats normalized both cardiac AMPK and ACC phosphorylation, our results suggest that following acute diabetes, reduction in insulin may be a key regulator of cardiac AMPK.

Insulin is the primary hormone that controls glucose uptake and oxidation, and STZ induced reduction in insulin would compromise cardiac glucose utilization. Indeed, glucose utilization was compromised in D55-A hearts that were forced to switch to using higher levels of FA. The mechanisms underlying this change towards increased FA utilization in acute D55-A diabetic hearts is unclear. In chronic diabetes, activation of PPAR- α is believed to promote FA oxidation (3). To determine whether PPAR- α is activated and contributes to high cardiac FA oxidation in acute D55-A animals, we measured gene expression of cardiac PPAR- α and its targets, CPT-1, ACO, MCD and CD36. Interestingly, we did not observe any change in expression of genes in these animals. Given that augmented FA and its metabolites activate PPAR- α (26), we also assessed plasma and cardiac FA and TG. D55-A diabetes did not change plasma and

cardiac lipids, and this could explain the absence of PPAR- α activation in these animals. Using real-time PCR, a previous study has also reported that following 1 week of STZ, no change in expression of PPAR- α and CPT-1 were observed (27). Taken together, our results indicate that mechanisms other than PPAR- α activation promote FA oxidation in acute D55-A diabetic hearts. Given that cardiac AMPK was activated in these animals, it is likely that through phosphorylation and inhibition of ACC, this arrangement may contribute towards the increase in cardiac FA oxidation. As ACC controls conversion of acetyl-CoA to malonyl-CoA (15) which inhibits CPT-1, the rate limiting enzyme regulating transfer of FA into the mitochondria, inhibition of ACC decreases malonyl-CoA production, therefore relieving CPT-1 inhibition, and promoting FA oxidation (28). This acute adaptation via AMPK activation would ensure adequate cardiac energy production, when glucose utilization is compromised. It should be noted that a previous study from our laboratory has reported that coronary luminal lipoprotein lipase (LPL), the rate-limiting enzyme that breaks down lipoprotein triglyceride to FA, is acutely increased following STZ induced diabetes (D55-A) (29). It is possible that when plasma TG and FA remain unchanged in D55-A, this increase in LPL is an additional adaptation to increase FA supply to the diabetic heart.

To examine whether cardiac AMPK activation persists following chronic diabetes, D55-C rats were kept for 6 weeks. Despite the presence of hypoinsulinemia in these rats, AMPK and ACC phosphorylation remained unchanged compared to control. Similar results of unchanged AMPK and ACC activity in control and chronic 6-week diabetic hearts have also been previously reported (30). One striking difference between acute and chronic diabetes was the occurrence of hyperlipidemia and augmented cardiac FA

and TG, only in chronic D55-C diabetes. Additionally, measurement of individual cardiac FA species revealed that only chronic D55-C diabetic animals exhibit higher linoleic, oleic, palmitic and arachidonic acid levels. This data suggest that accumulation of intracellular FA following chronic diabetes potentially counteracts cardiac AMPK activation seen after acute hypoinsulinemia. The mechanisms that mediate such an action are currently unclear. Interestingly, a recent study has demonstrated that long chain acyl-CoA esters prevent AMPK phosphorylation by the upstream kinase AMPKK (22). In another study using ob/ob mice or ZDF rats, decreased cardiac AMPK phosphorylation was found to be associated with augmented lipid oversupply and overexpression of protein phosphatase 2C, which is known to dephosphorylate and inactivate AMPK (31). Treating these animals with troglitazone or rosiglitazone normalized plasma lipids, reduced protein phosphatase 2C expression, and increased cardiac AMPK phosphorylation. Finally, in insulin resistant JCR:LA-cp rats where cardiac TG content is increased by 50%, no significant difference in AMPK activity was noted (32).

Given the apparent link between lipids and cardiac AMPK, we used two strategies to confirm this association. Initially, we made animals severely diabetic by injecting higher doses of STZ to produce absolute insulin deficiency, severe hyperglycemia, and enlargement in both plasma and cardiac FA and TG levels. Associated with this augmented lipids, AMPK remained unchanged in these acute but severely diabetic animals. Another approach used IL infusion of control and D55-A rats to increase circulating TG and FA. Measurement of cardiac AMPK and ACC phosphorylation revealed that IL lowered phosphorylation of AMPK and ACC in control rat hearts. More importantly, the high AMPK activation observed in D55-A hearts was reversed by 1% IL

infusion for four hours. Taken together, our data suggest that accumulation of FA could negatively influence the AMPK cascade. In this regard, a recent study has suggested that the ability of insulin to inhibit AMPK activity is lost in the presence of high concentrations of FA (33). It should be noted that other studies have reported activation of AMPK by FA (34). The reason for this disagreement may be explained by the quantity of FA (low concentrations that varied from 0.075-0.8 mM) used in these studies, and the duration of lipid overload (hearts were perfused with FA for 1 hr, cells were incubated with FA for 24 hr, or animals were fasted for 24 hr to increase plasma FA). Given that intracellular FA or TG were not measured in these studies, and that AMPK activation was not determined following chronic treatment, it is likely that intracellular FA levels have dual effects on AMPK activation.

In the absence of AMPK activation in hearts from D55-C animals, it is likely that the increased FA oxidation in these animals is through PPAR- α . Indeed, measurement of gene expression in D55-C hearts revealed increased expression of the downstream targets of PPAR- α (CPT-1, MCD, CD36 and ACO). As previous studies have demonstrated that augmented intracellular FA activates PPAR- α , with subsequent overexpression of genes involved in FA utilization, (35) it is possible that in the present study, augmented plasma and cardiac FA and TG may activate PPAR- α , leading to increased expression of its downstream targets.

In summary, we document that the control of myocardial fatty acid metabolism fluctuates with the intensity of insulin-deficient diabetes. In hyperglycemia and hypoinsulinemia, without any changes in plasma or cardiac FA, AMPK is activated. This activation of AMPK likely increases FA oxidation through phosphorylation and

inhibition of ACC. Given that glucose utilization is compromised under these conditions, this adaptation would ensure adequate cardiac energy production. In severe diabetes, the additional drop in insulin initiates changes in both carbohydrate and lipids. With the addition of augmented plasma and heart lipids, AMPK activation is prevented, and control of FA oxidation is likely through PPAR- α . Whether this negative effect of FA on AMPK activation contributes to diabetic heart disease requires further studies. In patients with diabetes, the rate of mortality following a myocardial infarction is almost twice that compared to non-diabetics (36). AMPK plays an important role in preventing cardiac ischemic/reperfusion damage (37; 38). Thus, when hearts from AMPK knockout animals were exposed to ischemia/reperfusion, they showed poor cellular energy control, severe cell damage, and inadequate functional recovery compared to hearts from wild type animals. It is possible that in these diabetic hearts, the accelerated damage observed during exposure to ischemia/reperfusion could be a likely outcome of a compromised activation of AMPK (39).

2.5 TABLES AND FIGURES

Table 2-1 General characteristics of the experimental animals

	STZ-DIABETES		
	CONTROL	D55-A	D100-A
Body Weight (g)	319 ± 2	298 ± 4*	277 ± 13.9*
Plasma Glucose (mM)	5.8 ± 0.5	22 ± 1.1*	28 ± 0.5* [†]
Plasma Insulin (ng/ml)	2.4 ± 0.13	0.93 ± 0.04*	0.60 ± 0.02* [†]

Diabetes was induced with either 55 (D55) or 100 (D100) mg/kg streptozotocin (STZ). Following termination, animals from all groups were killed, blood collected and plasma separated for measurement of various parameters. Values are mean ± SE for 6 animals in each group. *Significantly different from control; [†]Significantly different from D55-A; *P*<0.05. A=Four days of acute diabetes.

Table 2-2 Effects of diabetes on cardiac fatty acid composition

	STZ DIABETES			
	CONTROL	D55-A	D55-C	D100-A
Linoleic acid (18:2n6)	0.33 ± 0.03	0.41 ± 0.02	0.86 ± 0.10*	0.83 ± 0.11*
Oleic acid (18:1n9)	0.29 ± 0.03	0.29 ± 0.02	0.93 ± 0.12*	0.68 ± 0.11*
Palmitic acid (16:0)	0.39 ± 0.04	0.47 ± 0.02	0.64 ± 0.07*	0.70 ± 0.05*
Arachidonic Acid (20:4n6)	0.013 ± 0.001	0.019 ± 0.001	0.027 ± 0.001*	0.021 ± 0.001*

Diabetes was induced with either 55 (D55) or 100 (D100) mg/kg streptozotocin (STZ). Following termination, cardiac free fatty acids were extracted with chloroform-methanol-acetone-hexane solvent, converted to their respective methyl esters, and separated by gas chromatography. Values are mean ± SE of 3-4 rats in each group and are expressed as micrograms per milligram protein. * $P < 0.05$ vs. control only. A=Four days of acute diabetes; C=Six weeks of chronic diabetes.

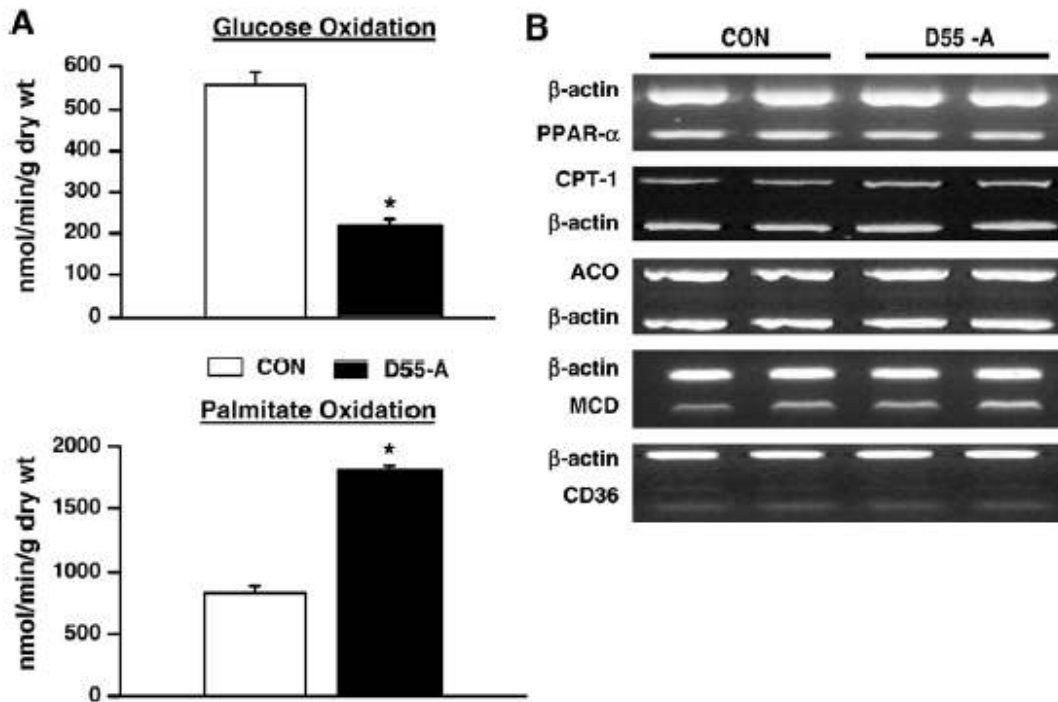


Fig. 2-1 Cardiac glucose and palmitate oxidation in STZ treated hearts. 4 days after control rats were treated with 55 mg/kg STZ, animals were killed and hearts collected. Isolated hearts were perfused in the working mode for 1h (preload of 11.5 mmHg; afterload of 80 mmHg), and rates of glucose (2-1A, top panel) and palmitate (2-1A, lower panel) oxidation determined. Mean steady state rates of substrate oxidation were determined from data obtained during the initial portion of the heart perfusion, and from samples of perfusate and hyamine hydroxide taken every 10 min. Results are the means \pm SE of 6 rats in each group. CON-control; D55-A, acute four days diabetes induced by 55 mg/kg STZ. *Significantly different from control; $P < 0.05$. Gene expression of PPAR- α , CPT-1, ACO, MCD, and CD36 in 4-day 55 mg/kg STZ diabetic hearts is depicted in Fig. 2-1B. Hearts from control and 4-day STZ diabetic animals were removed and immediately snap frozen in liquid nitrogen. Gene expression of PPAR- α , CPT-1, ACO, MCD, and CD36 were measured using rt-PCR. Data are means \pm SE; $n=3$. t-test was used to determine differences between means. CON-control; D55-A, acute four days diabetes induced by 55 mg/kg STZ.

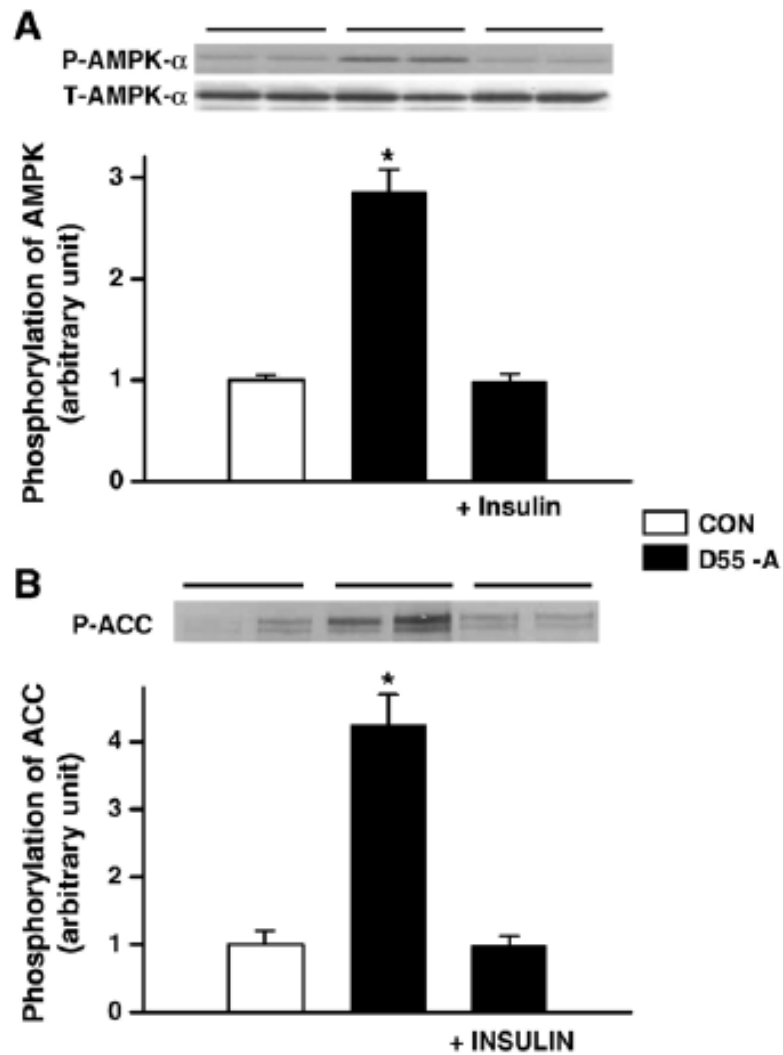


Fig. 2-2 Cardiac AMPK and ACC phosphorylation in 4-day 55 mg/kg STZ diabetic hearts. Hearts from control, 4-day STZ diabetic rats, or diabetic animals treated with insulin were removed and immediately snap frozen in liquid nitrogen. AMPK- α (total and phosphorylated) (A) and phospho-ACC (B) were measured using Western Blotting. Data are means \pm SE; n=4. One-way ANOVA followed by the Tukey test was used to determine differences between means. *Significantly different from other groups, $P < 0.05$. CON-control; D55-A, acute four days diabetes induced by 55 mg/kg STZ.

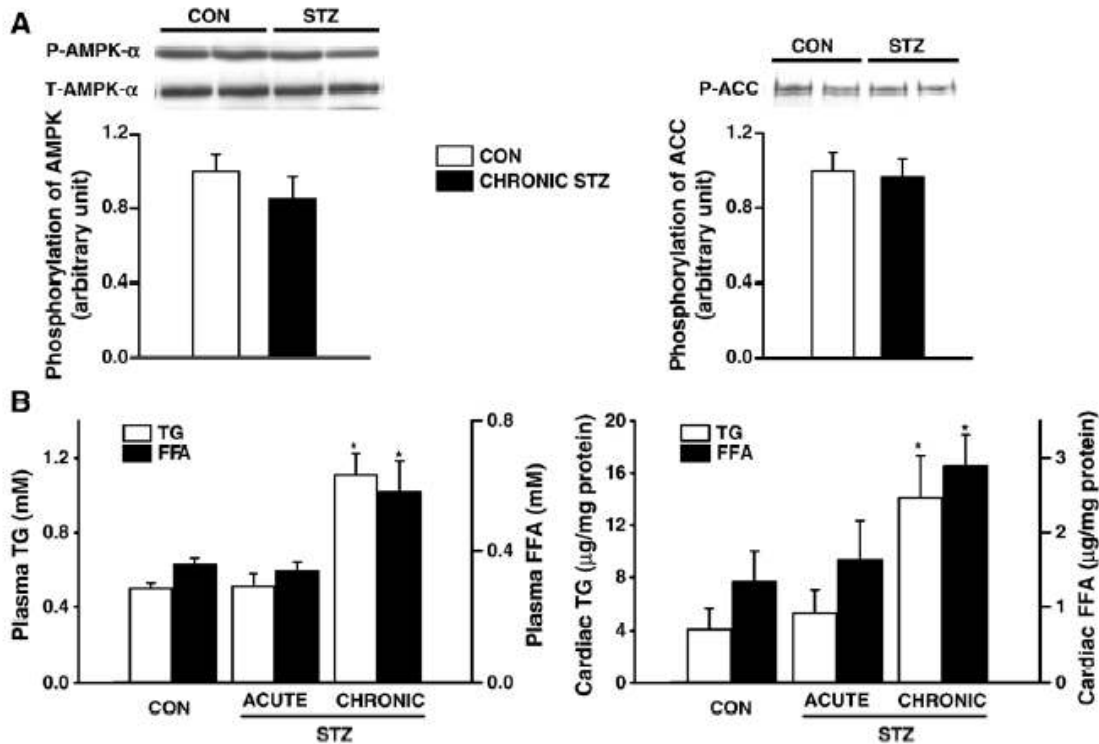


Fig. 2-3 Cardiac AMPK and ACC phosphorylation and plasma and cardiac lipids. Hearts from control and chronic 6 weeks STZ diabetic rats were removed and immediately snap frozen in liquid nitrogen. AMPK- α (total and phosphorylated) (A, left panel) and phospho-ACC (A, right panel) were measured using Western Blotting. Data are means \pm SE; $n=4$. t-test was used to determine differences between means. CON-control; D55-C, chronic 6 weeks diabetes induced by 55 mg/kg STZ. Plasma and cardiac lipids were also determined subsequent to different durations of diabetes. At termination, blood samples were obtained from the tail vein, and plasma separated and assayed for triglycerides (TG) and non-esterified fatty acids (FFA) using diagnostic kits (B, left panel). Cardiac TG and fatty acids (FA) were extracted with chloroform:methanol:acetone:hexane solvent, and determined using HPLC (B, right panel). Results are the means \pm SE of 4 rats in each group. CON-control; D55-diabetes induced by 55 mg/kg STZ; acute-four days of diabetes; chronic-six weeks of diabetes. One-way ANOVA followed by the Tukey test was used to determine differences between means. *Significantly different from all other groups; $P < 0.05$.

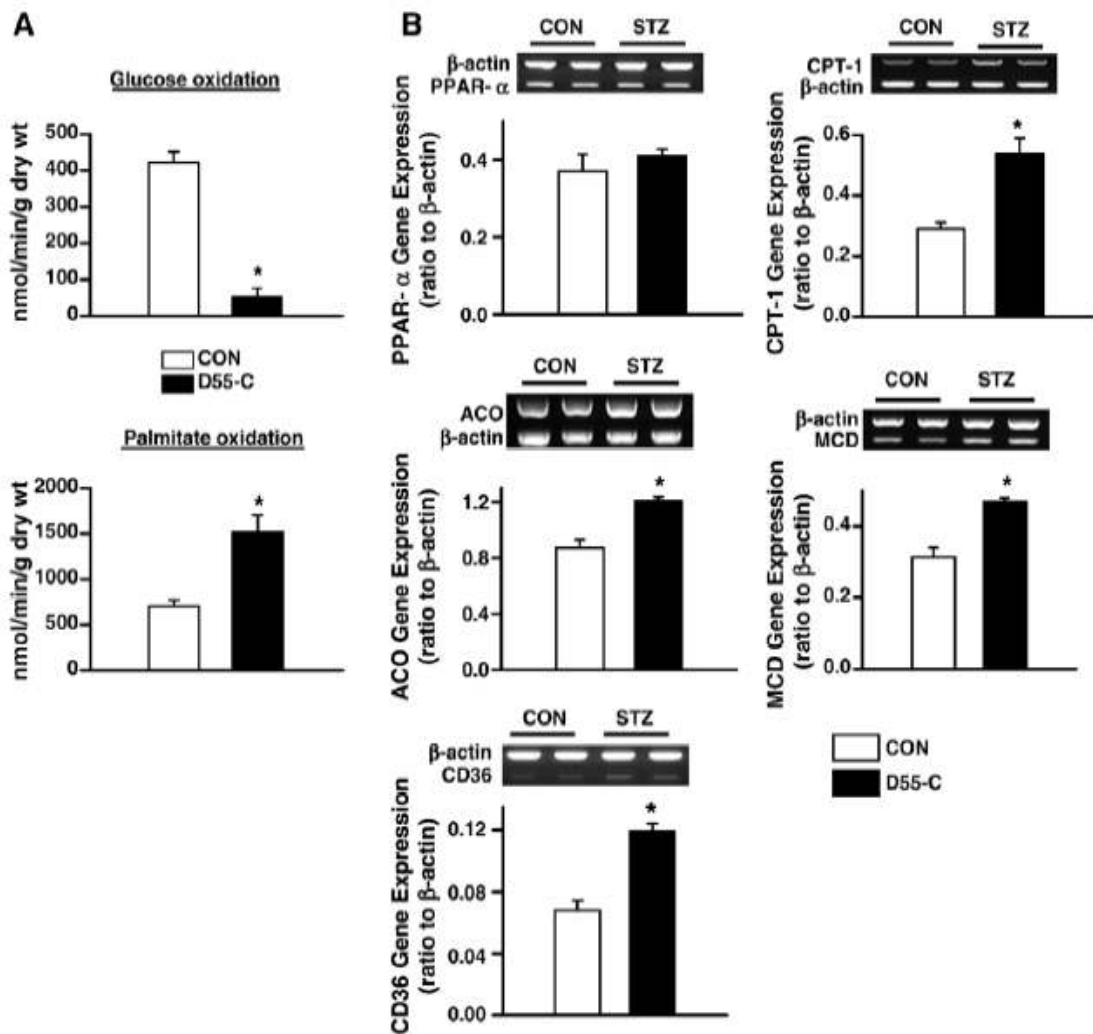


Fig. 2-4 Cardiac glucose and palmitate oxidation in chronic STZ diabetic hearts. Six weeks after control rats were treated with 55 mg/kg STZ, animals were killed and hearts collected. Isolated hearts were perfused in the working mode for 1h (preload of 11.5 mmHg; afterload of 80 mmHg), and rates of glucose (2-3A, top panel) and palmitate (2-3A, lower panel) oxidation determined. Results are the means \pm SE of 5 rats in each group. CON-control; D55-C, chronic six weeks diabetes induced by 55 mg/kg STZ. *Significantly different from control; $P < 0.05$. Gene expression of PPAR- α , CPT-1, ACO, MCD, and CD36 in 6-week 55 mg/kg STZ diabetic hearts is depicted in Fig. 2-3B. Hearts from control and 6-week STZ diabetic animals were removed and immediately snap frozen in liquid nitrogen. Gene expression was measured using rt-PCR. CON-control; D55-C, chronic six weeks diabetes induced by 55 mg/kg STZ.

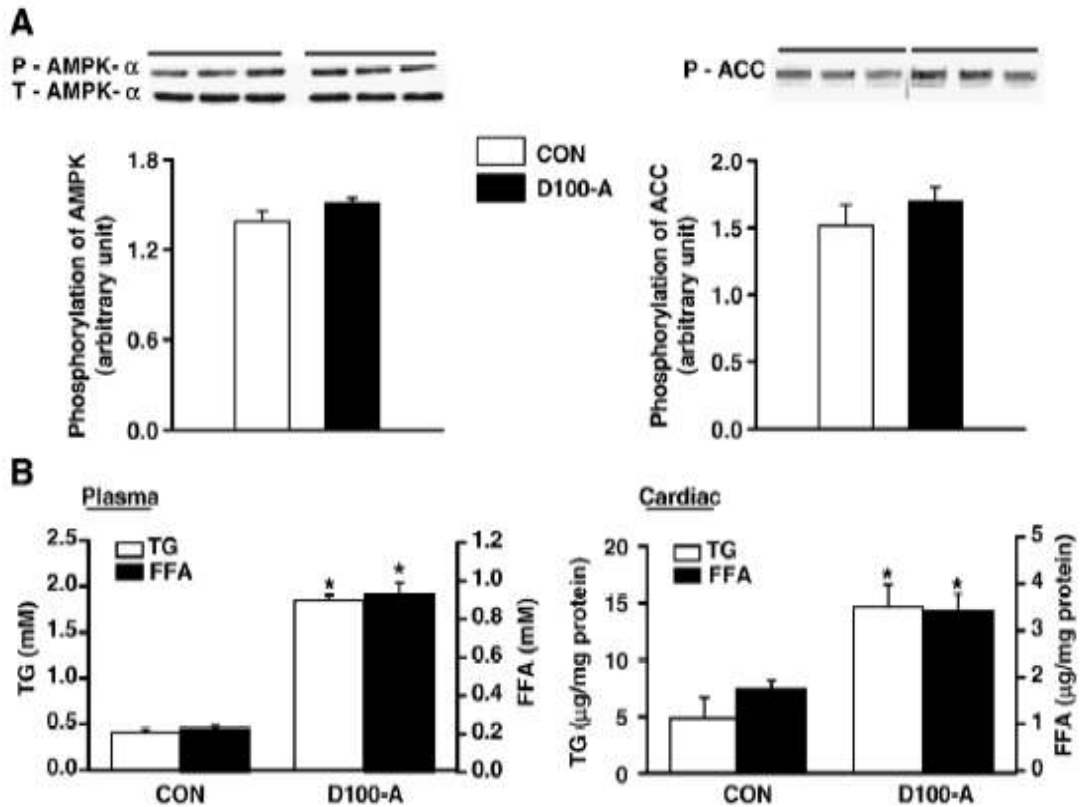


Fig. 2-5 Cardiac AMPK and ACC phosphorylation and plasma and cardiac lipids in 4-day 100 mg/kg STZ diabetic hearts. Hearts from control and acute four-day 100 mg/kg STZ diabetic rats were removed and immediately snap frozen in liquid nitrogen. AMPK- α (total and phosphorylated) (A, left panel) and phospho-ACC (A, right panel) were measured using Western Blotting. Plasma and cardiac lipids were also determined in these severely diabetic rats. At termination, blood samples were obtained from the tail vein, and plasma separated and assayed for triglycerides (TG) and non-esterified fatty acids (FFA) using diagnostic kits (B, left panel). Cardiac TG and fatty acids (FA) were extracted with chloroform:methanol:acetone:hexane solvent, and determined using HPLC (B, right panel). Data are means \pm SE; $n=4$. CON-control; D100-A, acute four-day diabetes induced by 100 mg/kg STZ. t-test was used to determine differences between means. *Significantly different from control; $P < 0.05$.

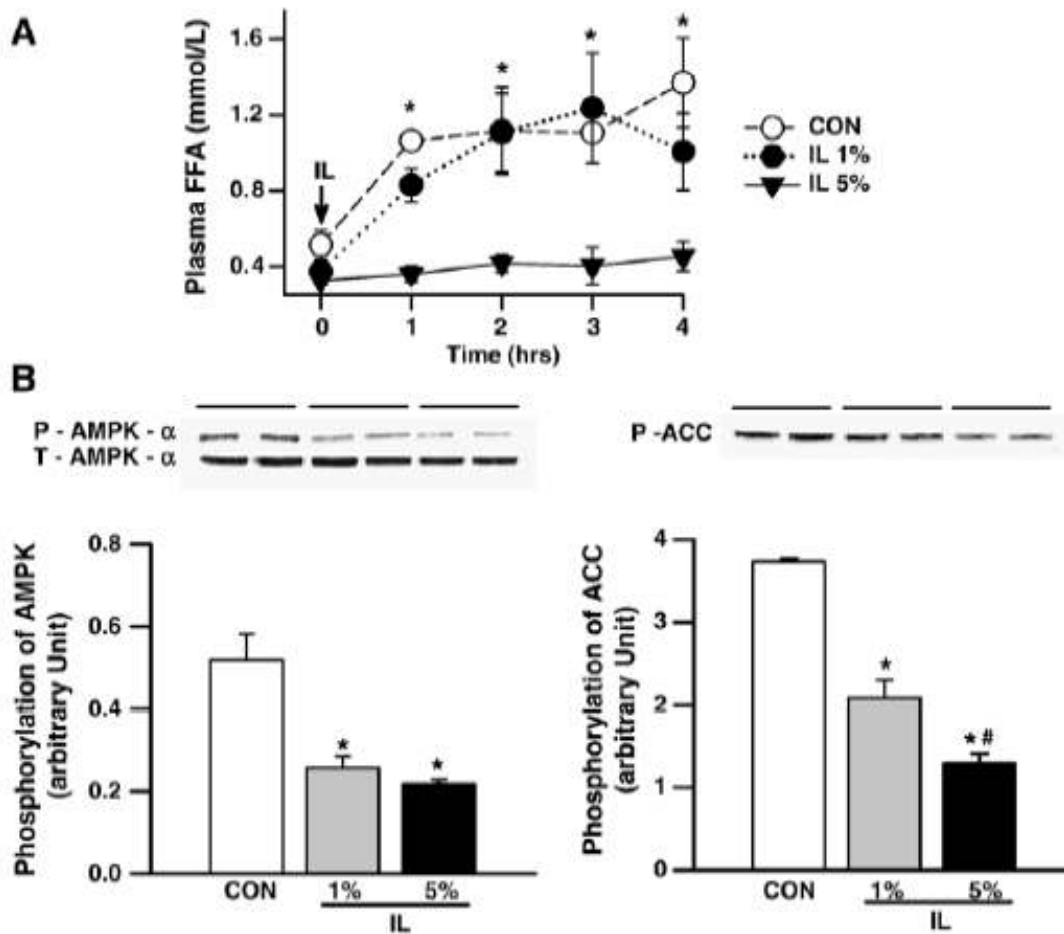


Fig. 2-6 Effects of intralipid on cardiac AMPK and ACC phosphorylation. Control rats were anaesthetized and the left jugular vein cannulated. Intralipid (IL, 1% and 5%; 1.2 ml/kg/h) was infused over a period of 4h, with blood samples collected every hour from the tail vein for measurement of plasma FFA (A). After 4h of IL infusion, hearts were removed and immediately snap frozen in liquid nitrogen. AMPK- α (total and phosphorylated) (B, left panel) and phospho-ACC (B, right panel) were measured using Western Blotting. Data are mean \pm SE for 4 rats in each group. Two-way ANOVA followed by the Tukey test was used to determine differences between means. *Significantly different from control; $P < 0.05$. #Significantly different from 1% IL; $P < 0.05$.

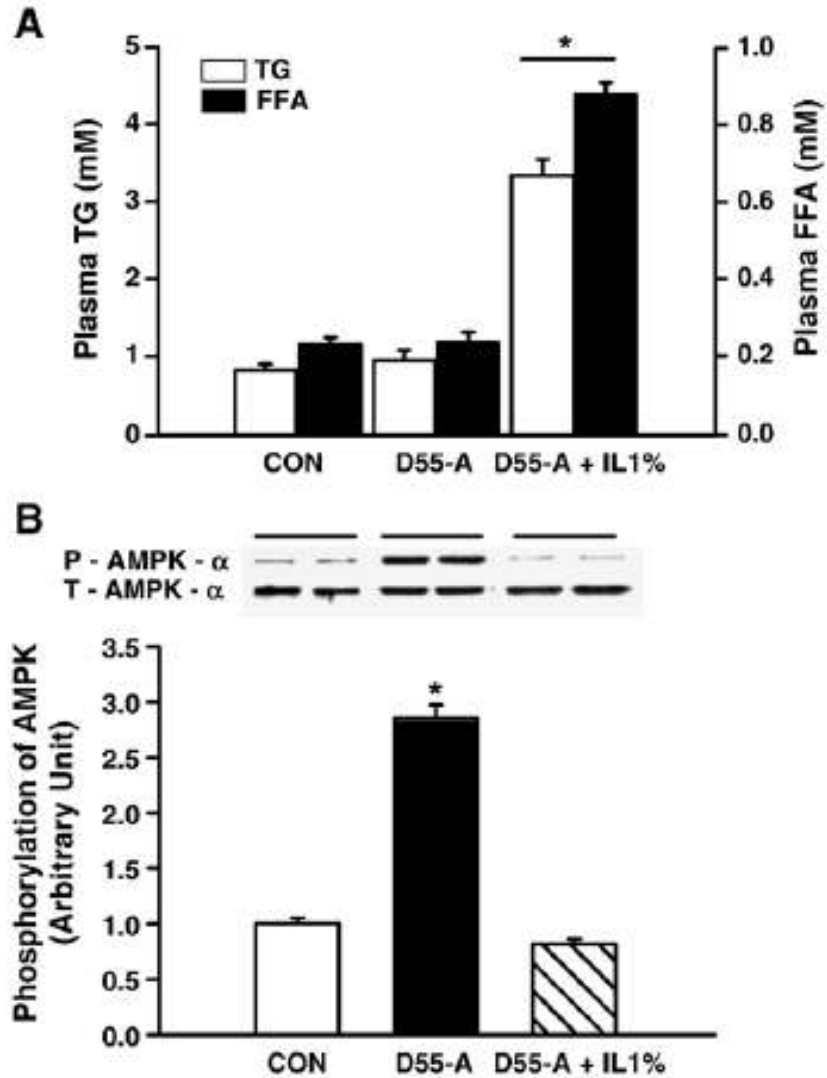


Fig. 2-7 Effects of intralipid on cardiac AMPK phosphorylation in acute D55-A diabetic rats. Acute D55-A rats were anaesthetized and the left jugular vein cannulated. Intralipid (IL, 1%; 1.2 ml/kg/h) was infused over a period of 4h, at which time the animals were killed. Prior to termination, blood samples were collected from the tail vein for measurement of plasma FFA and TG (A, top panel). Data are mean \pm SE for 4 rats in each group. One-way ANOVA followed by the Tukey test was used to determine differences between means. *Significantly different from all other groups; $P < 0.05$. CON-control; D55-A, acute four days diabetes induced by 55 mg/kg STZ; D55-A + IL 1%, acute four days diabetes induced by 55 mg/kg STZ perfused with 1% IL for four hours. After 4h of IL infusion, hearts were removed and immediately snap frozen in liquid nitrogen. AMPK- α (total and phosphorylated) (B, lower panel) was measured using Western Blotting. Data are mean \pm SE for 4 rats in each group. One-way ANOVA was used to determine differences between means. *Significantly different from D55-A; $P < 0.05$. D55-A, acute four days diabetes induced by 55 mg/kg STZ; D55-A + IL 1%, acute four days diabetes induced by 55 mg/kg STZ perfused with 1% IL for four hours.

2.6 BIBLIOGRAPHY

1. Rodrigues B, McNeill JH. The diabetic heart: metabolic causes for the development of a cardiomyopathy. *Cardiovasc Res* 1992;26:913-922.
2. Randle PJ, Garland PB, Hales CN, Newsholme EA. The glucose fatty-acid cycle. Its role in insulin sensitivity and the metabolic disturbances of diabetes mellitus. *Lancet* 1963;1:785-789.
3. Finck BN, Lehman JJ, Leone TC, Welch MJ, Bennett MJ, Kovacs A, Han X, Gross RW, Kozak R, Lopaschuk GD, Kelly DP. The cardiac phenotype induced by PPARalpha overexpression mimics that caused by diabetes mellitus. *J Clin Invest* 2002;109:121-130.
4. Martin G, Schoonjans K, Lefebvre AM, Staels B, Auwerx J. Coordinate regulation of the expression of the fatty acid transport protein and acyl-CoA synthetase genes by PPARalpha and PPARgamma activators. *J Biol Chem* 1997;272:28210-28217.
5. Brandt JM, Djouadi F, Kelly DP. Fatty acids activate transcription of the muscle carnitine palmitoyltransferase I gene in cardiac myocytes via the peroxisome proliferator-activated receptor alpha. *J Biol Chem* 1998;273:23786-23792.
6. Varanasi U, Chu R, Huang Q, Castellon R, Yeldandi AV, Reddy JK. Identification of a peroxisome proliferator-responsive element upstream of the human peroxisomal fatty acyl coenzyme A oxidase gene. *J Biol Chem* 1996;271:2147-2155.
7. Hardie DG. Minireview: the AMP-activated protein kinase cascade: the key sensor of cellular energy status. *Endocrinology* 2003;144:5179-5183.
8. Horman S, Browne G, Krause U, Patel J, Vertommen D, Bertrand L, Lavoinnie A, Hue L, Proud C, Rider M. Activation of AMP-activated protein kinase leads to the

phosphorylation of elongation factor 2 and an inhibition of protein synthesis. *Curr Biol*, 2002, 12:1419-1423.

9. Hayashi T, Hirshman MF, Fujii N, Habinowski SA, Witters LA, Goodyear LJ. Metabolic stress and altered glucose transport: activation of AMP-activated protein kinase as a unifying coupling mechanism. *Diabetes* 2000;49:527-531.

10. Marsin AS, Bertrand L, Rider MH, Deprez J, Beauloye C, Vincent MF, Van den Berghe G, Carling D, Hue L. Phosphorylation and activation of heart PFK-2 by AMPK has a role in the stimulation of glycolysis during ischaemia. *Curr Biol* 2000;10:1247-1255.

11. Kudo N, Barr AJ, Barr RL, Desai S, Lopaschuk GD. High rates of fatty acid oxidation during reperfusion of ischemic hearts are associated with a decrease in malonyl-CoA levels due to an increase in 5'-AMP-activated protein kinase inhibition of acetyl-CoA carboxylase. *J Biol Chem* 1995;270:17513-17520.

12. Kudo N, Gillespie JG, Kung L, Witters LA, Schulz R, Clanachan AS, Lopaschuk GD. Characterization of 5'AMP-activated protein kinase activity in the heart and its role in inhibiting acetyl-CoA carboxylase during reperfusion following ischemia. *Biochim Biophys Acta* 1996;1301:67-75.

13. Luiken JJ, Coort SL, Willems J, Coumans WA, Bonen A, van der Vusse GJ, Glatz JF. Contraction-induced fatty acid translocase/CD36 translocation in rat cardiac myocytes is mediated through AMP-activated protein kinase signaling. *Diabetes* 2003;52:1627-1634.

14. An D, Pulinilkunnil T, Qi D, Ghosh S, Abrahani A, Rodrigues B. The metabolic "switch" AMPK regulates cardiac heparin-releasable lipoprotein lipase. *Am J Physiol Endocrinol Metab* 2005;288:246-253.

- 15 Kudo N, Gillespie JG, Kung L, Witters LA, Schulz R, Clanachan AS, Lopaschuk GD. Characterization of 5'AMP-activated protein kinase activity in the heart and its role in inhibiting acetyl-CoA carboxylase during reperfusion following ischemia. *Biochim Biophys Acta* 1996;1301:67-75.
- 16 Soltys CL, Kovacic S, Dyck JR. Activation of cardiac AMP-activated protein kinase by LKB1 expression or chemical hypoxia is blunted by increased Akt activity. *Am J Physiol Heart Circ Physiol* 2006;290:H2472-2479.
- 17 Coven DL, Hu X, Cong L, Bergeron R, Shulman GI, Hardie DG, Young LH. Physiological role of AMP-activated protein kinase in the heart: graded activation during exercise. *Am J Physiol Endocrinol Metab* 2003;285:E629-636.
- 18 Sambandam N, Abrahani MA, St Pierre E, Al-Atar O, Cam MC, Rodrigues B. Localization of lipoprotein lipase in the diabetic heart: regulation by acute changes in insulin. *Arterioscler Thromb Vasc Biol* 1999;19:1526-1534.
- 19 Ghosh S, Qi D, An D, Pulinilkunnil T, Abrahani A, Kuo KH, Wambolt RB, Allard M, Innis SM, Rodrigues B. Brief episode of STZ-induced hyperglycemia produces cardiac abnormalities in rats fed a diet rich in n-6 PUFA. *Am J Physiol Heart Circ Physiol* 2004;287:H2518-2527.
- 20 Stanley WC, Recchia FA, Lopaschuk GD. Myocardial substrate metabolism in the normal and failing heart. *Physiol Rev* 2005;85:1093-1129.
- 21 Huss JM, Kelly DP. Nuclear receptor signaling and cardiac energetics. *Circ Res* 2004;95:568-578.

- 22 Taylor EB, Ellingson WJ, Lamb JD, Chesser DG, Winder WW. Long-chain acyl-CoA esters inhibit phosphorylation of AMP-activated protein kinase at threonine-172 by LKB1/STRAD/MO25. *Am J Physiol Endocrinol Metab* 2005;288:E1055-1061.
- 23 Kahn BB, Alquier T, Carling D, Hardie DG. AMP-activated protein kinase: ancient energy gauge provides clues to modern understanding of metabolism. *Cell Metab* 2005;1:15-25.
- 24 Beauloye C, Marsin AS, Bertrand L, Krause U, Hardie DG, Vanovershelde JL, Hue L. Insulin antagonizes AMP-activated protein kinase activation by ischemia or anoxia in rat hearts, without affecting total adenine nucleotides. *FEBS Lett* 2001;505:348-352.
- 25 Kovacic S, Soltys CL, Barr AJ, Shiojima I, Walsh K, Dyck JR. Akt activity negatively regulates phosphorylation of AMP-activated protein kinase in the heart. *J Biol Chem* 2003;278:39422-39427.
- 26 Kliewer SA, Sundseth SS, Jones SA, Brown PJ, Wisely GB, Koble CS, Devchand P, Wahli W, Willson TM, Lenhard JM, Lehmann JM. Fatty acids and eicosanoids regulate gene expression through direct interactions with peroxisome proliferator-activated receptors alpha and gamma. *Proc Natl Acad Sci U S A* 1997;94:4318-4323.
- 27 Depre C, Young ME, Ying J, Ahuja HS, Han Q, Garza N, Davies PJ, Taegtmeyer H. Streptozotocin-induced changes in cardiac gene expression in the absence of severe contractile dysfunction. *J Mol Cell Cardiol* 2000;32:985-996.
- 28 Saddik M, Gamble J, Witters LA, Lopaschuk GD. Acetyl-CoA carboxylase regulation of fatty acid oxidation in the heart. *J Biol Chem* 1993;268:25836-25845.
- 29 Pulinilkunnil T, Abrahani A, Varghese J, Chan N, Tang I, Ghosh S, Kulpa J, Allard M, Brownsey R, Rodrigues B. Evidence for rapid "metabolic switching" through

lipoprotein lipase occupation of endothelial-binding sites. *J Mol Cell Cardiol* 2003; 35:1093-103.

30 Sakamoto J, Barr RL, Kavanagh KM, Lopaschuk GD. Contribution of malonyl-CoA decarboxylase to the high fatty acid oxidation rates seen in the diabetic heart. *Am J Physiol Heart Circ Physiol* 2000;278:196-204.

31 Wang MY, Unger RH. Role of PP2C in cardiac lipid accumulation in obese rodents and its prevention by troglitazone. *Am J Physiol Endocrinol Metab* 2005;288:E216-221.

32 Atkinson LL, Kozak R, Kelly SE, Onay Besikci A, Russell JC, Lopaschuk GD. Potential mechanisms and consequences of cardiac triacylglycerol accumulation in insulin-resistant rats. *Am J Physiol Endocrinol Metab* 2003;284:E923-930.

33 Folmes CD, Clanachan AS, Lopaschuk GD. Fatty acids attenuate insulin regulation of 5'-AMP-activated protein kinase and insulin cardioprotection after ischemia. *Circ Res* 2006;99:61-68.

34 Clark H, Carling D, Saggerson D. Covalent activation of heart AMP-activated protein kinase in response to physiological concentrations of long-chain fatty acids. *Eur J Biochem* 2004;271:2215-2224.

35 Finck, B.N. Lehman JJ, Leone TC, Welch MJ, Bennett MJ, Kovacs A, Han X, Gross RW, Kozak R, Lopaschuk GD, Kelly DP. The cardiac phenotype induced by PPARalpha overexpression mimics that caused by diabetes mellitus. *J Clin Invest* 2002 109;121-30.

36 Stone PH, Muller JE, Hartwell T, York BJ, Rutherford JD, Parker CB et al. The effect of diabetes mellitus on prognosis and serial left ventricular function after acute myocardial infarction: contribution of both coronary disease and diastolic left ventricular

dysfunction to the adverse prognosis. The MILIS Study Group. *J Am Coll Cardiol* 1989;14:49-57.

37 Russell RR, 3rd, Li J, Coven DL, Pypaert M, Zechner C, Palmeri M, Giordano FJ, Mu J, Birnbaum MJ, Young LH. AMP-activated protein kinase mediates ischemic glucose uptake and prevents postischemic cardiac dysfunction, apoptosis, and injury. *J Clin Invest* 2004;114:495-503.

38 Xing Y, Musi N, Fujii N, Zou L, Luptak I, Hirshman MF, Goodyear LJ, Tian R. Glucose metabolism and energy homeostasis in mouse hearts overexpressing dominant negative alpha2 subunit of AMP-activated protein kinase. *J Biol Chem* 2003;278:28372-28377.

39 Di Filippo C, Marfella R, Cuzzocrea S, Piegari E, Petronella PI, Giugliano D, Rossi F, D'Amico M. Hyperglycemia in streptozotocin-induced diabetic rat increases infarct size associated with low levels of myocardial HO-1 during ischemia/reperfusion. *Diabetes* 2005;54:803-810.

3 ACUTE DEXAMETHASONE-INDUCED INCREASE IN CARDIAC LIPOPROTEIN LIPASE REQUIRES ACTIVATION OF BOTH AKT AND STRESS KINASES³

3.1 INTRODUCTION

Glucocorticoids are used widely as anti-inflammatory and immunosuppressive agents (42). However, chronic glucocorticoid therapy is often associated with adverse effects including Cushing's syndrome, osteoporosis, gastrointestinal bleeding, and dyslipidemia (42). In addition, both excess endogenous (32) and exogenous (43) glucocorticoids contribute towards the generation of the metabolic syndrome including obesity, hypertension, and insulin resistance. In the human body, insulin resistance is viewed as an insufficiency in insulin action, which can lead to a cardiac pathology. In the San Antonio Heart Study, patients with insulin resistance had a 2.5 times increased risk to die of cardiovascular disease than those without insulin resistance (20). Additionally, patients who have insulin resistance can develop Type 2 diabetes. Diabetes itself promotes vascular diseases and non-vascular cardiac injury (2). With insulin resistance or diabetes, metabolism in multiple organ systems including the heart is altered, which is believed to be an important factor in increased morbidity and mortality (27). Compared to glucose, fatty acids (FA) are the preferred substrate consumed by cardiac tissue (31), with hydrolysis of triglyceride (TG)-rich lipoproteins by lipoprotein lipase (LPL) positioned at the endothelial surface of the coronary lumen being suggested to be the principal source of FA for cardiac utilization (3). Increasing FA uptake through

³ "A version of this chapter has been published. Kewalramani, G. Puthanveetil, P. Kim, MS. Wang, F. Lee, V. Hau, N. Beheshti, E. Ng, N. Abrahani, A. Rodrigues, B. (2008) Acute dexamethasone-induced increase in cardiac lipoprotein lipase requires activation of both Akt and stress kinases. *Am J Physiol Endocrinol Metab.* 295:E137-E147."

overexpression of cardiac human LPL (47) or fatty acid transport protein (9), or augmenting FA oxidation through overexpression of cardiac PPAR- α (17) or long-chain acyl CoA synthase (10), results in a severe cardiac pathology.

Glucocorticoids act through genomic and non-genomic pathways (6). Genomic mechanisms include binding of the glucocorticoid to its cytosolic receptor, relocation into the nucleus, and an increase or decrease in gene expression (6). Non-genomic modes of glucocorticoid action occur rapidly (few seconds to minutes), and include activation of numerous cellular processes like mitogen-activated protein kinases (MAPKs) and heterotrimeric guanosine triphosphate-binding proteins (G-proteins) (8). Through its non-genomic effects in uncoupling oxidative phosphorylation, glucocorticoids decrease ATP in cells within the immune system leading to cell death, thereby preventing acute immune responses (7). If this effect of glucocorticoids were mimicked in cardiac tissue, the heart would be expected to change its substrate utilization in an effort to maintain its levels of ATP. Indeed, using an acute dexamethasone model, our laboratory has reported that glucocorticoid treatment leads to amplification in coronary LPL (both LPL activity and LPL protein) (37). The resulting clearance of plasma TG increases FA delivery to the heart, augments FA (but decreases glucose) oxidation (37; 36), and ensures continuous ATP generation to maintain normal heart function. Under these conditions, an increase in oxygen demand and generation of reactive oxygen species could lead to the cardiac damage seen following chronic glucocorticoid use.

In the heart, as endothelial cells do not express the LPL gene, this enzyme is synthesized in myocytes and subsequently transported onto heparan sulfate proteoglycan (HSPG) binding sites on the myocyte cell surface (14). From here, the enzyme is then transported

onto HSPG binding sites on the luminal surface of the capillary endothelium (33). At this location, LPL plays a crucial role in hydrolysis of TG rich lipoproteins to FA, which are transported to the heart and used either for energy production or for re-synthesis of TG. The objective of the present study was to determine the mechanisms by which dexamethasone increases cardiac LPL at the coronary lumen. We demonstrate that following a single dose of dexamethasone, although genomic mechanisms are activated, it is a novel, rapid non-genomic phosphorylation of stress kinases like AMPK and p38 mitogen-activated protein kinase (MAPK) which together with insulin, act in unison to facilitate LPL translocation to the myocyte cell surface.

3.2 MATERIALS AND METHODS

3.2.1 Experimental animals

The investigation conforms to the guide for the care and use of laboratory animals published by the US National Institutes of Health, and the University of British Columbia. Adult male Wistar rats (260-300 g) were obtained from the UBC Animal Care Unit. The synthetic glucocorticoid hormone dexamethasone (DEX; 1 mg/kg) or an equivalent volume of ethanol was administered by i.p. injection to non-fasted rats, and the animals were euthanized at various times (0-4h; plasma half life of DEX is approximately 279 min). In the human body, the basal daily secretion of cortisol is approximately 6-8 mg/m² (in a 70 Kg adult male, this translates to approximately 0.2 mg/Kg). In response to stress, cortisol release is increased up to 10-fold of the basal value (2 mg/kg). For exogenous administration, the dosing with corticosteroids depends on the disease condition, and varies from 75-300 mg/day (approximately 1-4 mg/Kg). Previous studies have determined that using the euglycemic-hyperinsulinemic clamp, a direct measure of insulin sensitivity, this dose of DEX induces whole-body insulin resistance (37). Subsequently, hearts were removed for measurement of coronary luminal LPL activity and Western blotting.

3.2.2 Euglycemic-hyperinsulinemic clamp.

Whole-animal insulin resistance was assessed using a euglycemic-hyperinsulinemic clamp, as described previously (37).

3.2.3 Tissue specific response to insulin

To assess tissue specific insulin resistance, skeletal muscle (gastrocnemius and soleus from hind leg) and heart from control and 4h DEX treated animals were evaluated for

total and phospho-IRS-1 (tyr⁹⁸⁹) and total and phospho-Akt, prior to and after 15 min of injecting a rapid acting insulin into the tail vein (8 U, HumulinR) using Western Blot (26; 21).

3.2.4 LPL and AMPK gene expression

LPL and AMPK gene expression were measured in the indicated groups using RT-PCR as described previously (37).

3.2.5 Heart tissue homogenization

Hearts from control and DEX rats were cleared of blood by flushing buffer through the aorta, and atria and other tissues removed. Ventricles were freeze-clamped in liquid nitrogen, and stored until total cardiac LPL activity was measured as described previously (39).

3.2.6 Coronary lumen LPL activity

To measure coronary endothelium-bound LPL, hearts were perfused retrogradely by the nonrecirculating Langendorff technique with Krebs-Henseleit buffer containing 10 mM glucose (39). The perfusion solution was changed to buffer containing fatty acid free BSA (1%) and heparin (5 U/ml). The coronary effluent was collected in timed fractions (10 sec) over 5 min, and assayed for LPL activity by measuring the hydrolysis of a [³H] triolein substrate emulsion (39; 41).

3.2.7 Western blotting

Western blot was carried out as described previously (24). Measuring the phospho form of AMPK and p38 MAPK is a surrogate for estimation of their activities. For measuring whole heart LPL protein, we used 5D2, a monoclonal mouse anti bovine LPL

(generously provided by Dr. J. Brunzell, University of Washington, Seattle, WA) and sheep-anti-mouse IgG.

3.2.8 Isolated cardiac myocytes

Ventricular calcium-tolerant myocytes were prepared by a previously described procedure (39). To examine the direct influence of DEX and insulin on LPL activity, cardiomyocytes were plated on laminin-coated 6-well culture plates (to a density of 200,000 cells/well). Cells were maintained using Media-199, and incubated at 37°C under an atmosphere of 95% O₂/5% CO₂ for 16 hours. Subsequently, and where indicated, DEX (100 nM) or insulin (100 nM) (16) or LY294002 (50 μM, PI3K inhibitor) was added to the culture medium. Unlike other studies that have used high concentrations of insulin (24), 100 nM insulin has no inhibitory effect on AMPK phosphorylation. Following the indicated times, myocyte basal LPL activity released into the medium was measured. To release surface-bound LPL activity, heparin (8 U/mL; 1 min) was added to the culture plates, aliquots of cell medium removed, separated by centrifugation, and assayed for LPL activity. In separate experiments, following incubation of plated myocytes (0.4 x 10⁶ cells in a 60 x 15 mm tissue culture dish) with DEX and insulin, myocyte cell lysates were also used for immunoprecipitation and Western blotting. In addition, the effects of DEX+Insulin in myocytes were also determined in the presence or absence of 1 μM cytochalasin D (CTD, an actin polymerization inhibitor) or 50 μM LY294002 (a PI3-kinase inhibitor).

3.2.9 Nuclear localization of p38 MAPK.

Nuclear localization of p38 MAPK was determined as described previously (23). Using an antibody against Histone H3 as a nuclear marker, we show good purity of nuclear fractions (data not shown).

3.2.10 Filamentous (F) and globular (G) actin.

F-actin/G-actin ratio in the whole heart and isolated myocytes was determined by Western blotting using an in vivo assay kit.

3.2.11 Immunoprecipitation

Following incubation of plated cardiomyocytes with DEX (100 nM) or DEX+insulin (100 nM), cell lysates were immunoprecipitated using an Akt monoclonal antibody rotating overnight at 4°C. The immunocomplex and the supernatant were resuspended in Laemmli buffer and heated for 5 min at 95°C. The immunocomplex was separated into two equal portions, each of which was immunoblotted with anti-Hsp25 and anti-Akt.

3.2.12 Silencing of p38 MAPK by siRNA

siRNA transfection of p38 MAPK in cardiomyocytes was carried out using a kit from Santa Cruz. Briefly, in 6-well culture plates, 0.1×10^6 cells were plated and subsequently exposed to the siRNA (or scrambled, Scr) solution for 8h at 37°C in a CO₂ incubator. Following this, the media was changed to Media 199 and the cells incubated for another 16h. Subsequently, and where indicated, DEX (100 nM)+insulin (100 nM) were added to the culture medium for 8h, and LPL (released by heparin), p38 MAPK, AMPK and Hsp25 (using Western blotting) were determined.

3.2.13 Plasma measurements

Following DEX, blood samples from the tail vein were collected, and blood glucose determined using a glucometer and glucose test strips (Accu-Chek Advantage, Roche). Diagnostic kits were used to measure triglyceride (Sigma), non-esterified fatty acid (NEFA, Wako), and insulin (Linco).

3.2.14 Materials

[³H]triolein (Amersham Canada), Heparin sodium injection (Hapalean; 1000 USP U/ml, Organon Teknika), F-actin/G-actin kit (Cytoskeleton Inc., Denver, CO). Total AMPK- α , phospho-AMPK- α (Thr172), p38 MAPK, phospho-p38 MAPK (Thr180/Tyr182), phospho-IRS-1 (Tyr989), phospho-Akt (Ser473), total-IRS-1 and total-Akt antibodies were obtained from Cell Signaling, Danvers, MA. Hsp25 and phospho-Hsp25 (S86) antibodies were from GeneTex[®], Inc., San Antonio, TX. ECL[®] detection kit (Amersham). All other chemicals were obtained from Sigma Chemical.

3.2.15 Statistical analysis

Values are means \pm SE. Wherever appropriate, one-way ANOVA followed by the Bonferroni test was used to determine differences between group mean values. The level of statistical significance was set at $P < 0.05$.

3.3 RESULTS

3.3.1 General characteristics of the experimental animals

Chronic DEX treatment induces insulin resistance, hyperinsulinemia and hyperglycemia (4). In the present study, injection of DEX for 4h was not associated with either hyperinsulinemia or hyperglycemia (Table 3-1). However, the euglycemic-hyperinsulinemic clamp, a direct measure of insulin sensitivity, revealed that the glucose infusion rate necessary to maintain euglycemia was lower following DEX administration (Table 3-1). We also evaluated plasma TG and FA at 4h following DEX. Interestingly, although plasma TG declined, there was no effect on plasma FA (Table 3-1).

3.3.2 Tissue specific insulin resistance

Whole body insulin resistance could embrace metabolic abnormalities in multiple organs (38). We assessed the effects of DEX on the responses of skeletal muscle and cardiac tissue to insulin. In skeletal muscle, both basal and insulin stimulated tyrosine phosphorylation of IRS-1 (Fig. 3-1A) and Akt (Fig. 3-1B) were reduced after 4h of DEX. Unexpectedly, these effects were not observed in cardiac tissue, which demonstrated a normal response to insulin when IRS-1 (Fig. 3-1A) and Akt (Fig. 3-1B) phosphorylation were measured. Following 4h of DEX, total IRS1 and total Akt (basal and insulin stimulated) did not change in skeletal and cardiac muscle when compared to control (Fig. 3-1 A and B). Thus in cardiac tissue, any observed changes at 4h are likely due to a direct effect of DEX, and independent of insulin signaling.

3.3.3 Changes in LPL following DEX

LPL mediated hydrolysis of circulating TG-rich lipoproteins at the coronary lumen provides the heart with FA (35). DEX increased LPL mRNA levels, 60 to 240 min after

injection (Fig. 3-2A). To determine whether the change in LPL gene following DEX is related to augmented protein synthesis, we measured LPL protein and activity in heart homogenates. Interestingly, the change in gene expression was not reflected in an alteration in whole heart LPL protein (Fig. 3-2A, immunoblot) or activity (Fig. 3-2B) upto 240 min after DEX. However, when we measured LPL activity localized to the coronary lumen by retrogradely perfusing isolated hearts with heparin, an increase in LPL activity became apparent as early as 120 min subsequent to injection of DEX (Fig. 3-2C), and was maintained upto 4h (Fig. 3-2C). The DEX induced increase in heparin-releasable LPL activity at the vascular lumen after 120 to 240 min was substantial compared to control (~3 fold, Fig. 3-2C).

3.3.4 Influence of DEX on cardiac AMPK and p38 MAPK phosphorylation

Previous studies from our laboratory have reported significantly higher AMPK phosphorylation in hearts from STZ diabetic animals, a model of poorly controlled Type 1 diabetes (22). In the present study, an early (20 min) increase of cardiac AMPK phosphorylation was observed, that peaked at 40 min after injection of DEX (Fig. 3-3B). With time, AMPK phosphorylation in hearts from DEX treated animals declined, but was still higher than control after 4h (Fig. 3-3B). An increase in total AMPK protein only became apparent after 120 min of DEX, with a maximum observed after 4h (Fig. 3-3B, immunoblot). This change in AMPK total protein paralleled a rise in AMPK gene expression (Fig. 3-3A). p38 MAPK is a downstream target of AMPK (29). Estimation of cardiac cytosolic p38 MAPK phosphorylation showed a similar pattern to that seen with activation of AMPK; rapid activation followed by a decline (Fig. 3-3C). Once phosphorylated, p38 MAPK relocates to the nucleus (48). Separation of the nuclear

fraction revealed that concurrent to the decline in cytosolic p38 MAPK phosphorylation, nuclear p38 MAPK phosphorylation increased (Fig. 3-3C, immunoblot).

3.3.5 DEX stimulates cardiac actin polymerization

p38 MAPK phosphorylation is suggested to regulate actin polymerization through its phosphorylation of Hsp25. In turn, the actin cytoskeleton has been implicated in managing myocyte LPL secretion (15). Marked phosphorylation of Hsp25 was evident after 120 min of DEX, an effect that intensified at 4h (Fig. 3-4A). To determine whether Hsp25 phosphorylation elicits F-actin polymerization, we quantitated F-actin and G-actin cellular fractions using Western blot. In the resting cardiomyocyte, the proportion of polymerized F-actin is consistently higher than G-actin (90:10). Additionally, an increase in F-to-G actin ratio indicates actin polymerization. DEX increased the F/G actin ratio (Fig. 3-4B). Interestingly, the increase in F-actin polymerization closely mirrored the enlargement of LPL activity after DEX (Fig. 3-2C).

3.3.6 In vitro effects of DEX on isolated control myocytes

LPL at the coronary lumen is acquired from underlying cardiomyocytes. In these cells, following its synthesis, LPL is transported onto cell surface HSPG binding sites (34). To directly examine the effects of DEX on myocyte LPL, control cardiomyocytes were incubated with DEX for varying times. In the absence of DEX, no change in AMPK phosphorylation was observed over time (data not shown). Unlike its effects *in vivo*, DEX activated AMPK phosphorylation in cardiomyocytes was delayed (becoming apparent only at 60 min), and was maintained upto 8h after DEX treatment (Fig. 3-5A). In addition, no change in total AMPK protein was observed (Fig. 3-5A, immunoblot). The activation of AMPK was temporally related to phosphorylation of cytosolic p38

MAPK (Fig. 3-5B), which declined over time as a consequence of its nuclear translocation (Fig. 3-5B, immunoblot). Interestingly, p38 MAPK activation *in vitro* was not reflected in phosphorylation of Hsp25 (Fig. 3-5C, left panel), nor was there any evidence of F-actin polymerization (Fig. 3-5C, right panel), or an augmentation of heparin releasable LPL activity upto 4h after incubation with DEX (Fig. 3-6A, left panel).

3.3.7 Insulin mediates the *in vitro* effects of DEX on cardiomyocyte LPL activity

We evaluated whether insulin could explain the dissimilar effects of DEX observed *in vivo* and *in vitro*. Fig. 3-6A (right panel) illustrates both basal and heparin releasable LPL activity. Incubation of myocytes with either insulin or DEX alone for upto 8h had no effect on basal or heparin releasable LPL activity. The simultaneous addition of DEX with insulin for 4h also had no influence on this enzyme (data not shown). Interestingly, extending the incubation with DEX and insulin for 8h appreciably enhanced heparin releasable activity in the medium (3-6A, right panel). This increase in LPL following simultaneous addition of DEX and insulin closely mirrored the robust elevation in both phosphorylation of Hsp25 (3-6B, middle panel) and F-actin polymerization (3-6B, right panel). These data suggest that the effects of DEX on LPL are only apparent in the presence of insulin. In the presence of DEX, Hsp25 forms a complex with protein kinase B (Akt), as a means to safeguard this cell survival kinase. As insulin by phosphorylating Akt dissociates Hsp25 from its complex with Akt, allowing p38 MAPK to phosphorylate Hsp25, induce F-actin polymerization, and eventual LPL translocation to the myocyte cell surface, we examined the association between AKT and Hsp25 in the presence of DEX and DEX+insulin. In cardiomyocytes, DEX treatment increased the association between Akt and Hsp25, an effect that was reduced in the presence of insulin (Fig. 6B,

left panel). Presence of LY294002 prevented the disassociation of Akt from Hsp25 (Fig. 3-6B, left panel), and reduced phospho Hsp25 (Fig. 3-6B, middle panel) and F-actin polymerization (Fig. 3-6B, right panel). More importantly, LY294002 reduced the augmented heparin releasable LPL activity observed with DEX+Ins (Fig. 3-6A).

To investigate the involvement of the actin cytoskeleton in the DEX+insulin mediated augmentation of myocyte LPL, myocytes were pretreated with an actin polymerization inhibitor, CTD (34), before incubation with DEX and insulin. CTD reduced the effect of DEX+insulin to increase myocyte HR-LPL (heparin releasable LPL) without any effect on basal activity (Control-2222 \pm 89; DEX+insulin-5846 \pm 126; Dex+insulin+CTD-3149 \pm 186, nmol \cdot h $^{-1}\cdot$ 10 $^{-6}$ cells, $P<0.05$).

3.3.8 Silencing of p38 MAPK prevents cardiomyocyte LPL recruitment observed with DEX and insulin.

To confirm the relationship between p38 MAPK and LPL, we used short interfering RNA to silence p38 MAPK expression in isolated cardiomyocytes and then treated the cells with DEX and insulin. We first validated successful p38 MAPK inhibition using Western blotting (Fig. 3-7A, immunoblot). Interestingly, silencing p38 MAPK in myocytes treated with DEX+insulin for 8h demonstrated a decrease in phosphorylation of Hsp25 (Fig. 3-7B) with a concurrent decline in heparin releasable LPL activity (Fig. 3-7C). Silencing of p38 MAPK had no effect on phosphorylation of AMPK, which remained high following Dex+insulin (Fig. 3-7A, immunoblot).

3.4 DISCUSSION

Glucocorticoids are widely accepted to cause insufficiency in insulin action, with insulin resistance causing changes in metabolism in multiple organ systems such as skeletal muscle, liver and adipose tissue (12). In this study, we demonstrate that DEX produced whole-body insulin resistance, which was likely accounted for by changes in the responses of skeletal muscle to insulin. In other insulin sensitive tissues like the heart, although no changes were observed in insulin signaling, we describe rapid non-genomic alterations in cardiac metabolism following acute DEX treatment. These include phosphorylation of AMPK, p38 MAPK and Hsp25 that cause actin cytoskeleton rearrangement, facilitating LPL translocation to the myocyte cell surface. Transfer of the enzyme from the myocyte cell surface to the coronary lumen would be expected to increase LPL derived FA provision to the heart, likely compromising glucose utilization (36).

Skeletal muscle accounts for 80% of insulin-induced glucose disposal in the human body (12) and thus, it is a major target for glucocorticoid-induced insulin resistance. In skeletal muscle, insulin stimulates glucose uptake, utilization and storage. As cortisol administration does not alter the number of insulin receptors in skeletal muscle (5), it is likely that glucocorticoids alter glucose metabolism through its post-receptor effects on downstream insulin signaling or glucose utilization. Following chronic DEX treatment, even though its gene expression is unchanged, the phosphorylation of Akt/protein kinase B (PKB) induced by insulin significantly decreases (40). This reduction in insulin signal is paralleled with a decreased glucose uptake and disposal (13). The decreased Akt phosphorylation may be attributed to a decreased insulin receptor tyrosine

phosphorylation and insulin receptor substrate (IRS) protein expression (18). Our study demonstrates that a single dose of DEX also reduces tyrosine phosphorylation of IRS-1 and phosphorylation of Akt under both basal and insulin stimulated conditions in skeletal muscle. Surprisingly, unlike skeletal muscle, cardiac tissue displayed normal responses to insulin. At present, whether the heart requires an extended DEX exposure to become insulin resistant is unknown, and is under investigation.

The major source of FA for myocardial energy utilization is LPL mediated hydrolysis of TG-rich lipoproteins at the vascular endothelium. As glucocorticoids have previously been reported to influence the transcription of approximately 1% of the entire genome in humans (42), we examined cardiac LPL gene expression and establish that acute DEX increases LPL mRNA. However, this change was not coordinated to an increase in LPL protein or activity in whole heart homogenates, upto 4h after DEX treatment. It is possible that at this early time point, the change in LPL gene has not yet been translated to an increase in LPL protein, and may become apparent if the duration of DEX treatment is extended beyond 4h. Nevertheless, in the present study, we report that DEX increases cardiac luminal LPL activity, a change that was detectable within 2h of DEX injection and is likely due to novel and rapid non-genomic phosphorylation of stress kinases that increases movement of enzyme to the myocyte cell surface and from there, to the vascular lumen.

AMPK is the switch that regulates cellular energy during metabolic stress (19). Particularly related to FA, AMPK can regulate FA delivery through its regulation of CD36 (30), and FA oxidation through its effect on acetyl-CoA carboxylase (25). Recently, we have also demonstrated that following AMPK activation, heparin-releasable

coronary lumen LPL activity is amplified, providing an immediate compensatory response by the heart to guarantee FA supply and ATP production. In addition, in hearts from fasted animals (that demonstrate augmented AMPK phosphorylation and LPL activity), inhibition of AMPK phosphorylation using Ara-A or insulin reduced cardiac luminal LPL activity (1). In the present study, the augmentation in coronary LPL activity was preceded by a rapid (within 20 min) and intense phosphorylation in AMPK that was not sustainable, and decreased over time. The early increase in AMPK phosphorylation may well be a product of the rapid action of glucocorticoids to compromise ATP production that highlights its actions as an immunosuppressant to reduce inflammatory processes (44). The gradual decline in AMPK activation is likely a consequence of the excessive amount of cardiac LPL derived FA. Cardiac LPL is a major determinant of plasma TG (28), and the increase in cardiac luminal LPL is associated with a decline in circulating TG, and an increase in cardiac FA (palmitic and oleic acid) and TG levels (36). High FA or TG, through their formation of ceramide, has been shown to activate protein phosphatase 2A leading to dephosphorylation of AMPK (46). As AMPK phosphorylation following prolonged DEX never declined to control levels, it is possible that 2-4 h after DEX, AMPK phosphorylation is a balance between FA inhibition of AMPK (23), and activation of the AMPK gene resulting in higher total AMPK protein.

Given the delay between AMPK activation (within mins) and the increase in coronary lumen LPL activity (within hrs), we considered the possibility that the early activation of AMPK may have turned on other downstream signals. One downstream target of AMPK is p38 MAPK, and there was coincident activation of both AMPK and p38 MAPK following injection of DEX. Other studies have demonstrated that AMPK activates p38

MAPK through its interaction with transforming growth factor- β -activated protein kinase 1-binding protein 1 (29). Cytosolic activation of p38 MAPK results in its transfer to the nucleus, and gene activation through a number of transcription factors (45). In the nucleus, p38 MAPK can also activate MAPKAP kinase 2, which is then exported to phosphorylate Hsp25. Our studies in the heart confirmed that cytosolic activation of p38 MAPK was followed by its nuclear translocation. More importantly, with increasing duration of DEX, phosphorylation of Hsp25 progressively increased. Hsp25 is known to inhibit actin polymerization, and its phosphorylation results in a decline of this inhibitory function (11). In this setting, actin monomers are released from the phosphorylated Hsp25 to self-associate to form fibrillar actin. Within the myocyte, we (34) and others (15) have reported actin cytoskeleton reorganization as an important means by which LPL is secreted onto plasma membrane HSPG binding sites. Since the increase in luminal LPL activity at 2 and 4h after DEX corresponded to an enlargement in the F-actin/G-actin ratio, our data suggest that AMPK and p38 MAPK, through their control of Hsp25 and the actin cytoskeleton, act in unison to facilitate LPL translocation to the myocyte cell surface, and ultimately to the coronary lumen. The importance of p38 MAPK in modulating the effects of DEX on myocyte LPL was evident in our silencing experiment where p38 MAPK siRNA prevented Hsp25 phosphorylation and an increase in LPL activity (in the absence of any change in AMPK phosphorylation). Recently, observations from our lab have also shown that thrombin activates p38 MAPK and increases myocyte LPL activity, and that myocytes pre-incubated with a p38 MAPK inhibitor (SB202190, 20 μ M) abolished these effects of thrombin (23).

In the heart, LPL is synthesized in the underlying myocytes before it is translocated to the luminal side of the coronary vessel wall with the help of heparan sulfate oligosaccharides acting as extracellular chaperones (33). We next evaluated the direct effects of DEX on stress kinases, and their control of cardiomyocyte LPL. Unlike our *in vivo* data, although 100 nM DEX activated AMPK *in vitro*, the pattern of AMPK phosphorylation was different. In cardiomyocytes, AMPK stimulation occurred later (60 min), with no falling off over time. At present, an explanation for such effects is unknown. It is possible that the limited demand for energy in non-beating quiescent myocytes delays the activation of AMPK, whereas the absence of FA in the myocyte incubation medium prevents the gradual decline in AMPK observed *in vivo*. Activation of AMPK by DEX in isolated myocytes was associated with cytosolic phosphorylation of p38 MAPK, followed by its nuclear transfer. However, no phosphorylation of Hsp25 was observed in this setting, nor was there any actin polymerization, suggesting that Hsp25 phosphorylation requires additional elements. In mouse embryonic fibroblasts, Hsp25 associates with Akt to form an oligomer, and activation of Akt releases Hsp25 from its complex with Akt, facilitating Hsp25 phosphorylation, dissociation of the actin dimers and monomers (48), and ultimately actin polymerization. It is possible that in the presence of DEX, the cellular response of the heart to evade cell death is for Hsp25 to form a complex with protein kinase B (Akt), as a means to safeguard this cell survival kinase. Indeed, in cardiomyocytes incubated with DEX alone, there was a robust association between Akt and Hsp25. Our data suggest that insulin, by phosphorylating Akt, dissociates Hsp25 from its complex with Akt, allowing p38 MAPK to phosphorylate Hsp25, induce F-actin polymerization, and eventual LPL translocation to the myocyte

cell surface (Fig. 3-8). A previous study has also reported that the increase in LPL activity following DEX is only observed with the prolonged exposure of myocytes to both insulin and DEX (15).

In summary, following acute administration of DEX, it is LPL recruitment to the coronary lumen that supports an augmented FA supply to the heart. The mechanism underlying this process embraces activation of stress kinases like AMPK and p38 MAPK, a requirement of insulin, and an increase in actin cytoskeleton polymerization. As elevated FA use has been implicated in a number of metabolic, morphological, and mechanical changes, and more recently, in “lipotoxicity”, our data suggest that enlargement in LPL at the cardiomyocyte cell surface and likely transfer to the vascular lumen could play a crucial role in the development of heart disease when glucocorticoids are used chronically.

3.5 TABLES AND FIGURES

Table 3-1 General characteristics of experimental animals

	CON	DEX
Body Weight (gm)	265 ± 4	273 ± 4
Heart Weight (gm)	1.5 ± 0.1	1.3 ± 0.05
Glucose Infusion Rate (GIR)	15 ± 2.2	4.0 ± 0.7*
Plasma Glucose (mmol/l)	8.2 ± 0.2	8.0 ± 0.4
Plasma Insulin (ng/ml)	3.0 ± 0.01	3.0 ± 0.05
Plasma Fatty Acids (mmol/l)	0.6 ± 0.1	0.6 ± 0.1
Plasma Triglycerides (mmol/l)	1.5 ± 0.1	0.5 ± 0.1*

The table illustrates the general characteristics of the experimental animals after DEX (1 mg/kg) was administered by i.p injection into control rats and the animals killed after 4h. Whole-animal insulin resistance was also assessed using a euglycemic-hyperinsulinemic clamp. Briefly, 4h after the injection of vehicle or DEX, animals were anesthetized with sodium pentobarbital (Somnotol™; 65 mg/kg) and a cannula inserted into the left jugular vein. Insulin (HumulinR; 3 mU/min/kg) and d-glucose (50%) were continuously delivered for 3h with the glucose infusion started 4 min after commencement of insulin infusion. The table depicts the average GIR values (over 3h of infusion) that were adjusted accordingly to maintain euglycemia. Values are the mean ± SE for 3-5 rats in each group. CON, control; DEX, dexamethasone. *Significantly different from control, $P < 0.05$.

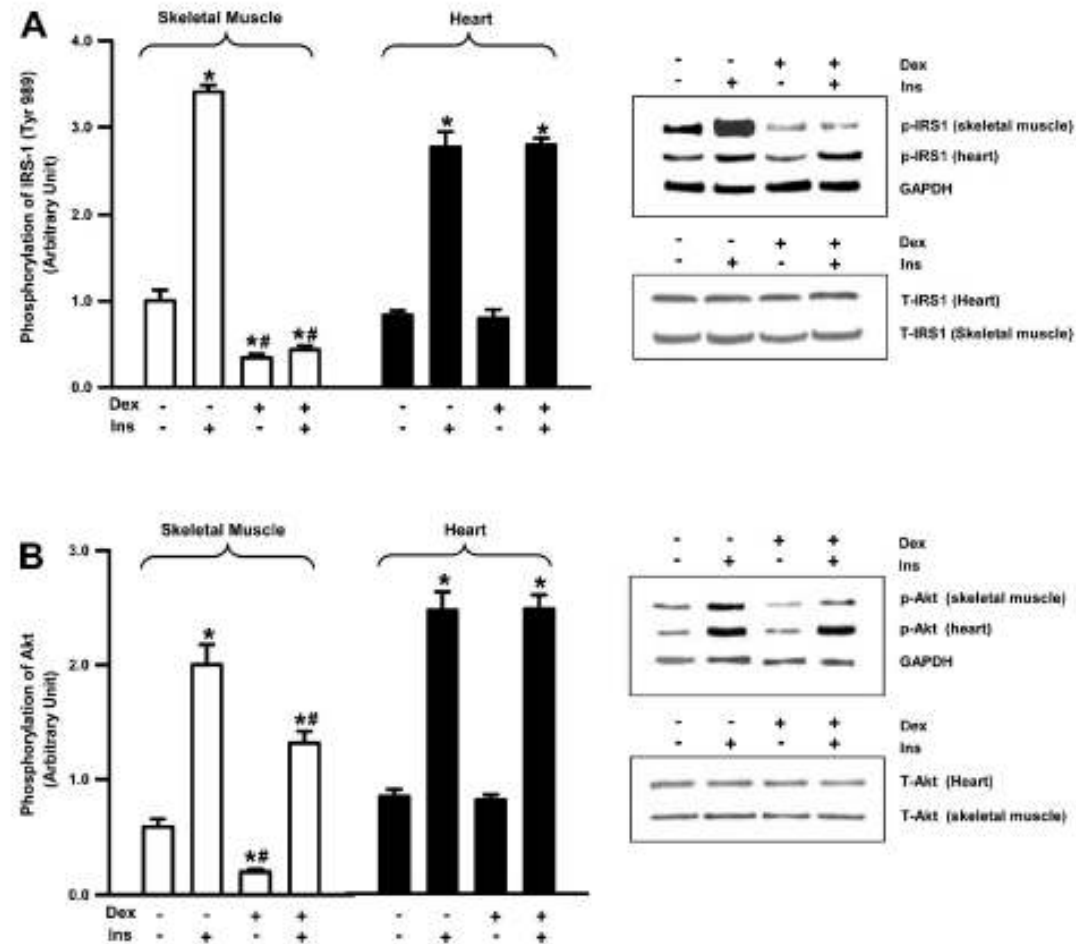


Fig. 3-1 Responses of skeletal muscle and heart to insulin. Skeletal muscle (gastrocnemius and soleus from hind leg) and heart from control and 4h DEX treated animals were evaluated for phospho-IRS-1 (at tyrosine 989) and total-IRS-1 (A) and phospho-Akt (at serine 473) and total-Akt (B), prior to and after 10 min of injecting rapid acting insulin into the tail vein (8 U, HumulinR) using Western Blot. Results are the means \pm SE of 5 rats in each group. *Significantly different from control (no DEX or insulin); #Significantly different from control given insulin, $P < 0.05$.

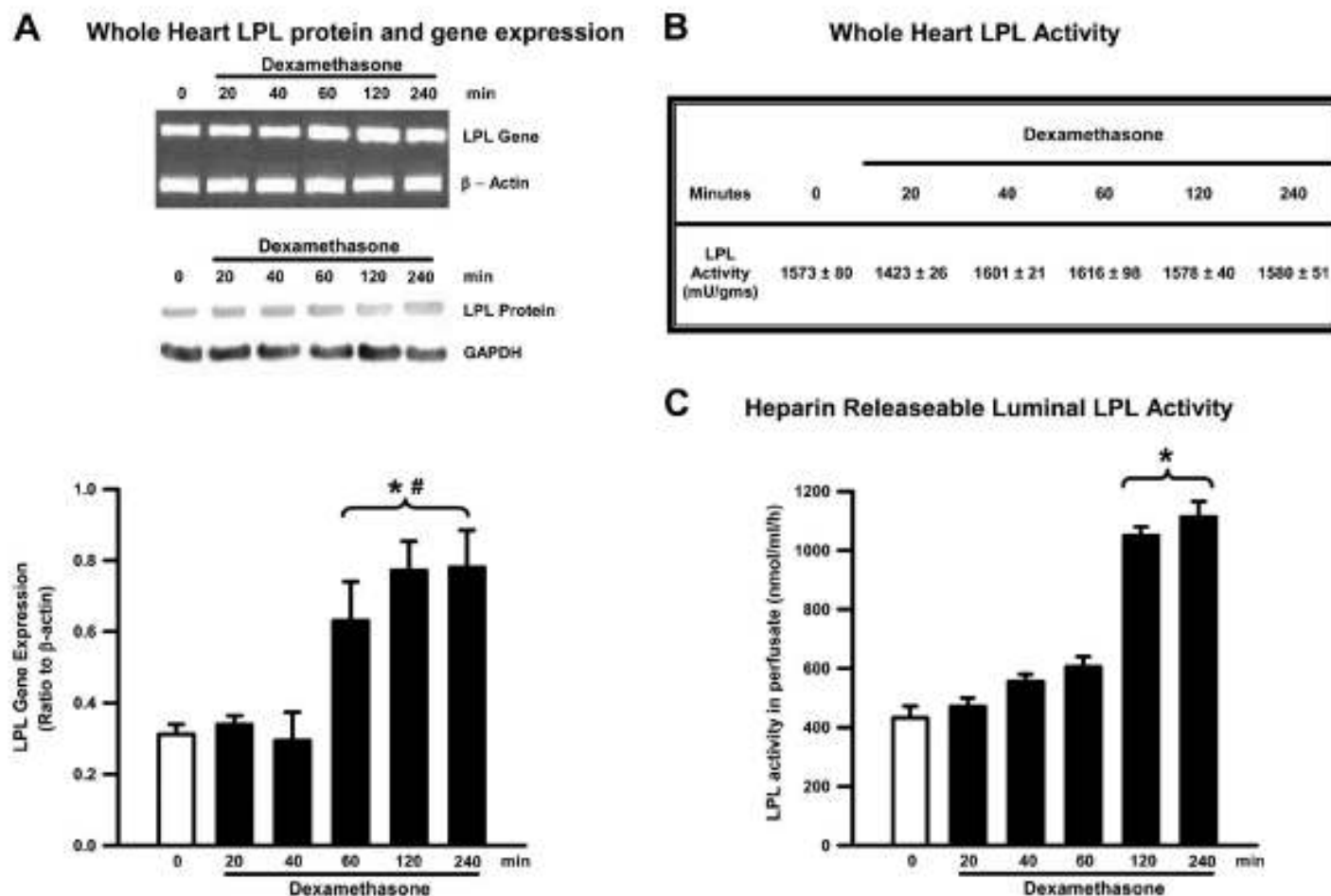


Fig. 3-2 LPL gene expression, protein and activity measurement in hearts from control and DEX treated animals. Using 50 mg of homogenized ventricular tissue from control, and animals given DEX for various intervals, LPL gene and protein (A), and activity (B) were determined. To evaluate LPL exclusively localized at the coronary lumen, hearts from the different groups were also perfused in the non-recirculating retrograde mode with heparin. Coronary effluents were collected (for 10 s) over 5 mins, but only peak LPL activities are illustrated (C). Results are the means \pm SE of 5 rats in each group *Significantly different from untreated control (0 min); #Significantly different from DEX (20-40 min), $P < 0.05$.

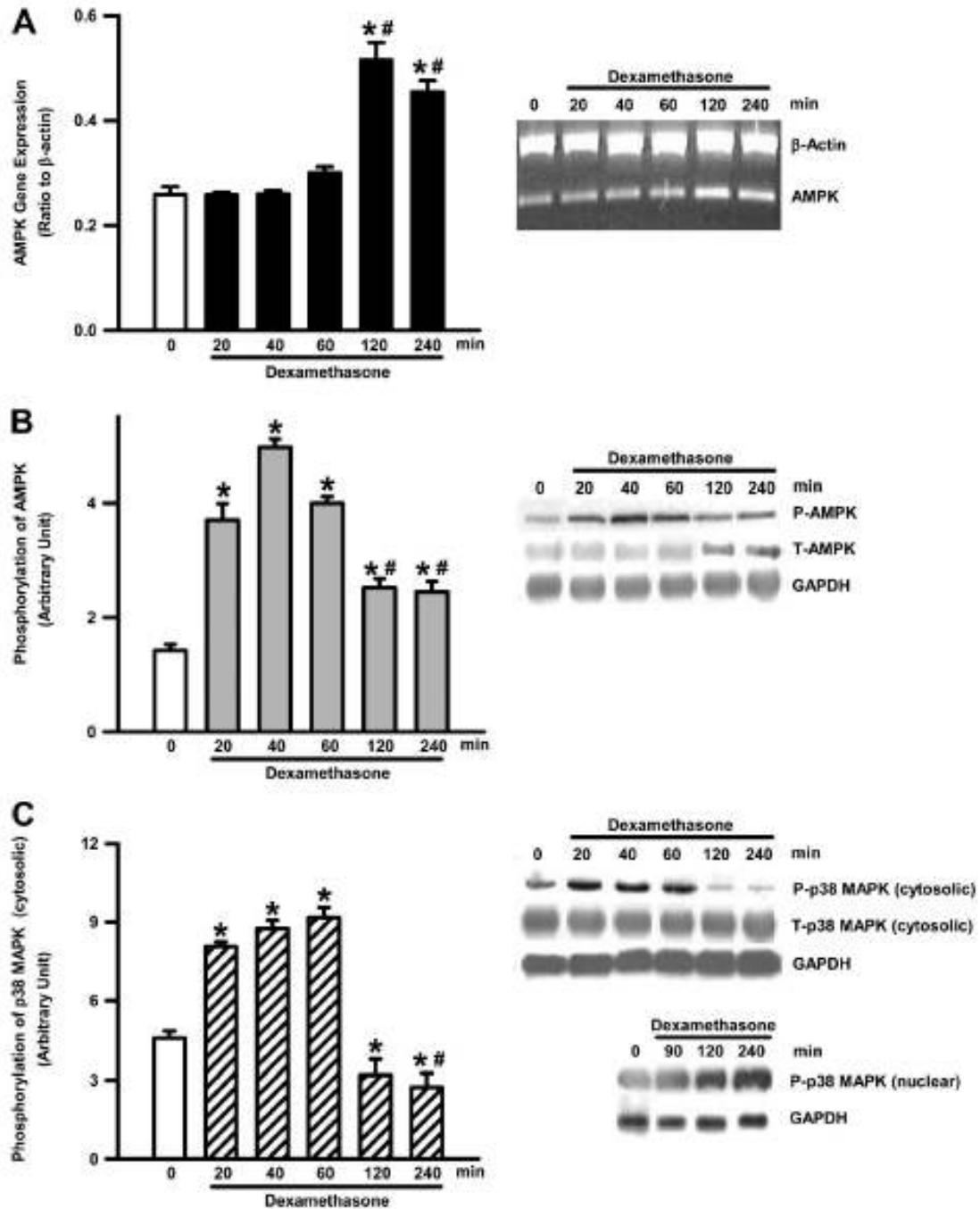


Fig. 3-3 Time dependent changes in AMPK gene expression, phosphorylation of AMPK and p38 MAPK in hearts isolated from DEX treated animals. Following DEX for different intervals, AMPK gene expression was measured using rtPCR (A). Total and phosphorylated AMPK- α was measured using rabbit AMPK- α or phospho-AMPK (Thr 172) antibodies respectively (B). Cytosolic and nuclear p38 MAPK were evaluated using rabbit p38 MAPK or phospho-p38 MAPK (Thr180/Tyr182) antibodies (C). Results are the means \pm SE of 5 rats in each group. ^{*}Significantly different from untreated control (0 min); [#]Significantly different from DEX (20-60 min), $P < 0.05$.

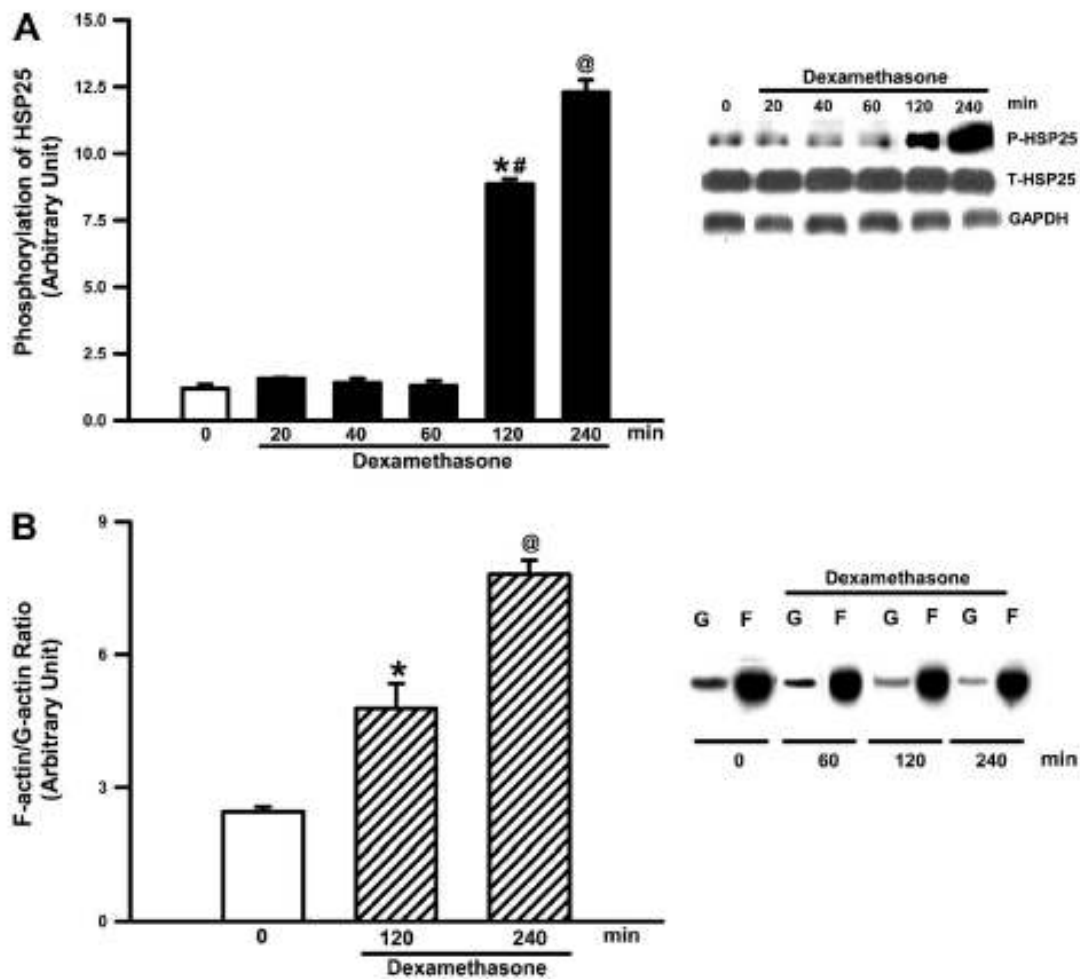


Fig. 3-4 Phosphorylation of Hsp25 and actin polymerization following DEX. Total or phosphorylated Hsp25 was determined immediately upon removal of the heart using rabbit Hsp25 or phospho-Hsp25 (S86) antibodies, and Western blotting (A) Cardiac actin rearrangement following DEX was determined using a G-actin/F-actin in vivo assay kit (B). Data are means \pm SE of 5 different hearts in each group. *Significantly different from control (0 min); #Significantly different from DEX (20-60 min); @Significantly different from all other groups, $P < 0.05$.

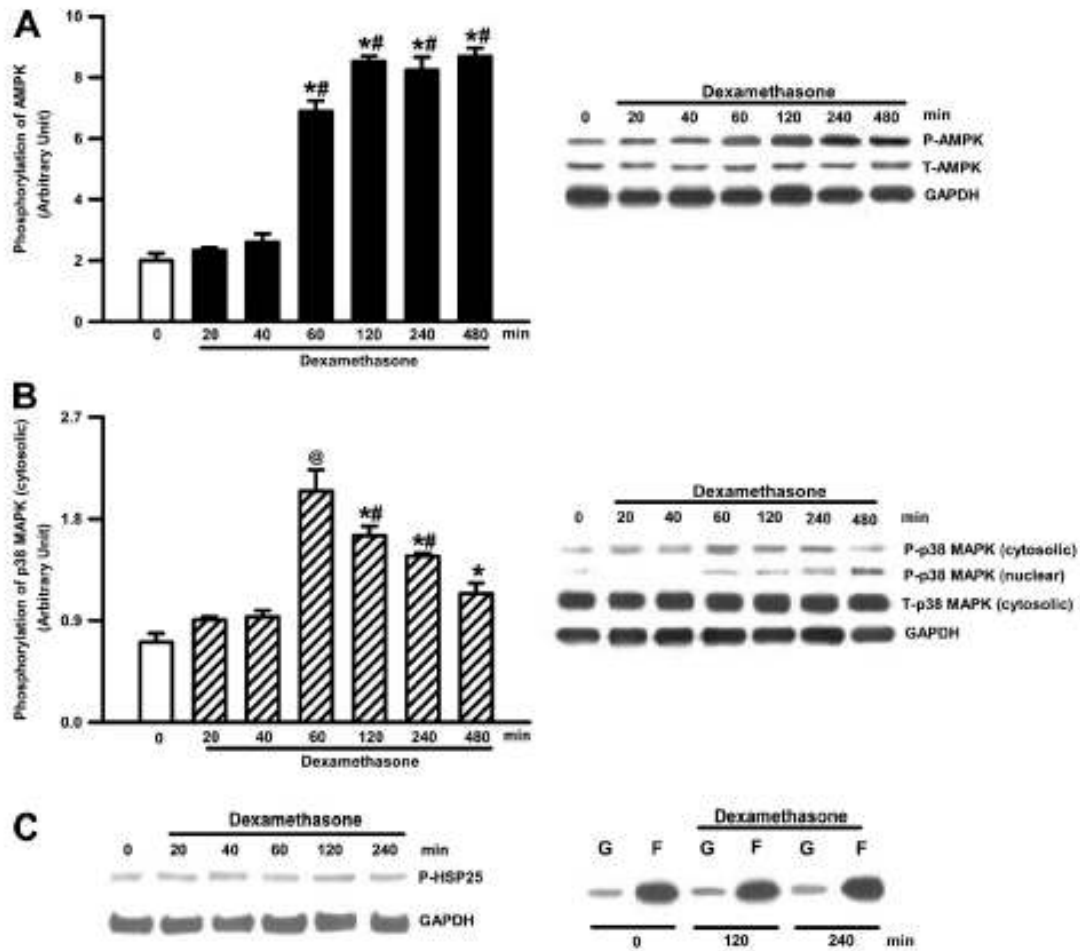


Fig. 3-5 Consequence of incubating cardiomyocytes with DEX *in vitro*. Cardiomyocytes were plated on laminin-coated culture plates. Cells were maintained using Media-199, and incubated at 37°C under an atmosphere of 95% O₂/5% CO₂ for 16 hours. Subsequently, DEX (100 nM) was added to the culture medium. At the indicated times, protein was extracted to determine AMPK (A), cytosolic and nuclear p38 MAPK (B) (both total and phosphorylated), and phosphorylation of Hsp25 (C, left panel) and actin polymerization (C, right panel) using Western Blotting. Data are means ± SE. n=5 myocyte preparations from different animals. For measuring Hsp25 and F and G-actin, only a representative value is indicated. *Significantly different from control (0 min); #Significantly different from DEX (20-40 min); @Significantly different from all other groups, $P < 0.05$.

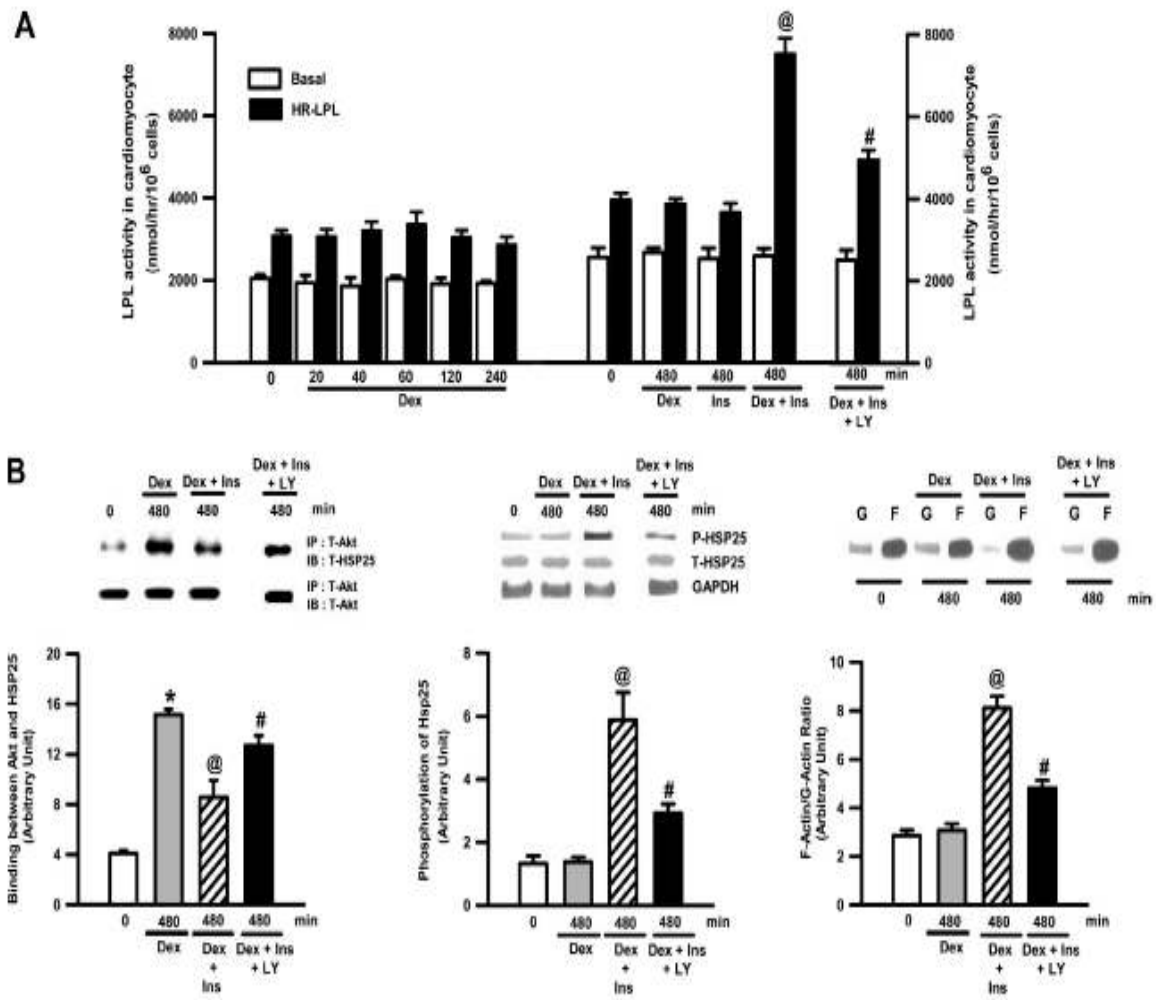


Fig. 3-6 Changes in cardiomyocyte heparin-releasable LPL activity with DEX and insulin. Cardiomyocytes were pre-incubated in the absence or presence of DEX (100 nM), insulin (100 nM), DEX+insulin and DEX+insulin+LY294002 added to the culture medium for varying times. To release surface-bound LPL activity, heparin (8 U/mL; 1 min) was added to the culture plates, aliquots of cell medium removed, separated by centrifugation, and assayed for LPL activity (A). At the indicated time (480 min), protein was extracted to determine the association between Akt and Hsp25 (B, left panel), phosphorylated Hsp25 (B, middle panel) and actin polymerization (B, right panel) using Western Blotting. Data are means \pm SE; n=5 myocyte preparations from different animals. *Significantly different from control, @Significantly different from all other groups, #Significantly different from Dex+Ins (480 min), $P < 0.05$.

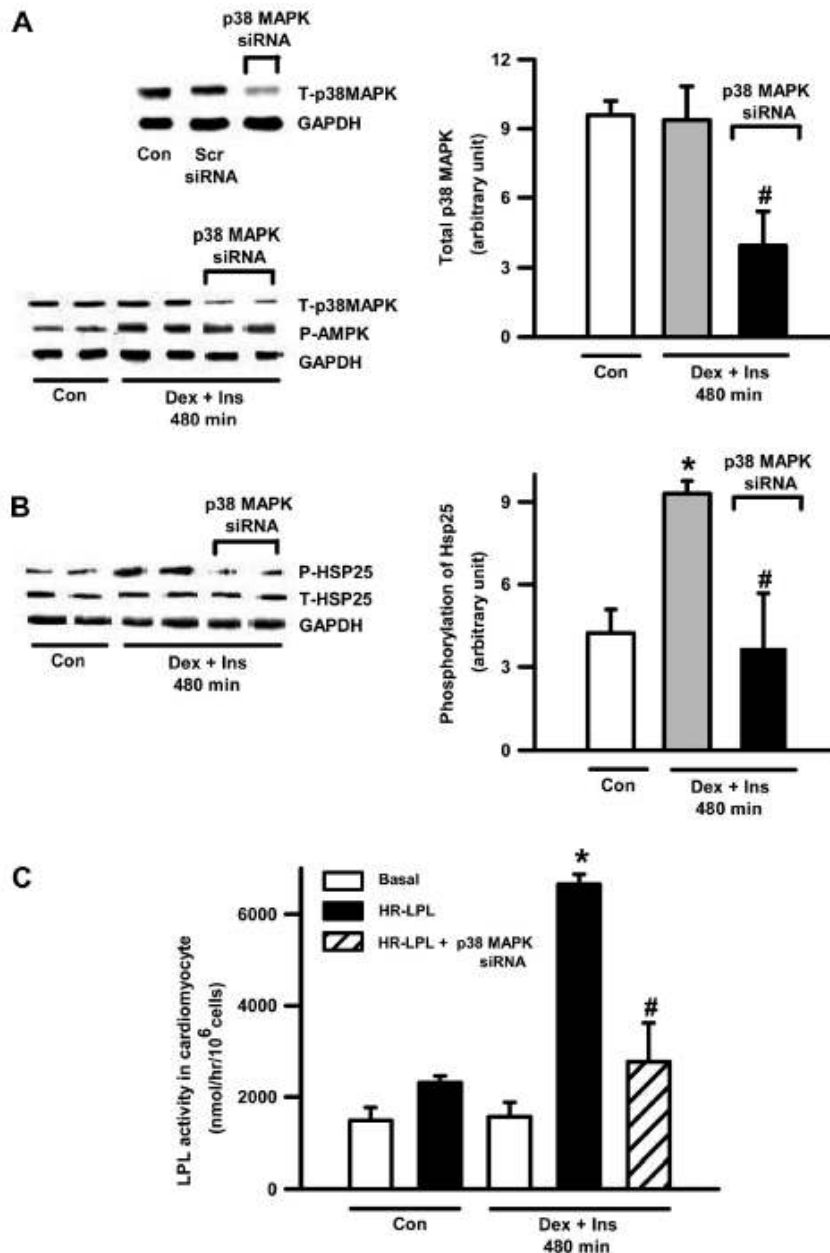


Fig. 3-7 Silencing of p38 MAPK by siRNA. siRNA transfection of p38 MAPK in cardiomyocytes was carried out using a kit from Santa Cruz. Plated myocytes were exposed to the siRNA (or scrambled, Scr). The figure depicts transfection efficiency (A, immunoblot). After this, where indicated, DEX (100 nM) + insulin (100 nM) was added to the culture medium for 8h, and p38 MAPK, phosphorylation of AMPK (A) and Hsp25 (B) (using Western blot) and LPL activity determined (C). Data are means \pm SE; n=5 myocyte preparations from different animals. *Significantly different from control, #Significantly different from Dex + Ins (480 min), $P < 0.05$.

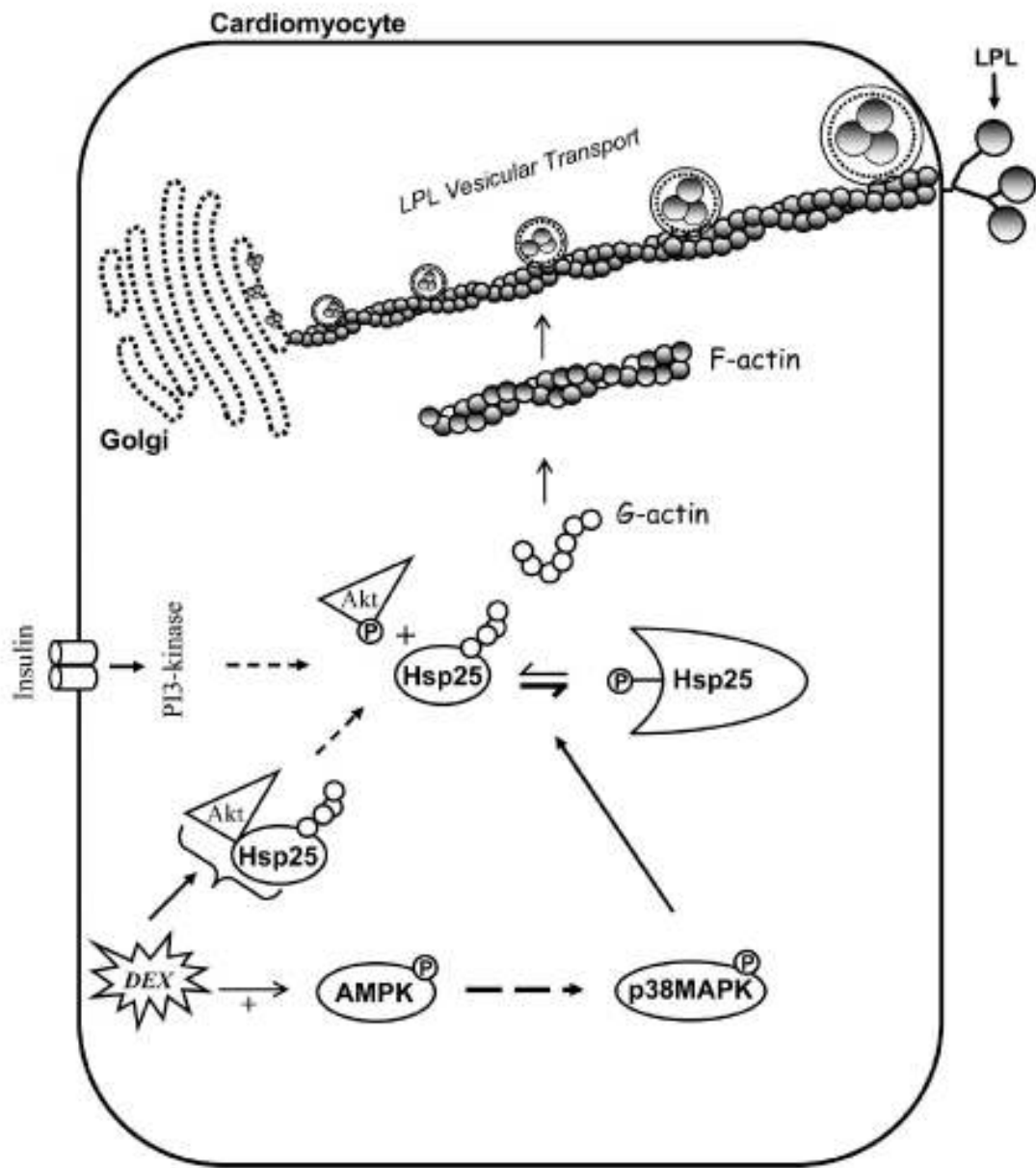


Fig. 3-8 Schematic of mechanisms that are likely involved in regulating the effects of DEX and insulin on cardiac LPL.

3.6 BIBLIOGRAPHY

- 1 An, D, Pulinillunnil, T, Qi D, Ghosh S, Abrahani A, Rodrigues B. The metabolic "switch" AMPK regulates cardiac heparin-releasable lipoprotein lipase. *Am J Physiol Endocrinol Metab* 2005;288:E246-253.
- 2 An D, Rodrigues B. Role of changes in cardiac metabolism in development of diabetic cardiomyopathy. *Am J Physiol Heart Circ Physiol* 2006;291:H1489-1506.
- 3 Augustus AS, Kako Y, Yagyu H, Goldberg IJ. Routes of FA delivery to cardiac muscle: modulation of lipoprotein lipolysis alters uptake of TG-derived FA. *Am J Physiol Endocrinol Metab* 2003;284:E331-339.
- 4 Bernal-Mizrachi C, Weng S, Feng C, Finck B.N, Knutsen RH, Leone TC. Dexamethasone induction of hypertension and diabetes is PPAR-alpha dependent in LDL receptor-null mice. *Nat Med* 2003;9:1069-1075.
- 5 Block NE, Buse MG. Effects of hypercortisolemia and diabetes on skeletal muscle insulin receptor function in vitro and in vivo. *Am J Physiol* 256:E39-48, 1989.
- 6 Buttgerit F, Scheffold A. Rapid glucocorticoid effects on immune cells. *Steroids* 2002;67:529-534.
- 7 Buttgerit F. Mechanisms and clinical relevance of nongenomic glucocorticoid actions. *Z Rheumatol* 2000;59:II/119-123.
- 8 Cato AC, Nestl A, Mink S. Rapid actions of steroid receptors in cellular signaling pathways. *Sci STKE* 2002;138:RE9.
- 9 Chiu HC, Kovacs A, Blanton RM, Han X, Courtois M, Weinheimer CJ, Yamada KA, Brunet S, Xu H, Nerbonne JM, Welch MJ, Fettig NM, Sharp TL, Sambandam N, Olson

KM, Ory DS, Schaffer JE. Transgenic expression of fatty acid transport protein 1 in the heart causes lipotoxic cardiomyopathy. *Circ Res* 2005;96:225-233.

10 Chiu HC, Kovacs A, Ford DA, Hsu FF, Garcia R, Herrero P, Saffitz JE, Schaffer JE. A novel mouse model of lipotoxic cardiomyopathy. *J Clin Invest* 2001;107:813-822.

11 Dai T, Natarajan R, Nast C.C, LaPage J, Chuang P, Sim J. Glucose and diabetes: effects on podocyte and glomerular p38MAPK, heat shock protein 25, and actin cytoskeleton. *Kidney Int* 2006;69:806-814.

12 DeFronzo RA, Jacot E, Jequier E, Maeder E, Wahren J, Felber JP. The effect of insulin on the disposal of intravenous glucose. Results from indirect calorimetry and hepatic and femoral venous catheterization. *Diabetes* 1981;30:1000-1007.

13 Dimitriadis G, Leighton B, Parry-Billings M, Sasson S, Young M, Krause U. Effects of glucocorticoid excess on the sensitivity of glucose transport and metabolism to insulin in rat skeletal muscle. *Biochem J* 1997;321 (Pt 3):707-712.

14 Eckel RH. Lipoprotein lipase. A multifunctional enzyme relevant to common metabolic diseases. *N Engl J Med* 1989;320:1060-1068.

15 Ewart H.S, Severson DL. Insulin and dexamethasone stimulation of cardiac lipoprotein lipase activity involves the actin-based cytoskeleton. *Biochem J* 1999;340 (Pt 2):485-490.

16 Ewart HS, Carroll R, Severson DL. Lipoprotein lipase activity in rat cardiomyocytes is stimulated by insulin and dexamethasone. *Biochem J* 1997;327:439-442.

17 Finck BN, Lehman JJ, Leone TC, Welch MJ, Bennett MJ, Kovacs A, Han X, Gross RW, Kozak R, Lopaschuk GD, Kelly DP. The cardiac phenotype induced by PPARalpha overexpression mimics that caused by diabetes mellitus. *J Clin Invest* 2002;109:121-130.

- 18 Giorgino F, Almahfouz A, Goodyear LJ, Smith RJ. Glucocorticoid regulation of insulin receptor and substrate IRS-1 tyrosine phosphorylation in rat skeletal muscle in vivo. *J Clin Invest* 1993;91:2020-2030.
- 19 Hardie DG, Hawley SA. AMP-activated protein kinase: the energy charge hypothesis revisited, *Bioessays* 2001;23:1112-1119.
- 20 Hunt KJ, Resendez RG, Williams K, Haffner SM, Stern MP. National Cholesterol Education Program versus World Health Organization metabolic syndrome in relation to all-cause and cardiovascular mortality in the San Antonio Heart Study. *Circulation* 2004;110:1251-1257.
- 21 Jessen N, Goodyear LJ. Contraction signaling to glucose transport in skeletal muscle. *J Appl Physiol* 2005;99:330-337.
- 22 Kewalramani G, An D, Kim MS, Ghosh, S, Qi, D, Abrahani A, Pulinilkunnil T, Shrama V, Wambolt RB, Allard MF, Innis SM, Rodrigues B. AMPK control of myocardial fatty acid metabolism fluctuates with the intensity of insulin-deficient diabetes. *J Mol Cell Cardiol* 2007;42:333-342.
- 23 Kim M, Kewalramani G, Puthanveetil P, Lee V, Kumar U, An D, Abrahani A, Rodrigues B. Acute diabetes moderates trafficking of cardiac lipoprotein lipase through p38 mitogen-activated protein kinase-dependant actin cytoskeleton organization. *Diabetes* 2007;57(1):64-76.
- 24 Kovacic C, Soltys CL, Barr AJ, Shiojima I, Walsh K, Dyck JR. Akt activity negatively regulates phosphorylation of AMP-activated protein kinase in the heart. *J Biol Chem* 2003;278:39422-39427.

- 25 Kudo N, Barr AJ, Barr RL, Desai S, Lopaschuk GD. High rates of fatty acid oxidation during reperfusion of ischemic hearts are associated with a decrease in malonyl-CoA levels due to an increase in 5'-AMP-activated protein kinase inhibition of acetyl-CoA carboxylase. *J Biol Chem* 1995;270:17513-17520.
- 26 Lee YH, White MF. Insulin receptor substrate proteins and diabetes. *Arch Pharm Res* 2004;27:361-370.
- 27 Lesnefsky EJ, Moghaddas S, Tandler B, Kerner J, Hoppel CL. Mitochondrial dysfunction in cardiac disease: ischemia--reperfusion, aging, and heart failure. *J Mol Cell Cardiol* 2001;33:1065-1089.
- 28 Levak-Frank S, Hofmann W, Weinstock PH, Radner H, Sattler W, Breslow JL. Induced mutant mouse lines that express lipoprotein lipase in cardiac muscle, but not in skeletal muscle and adipose tissue, have normal plasma triglyceride and high-density lipoprotein-cholesterol levels. *Proc Natl Acad Sci U S A* 1999;96:3165-3170.
- 29 Li J, Miller EJ, Ninomiya-Tsuji J, Russell RR, 3rd and Young LH. AMP-activated protein kinase activates p38 mitogen-activated protein kinase by increasing recruitment of p38 MAPK to TAB1 in the ischemic heart. *Circ Res* 2005;97:872-879.
- 30 Luiken JJ, Coort SL, Willems J, Coumans WA, Bonen A, van der Vusse GJ. Contraction-induced fatty acid translocase/CD36 translocation in rat cardiac myocytes is mediated through AMP-activated protein kinase signaling. *Diabetes* 52:1627-1634, 2003.
- 31 Opie LH. Cardiac metabolism--emergence, decline, and resurgence. Part II. *Cardiovasc Res* 1992;26:817-830.

- 32 Phillips DI, Barker DJ, Fall CH, Seckl JR, Whorwood CB, Wood PJ, Walker BR. Elevated plasma cortisol concentrations: a link between low birth weight and the insulin resistance syndrome? *J Clin Endocrinol Metab* 1998;83:757-760.
- 33 Pillarisetti S, Paka L, Sasaki A, Vanni-Reyes T, Yin B, Parthasarathy N, Wagner WD, Goldberg IJ. Endothelial cell heparanase modulation of lipoprotein lipase activity. Evidence that heparan sulfate oligosaccharide is an extracellular chaperone. *J Biol Chem* 1997;272:15753-15759.
- 34 Pulinilkunnil T, An D, Ghosh S, Qi D, Kewalramani G, Yuen G, Virk N, Abrahani A, Rodrigues B. Lysophosphatidic acid-mediated augmentation of cardiomyocyte lipoprotein lipase involves actin cytoskeleton reorganization. *Am J Physiol Heart Circ Physiol* 2005;288:H2802-2810.
- 35 Pulinilkunnil T, Rodrigues B. Cardiac lipoprotein lipase: metabolic basis for diabetic heart disease. *Cardiovasc Res* 2006;69(2):329-340.
- 36 Qi D, An D, Kewalramani G, Qi Y, Pulinilkunnil T, Abrahani A, Al-Atar U, Ghosh S, Wambolt RB, Allard MF, Innis SM, Rodrigues B. Altered cardiac fatty acid composition and utilization following dexamethasone-induced insulin resistance. *Am J Physiol Endocrinol Metab* 2006;291:E420-427.
- 37 Qi D, Pulinilkunnil T, An D, Ghosh S, Abrahani A, Pospisilik JA, Brownsey R, Wambolt R, Allard M, Rodrigues B. Single-dose dexamethasone induces whole-body insulin resistance and alters both cardiac fatty acid and carbohydrate metabolism. *Diabetes* 2004;53:1790-1797.
- 38 Qi D, Rodrigues B. Glucocorticoids produce whole body insulin resistance with changes in cardiac metabolism. *Am J Physiol Endocrinol Metab* 2007;292(3):E654-E657.

- 39 Rodrigues B, Cam MC, Jian K, Lim F, Sambandam N, Shepherd G. Differential effects of streptozotocin-induced diabetes on cardiac lipoprotein lipase activity. *Diabetes* 1997;46:1346-1353.
- 40 Ruzzin J, Wagman AS, Jensen, J. Glucocorticoid-induced insulin resistance in skeletal muscles: defects in insulin signalling and the effects of a selective glycogen synthase kinase-3 inhibitor. *Diabetologia* 2005;48:2119-2130.
- 41 Sambandam N, Abrahani MA, St Pierre E, Al-Atar O, Cam MC, Rodrigues B. Localization of lipoprotein lipase in the diabetic heart: regulation by acute changes in insulin. *Arterioscler Thromb Vasc Biol* 1999;19:1526-1534.
- 42 Schacke H, Docke WD, Asadullah K. Mechanisms involved in the side effects of glucocorticoids. *Pharmacol Ther* 2002;96:23-43.
- 43 Severino C, Brizzi P, Solinas A, Secchi G, Maioli M, Tonolo G. Low-dose dexamethasone in the rat: a model to study insulin resistance. *Am J Physiol Endocrinol Metab* 2002;283:E367-373.
- 44 Song IH, Buttgerit F. Non-genomic glucocorticoid effects to provide the basis for new drug developments. *Mol Cell Endocrinol* 2006;246:142-146.
- 45 Tan Y, Rouse J, Zhang A, Cariati S, Cohen P, Comb MJ. FGF and stress regulate CREB and ATF-1 via a pathway involving p38 MAP kinase and MAPKAP kinase-2. *Embo J* 1996;15:4629-4642.
- 46 Wu Y, Song P, Xu J, Zhang M, Zou MH. Activation of protein phosphatase 2A by palmitate inhibits AMP-activated protein kinase. *J Biol Chem* 2007;282:9777-9788.
- 47 Yagyu H, Chen G, Yokoyama M, Hirata K, Augustus A, Kako Y, Seo T, Hu Y, Lutz EP, Merkel M, Bensadoun A, Homma S, Goldberg IJ. Lipoprotein lipase (LpL) on the

surface of cardiomyocytes increases lipid uptake and produces a cardiomyopathy. *J Clin Invest* 2003;111:419-426.

48 Zheng, C, Lin Z, Zhao ZJ, Yang Y, Niu H, Shen X. MAPK-activated protein kinase-2 (MK2)-mediated formation and phosphorylation-regulated dissociation of the signal complex consisting of p38, MK2, Akt, and Hsp27. *J Biol Chem* 2006;281:37215-37226.

4 AMP-ACTIVATED PROTEIN KINASE CONFERS PROTECTION AGAINST TNF-ALPHA INDUCED CARDIAC CELL DEATH⁴

4.1 INTRODUCTION

Tumor necrosis factor-alpha (TNF- α), expressed as a 26 kDa membrane bound protein, is cleaved by TNF- α converting enzyme to produce a soluble 17 kDa biologically active protein (1; 2). Primarily produced by macrophages (3; 4), TNF- α is also synthesized by a variety of other cell types including lymphoid (5), endothelial (6) and mast cells (7), adipose (8) and neuronal tissue (9), fibroblasts (10) and cardiac myocytes (11). The effects of TNF- α are mediated by its binding to two distinct cellular receptors, TNFR1 and TNFR2. Although stimulation of cells with TNF- α regulates numerous cellular and biological processes such as immune function, cell proliferation, differentiation, and energy metabolism (12), binding of excess TNF- α to TNFR1 activates the programmed cell death (apoptosis) pathway. This includes formation of the death-inducing signaling complex, activation of the caspase cascade (13), impairment of mitochondrial integrity, cytochrome C release (14), and eventually apoptosis in a multitude of cells including fibroblasts, vascular smooth muscle, endothelial cells and cardiomyocytes.

Elevated plasma or endogenous cardiac TNF- α levels have been reported to cause myocyte apoptosis (15) leading to cardiomyocyte loss with associated cardiovascular diseases. For example, transgenic mice with cardiac specific overexpression of TNF- α demonstrate increased apoptosis and develop cardiac hypertrophy and dilated cardiomyopathy (16; 17). Stress can cause cardiomyocytes and resident macrophages to

⁴ "A version of this chapter has been accepted for publication. Kewalramani, G. Puthanveetil, P. Wang, F. Kim, MS. Deppe, S. Abrahani, A. Luciani, DS. Johnson, JD. Rodrigues, B. (2009) AMP-activated protein kinase confers protection against TNF-alpha induced cardiac cell death. Cardiovasc Res."

produce TNF- α that binds to myocardial TNFR1 and induces apoptosis. Augmented plasma TNF- α levels and increased expression of TNFR1 in the arterial wall have been found to promote atherosclerosis (18). This cytokine has also been suggested to contribute towards cardiomyocyte cell death and cardiac dysfunction in clinical conditions like sepsis (19), chronic heart failure and ischemia-reperfusion injury (20), and cardiac allograft rejection (21). Till date, a variety of apoptotic mediators have been proposed to facilitate TNF- α induced cardiomyocyte apoptosis, which include ceramides (22), nitric oxide (23) and mitogen-activated protein kinases (24). Regulation of myocardial apoptosis is also achieved by the Bcl-2 family of proteins (25), Bad, which initiates apoptosis induced signaling, and Bcl-xL that blocks activation of effector caspases and induction of apoptosis.

The fuel gauge AMP-activated protein kinase (AMPK) facilitates ATP production to meet energy demands during metabolic stress (26). Allosteric binding of AMP or phosphorylation by upstream kinases (tumor suppressor kinase-LKB1; Ca²⁺ calmodulin-dependent protein kinase kinases-CaMKK) activates AMPK (27). Once activated, AMPK facilitates substrate delivery and subsequent oxidation to generate ATP. Although a substantial role for AMPK has been established in regulating cardiac metabolism, a less studied action of AMPK is its ability to prevent cell death. In non-cardiac cells like endothelial cells or astrocytes, activation of AMPK has been shown to protect against hyperglycemia or high fat induced apoptotic cell death (28; 29). In H9c2 rat cardiac muscle cell lines or adult cardiomyocytes, AMPK activation protects against reactive oxygen species or high fat induced cell death (30). Using established AMPK activators like dexamethasone (DEX) or metformin (MET), the objective of the present

study was to determine if AMPK activation prevents TNF- α -induced apoptosis in adult rat ventricular cardiomyocytes. Our data demonstrate that by phosphorylating Bad and maintaining the anti-apoptotic property of Bcl-xL, AMPK confers protection against TNF- α -induced apoptosis.

4.2 MATERIALS AND METHODS

4.2.1 Experimental animals

The investigation conforms with the guide for the care and use of laboratory animals published by the US National Institutes of Health (NIH Publication No. 85-23, revised 1996), and the University of British Columbia. Adult male Wistar rats (260-300 g) were obtained from the UBC Animal Care Unit and given free access to a standard laboratory diet (PMI Feeds, Richmond, VA, USA) and water.

4.2.2 Isolation of cardiomyocytes

Ventricular myocytes were prepared by a previously described procedure (31). Briefly, myocytes were made calcium-tolerant by successive exposure to increasing concentrations of calcium. Our method of isolation yields a highly enriched population of calcium-tolerant myocardial cells that are rod-shaped (over 80%) in the presence of 1 mmol/l Ca^{2+} , with clear cross striations. Intolerant cells are intact but hypercontract into vesiculated spheres. Yield of myocytes was determined microscopically using an improved Neubauer haemocytometer. Myocyte viability was assessed as the percentage of elongated cells with clear cross striations that excluded 0.2% trypan blue. Cardiomyocytes were plated on laminin-coated six-well culture plates to a density of 200,000 cells/well. Following time for adhesion (3 hr), cells were counted again (approximately 160,000 cells adhere/plate), and incubations initiated. Cells were maintained using Media-199 at 37°C under an atmosphere of 95% O_2 /5% CO_2 . Where indicated, dexamethasone (DEX, 100 nM), metformin (MET, 2 mM) (we have previously reported that these concentrations of DEX and MET were optimal to activate AMPK)

(32; 33), or TNF- α (0-100 ng/ml) were added to the culture medium and myocytes kept for varying durations (0-12 hr). At the indicated times, cells were used for evaluation of intracellular calcium and apoptotic cell death. In separate experiments, cells were scraped and washed twice with 0.5 ml PBS. Samples were lysed in ice-cold buffer and myocyte cell lysates were used for Western blot, immunoprecipitation, and gene estimations. Where indicated, STO609 (2 μ M), RU486 (10 μ M) or Compound C (40 μ M) were used to inhibit CAMKK β , glucocorticoid receptor, or AMPK respectively. Compound C is a cell-permeable, selective and reversible, competitive inhibitor of AMPK.

4.2.3 Administration of DEX to control rats

To examine whether DEX administration in vivo would maintain its protective effect against TNF- α induced cell death in vitro, DEX (1 mg/kg) or an equivalent volume of ethanol was administered by intraperitoneal injection and the animals killed 4 hr later (plasma half-life of DEX is \sim 279 min). The hearts removed were used either for determination of whole heart AMPK or preparation of cardiomyocytes. For the latter procedure, myocytes from control and DEX treated hearts were plated for 8 hr in the presence or absence of TNF- α .

4.2.4 Estimation of cardiomyocyte intracellular free Ca²⁺

Ca²⁺ was measured using the Fura 2-AM method as described previously (34). Briefly, cardiomyocytes were plated on glass cover slips with etched grids. Plated cardiomyocytes were then transferred to an imaging chamber mounted on a temperature-controlled stage and held at 37°C on a Zeiss Axiovert 200 M inverted microscope equipped with a FLUAR 20 \times objective (Carl Zeiss, Thornwood, NY). For Ca²⁺

measurements, cells were loaded for 30 min with 5 μ M of the Ca^{2+} sensitive dye Fura-2 (Molecular Probes/Invitrogen) in Ringer's solution containing (in mM): NaCl 144, KCl 5.5, MgCl_2 1, CaCl_2 2, Hepes 20 (adjusted to pH 7.35 by NaOH) and washed twice to remove any extracellular dye. Fura-2 was excited at 340 nm and 380 nm and the emitted fluorescence was monitored through a D510/80m filter. The Ca^{2+} levels at rest as well as maximal increases evoked by DEX were determined and expressed as the ratio of the fluorescence emission intensities (F_{340}/F_{380}).

4.2.5 Measurement of apoptosis

To examine TNF- α induced apoptosis and the influence of DEX and MET on this process, cells were examined for a) morphological evidence of apoptosis using the fluorescent DNA-binding dye, Hoechst 33342 (Sigma) or b) changes in caspase-3 (enzyme that plays a key role in apoptosis) activity using an assay kit or Western blot. Cells were stained with 5 μ g/ml Hoechst 33342, and viewed on a Zeiss IM fluorescence microscope ($\times 400$) (Carl Zeiss Canada, Toronto, ON, Canada). Cells were scored as apoptotic if they exhibited unequivocal nuclear chromatin condensation and/or fragmentation. To quantify apoptosis, 500 nuclei from three different myocyte preparations were randomly picked and examined, and the results presented as apoptotic cells per 1,000 cells. Caspase-3 activity was determined using a fluorescent caspase-3 assay kit. Briefly, myocytes were lysed and protein extracted by centrifugation at 5,000 g for 5 min. 50 μ l of protein were added to an equal volume of reaction buffer that contained 50 μ mol/l of the respective substrate, and incubated at room temperature for 30 min. The enzyme-catalyzed release of aminomethylcoumarin was quantified in a fluorimeter (Perspective Biosystems, Framingham, MA, USA) at 380/450-nm

wavelengths. Protein was determined using a Bradford assay (Bio-Rad, Hercules, CA, USA). Caspase-3 activity is presented as activity per milligram of protein for each sample. Caspase-3 activation was also confirmed by measuring cleaved caspase-3 using Western blot.

4.2.6 Separation of mitochondrial and cytosolic fractions

Cardiomyocytes were collected in ice cold PBS, spun down, resuspended in cytosol extraction buffer mix, vortexed and incubated on ice for 10 min. Samples were centrifuged at 2600 rpm (700 xg) for 10 min and the supernatant transferred and spun at 9600 rpm (10000 xg) for 30 min to precipitate mitochondria. Supernatant was removed as the cytosolic fraction and the pellet was resuspended in mitochondrial extraction buffer mix as the mitochondrial fraction.

4.2.7 Western Blot

Western blot was carried out as described previously (35). Briefly, plated myocytes (0.4×10^6) were homogenized in ice-cold lysis buffer. After centrifugation at 5,000 g for 20 min, the protein content of the supernatant was quantified using a Bradford protein assay. Samples were diluted, boiled with sample loading dye, and 50 μ g used in SDS-polyacrylamide gel electrophoresis. After transfer, membranes were blocked in 5% skim milk in Tris-buffered saline containing 0.1% Tween-20. Membranes were incubated with rabbit total AMPK- α , phospho-AMPK (Thr-172), phospho-ACC, Bcl-xL, Prohibitin-1 (PHB1), GAPDH, cleaved caspase-3 (Asp175), caspase-3, total Bad, phospho-Bad (Ser112), phospho-CAMKI (Thr177), total CaMKI and cytochrome C antibodies and subsequently with secondary goat anti-rabbit or goat anti-mouse horseradish peroxidase-conjugated antibodies, and visualized using the ECL detection kit (Amersham).

4.2.8 Immunoprecipitation

Cell lysates were immunoprecipitated using a Bad monoclonal antibody rotating overnight at 4°C. The immunocomplex and the supernatant were resuspended in Laemmli buffer and heated for 5 min at 95°C. The immunocomplex was separated into two equal portions, each of which was immunoblotted with anti-Bcl-xL and anti-Bad using Western blot.

4.2.9 Cardiomyocyte AMPK gene expression

AMPK gene expression was measured in cardiac cells using RT-PCR (36). Briefly, total RNA from control and treated cardiomyocytes was extracted using TRIzol (Invitrogen), and reverse transcription was carried out using an oligo(dT) primer and SuperScript II RT (Invitrogen). cDNA was amplified using AMPK [5'-GCTGTGGATCGCCAAATTAT-3' (*left*) and 5'-GCATCAGCAGAGTGGCAATA-3' (*right*)]-specific primers. The β -actin gene was amplified as an internal control using 5'-TGGTGGGTATGGGTCAGAAGG-3' (*left*) and 5'-ATCCTGTCAGCGATGCCTGGG-3' (*right*). The amplification parameters were set at 94°C for 1 min, 58°C for 1 min, and 72°C for 1 min for a total of 30 cycles. The PCR products were electrophoresed on a 1.7% agarose gel containing ethidium bromide. Expression levels were represented as the ratio of signal intensity for AMPK mRNA relative to β -actin mRNA.

4.2.10 Materials

Total AMPK- α , phospho-AMPK- α (Thr¹⁷²), phospho ACC, Bcl-xL, GAPDH, prohibitin (PHB1), cleaved caspase-3 (Asp¹⁷⁵) and caspase-3 antibodies were obtained from Cell Signaling (Danvers, MA). Total Bad, phospho-Bad (Ser¹¹²), Total CaMKI, phospho-

CaMKI (Thr¹⁷⁷) and cytochrome C antibodies were obtained from Santa Cruz Biotechnology, Inc. (Santa Cruz, CA). EnzChek Caspase-3 Assay Kit was obtained from Molecular Probes, (Eugene, OR). The CAMKK β inhibitor STO609 was obtained from Calbiochem, (La Jolla, CA). All other chemicals were obtained from Sigma Chemical.

4.2.11 Statistical Analysis

Values are means \pm SE. Wherever appropriate, one-way ANOVA followed by Tukey's or Bonferroni tests to determine differences between group mean values. The level of statistical significance was set at $P < 0.05$.

4.3 RESULTS

4.3.1 Influence of DEX on total and phosphorylated AMPK in isolated cardiac

myocytes Previous studies from our laboratory have reported an increased phosphorylation and activation of AMPK in hearts from 4 hr DEX treated animals (37). To assess direct activation of AMPK, control cardiomyocytes were incubated with DEX for varying times. In the absence of DEX, no change in AMPK phosphorylation was observed over time (data not shown). DEX induced a time dependent increase in AMPK phosphorylation, an effect that peaked at 2 hr and was maintained upto 8 hr (Figure 4-1A). Once activated, AMPK phosphorylates and inactivates ACC. Similar to AMPK, ACC phosphorylation increased temporally in DEX treated cardiomyocytes (Figure 4-1A, immunoblot). The increase in AMPK phosphorylation (upto 4 hr) following DEX could not be explained by any changes in AMPK total protein or gene expression. An augmentation in total AMPK protein and gene expression only became apparent 8 hr after DEX incubation (Figure 4-1B and C).

4.3.2 Changes in cardiomyocyte intracellular calcium and CaMKI phosphorylation following DEX

Elevation in cytosolic calcium increases the phosphorylation of CaMKI (Thr177), an upstream regulator of AMPK (38; 39). To determine the mechanism by which DEX induces the early activation of AMPK, we measured intracellular calcium and CaMKI phosphorylation. Cells treated with DEX displayed a robust increase in intracellular calcium (Figure 4-2A). Peak responses were recorded within 5 min, and were maintained upto 25 min after DEX. Although the calcium response declined over time, it was

maintained above baseline upto 1 hr after DEX (Figure 4-2A). CaMKI (Thr¹⁷⁷) phosphorylation followed the rise in intracellular calcium observed with DEX; an increased phosphorylation was observed within 15 min of DEX incubation (Figure 4-2B). Interestingly, CAMKI phosphorylation peaked at 60 min followed by a return to near control levels after 8 hr of DEX (Figure 4-2B). No change in total CaMKI protein was observed with DEX treatment (Figure 4-2B, immunoblot).

4.3.3 Dual regulation of AMPK phosphorylation by DEX

To validate the impact of CAMKI on AMPK phosphorylation, cardiomyocytes were treated with DEX in the presence or absence of STO609, a specific inhibitor of CaMKK β , an upstream regulator of CaMKI. STO609 prevented the DEX induced phosphorylation of CAMKI (Figure 4-3A) and AMPK (Figure 4-3B) at 2 hr, an effect that was absent when the incubation with DEX was extended to 8 hr (Figure 4-3C). By itself, STO609 had no effect on CaMKI or AMPK phosphorylation (data not shown). Interestingly, the glucocorticoid receptor antagonist RU486 did not influence the early (2 hr) impact of DEX on CaMKI (Figure 4-3A), or AMPK phosphorylation (Figure 4-3B), suggesting that at this time, the effects of DEX are likely mediated by calcium. However, at 8 hr, RU486 abrogated the DEX induced increase in AMPK phosphorylation (Figure 4-3C) and total AMPK and gene expression (Figure 4-3C, immunoblots).

4.3.4 TNF- α mediated effects on cardiomyocyte cell death

An initial experiment was performed to determine the concentration and time required for TNF- α to induce optimal cardiomyocyte cell death. Cardiomyocytes were exposed to various concentrations of TNF- α (0-100 ng/ml) and caspase-3 activity determined. As concentrations of TNF- α between 10 and 100 ng/ml produced comparable levels of

caspase-3 activation (Figure 4-4A), a dose of 10 ng/ml was used for all subsequent experiments. Using this concentration of TNF- α , a time-dependant assay revealed similar levels of caspase-3 activation (Figure 4-4B) and apoptotic cell death (Figure 4-4C and supplementary Figure 4-S1) after 8 and 12 hr. Thus, 8 hr was chosen as the optimum period for all subsequent experiments utilizing TNF- α .

4.3.5 AMPK regulation of TNF- α mediated caspase-3 activation and cell death

MET is an established activator of AMPK in cardiomyocytes (33). Treatment of control myocytes with DEX or MET for 8 hr resulted in an increase in AMPK phosphorylation, with DEX displaying an approximate two-fold greater AMPK activation compared to MET (Figure 4-5A). Interestingly, the DEX induced changes in AMPK phosphorylation were accompanied by an increase in total AMPK protein, an effect that was absent with MET (Figure 4-5A, immunoblot). Although TNF- α by itself marginally suppressed AMPK phosphorylation, both DEX or MET were still able to activate AMPK in the presence of this cytokine (Figure 4-5A). TNF- α had no influence on total AMPK protein, either by itself or in the presence of DEX (Figure 4-5A, immunoblot). Both DEX or MET induced a robust reduction in the TNF- α induced activation of caspase-3 (Figure 4-5B and C). Figure 4-5D describes the protective effects of these AMPK activators on TNF- α induced cardiomyocyte cell death. In the control group, less than 60 of 1,000 cells were scored as apoptotic. TNF- α significantly increased apoptosis (623/1,000 cells). Introducing DEX and MET into the medium significantly lowered the number of apoptotic cells (DEX, 182/1,000; MET, 196/1,000). Counting the total number of surviving cells revealed that with TNF- α , a survival rate of 39% was observed. Addition of DEX and MET increased the survival of cardiomyocytes to 83% and 84%

respectively. These data suggest that under our experimental conditions, the TNF- α induced cell death is predominantly apoptotic in nature.

In vivo, DEX after 4 hr increased AMPK phosphorylation, an effect that was maintained until 8 hr (see supplementary, Figure 4-S2A). This change in AMPK phosphorylation paralleled a rise in total AMPK protein and gene expression (see supplementary material online, Figure 4-S2A, insets). Interestingly, AMPK remained activated in myocytes from DEX treated animals, an effect that remained unchanged on addition of TNF- α for 8 hr (see supplementary material online, Figure 4-S2B). More importantly, the protective effect of DEX against TNF- α induced caspase activation was maintained in these myocytes even in the direct absence of DEX in the culture media (see supplementary material online, Figure 4-S2C).

4.3.6 DEX induced effects on Bad phosphorylation and cytochrome C release

The pro-apoptotic protein Bad plays a significant role in activating the caspase cascade of cell death. To determine if DEX inhibits TNF- α induced apoptosis by phosphorylating and inactivating Bad, we examined Bad phosphorylation in control myocytes treated with DEX. Phospho Bad (Ser112) levels were significantly higher by 30 min, reached near maximal values by 2 hr, and remained activated upto 8 hr after DEX treatment (Figure 4-6A). No change in total Bad protein was observed over time (Figure 4-6A, immunoblot). Bad phosphorylation reduces its association with Bcl-xL, thus maintaining the anti-apoptotic function of this protein. In the presence of TNF- α , Bad phosphorylation was reduced (Figure 4-6B, immunoblot), with a corresponding increase in its interaction with Bcl-xL (Figure 4-6B). Addition of DEX to the incubation medium resulted in a dramatic loss of association between Bad and Bcl-xL (Figure 4-6B), and was consistent with a

phosphorylation-induced dissociation (Figure 4-6B, immunoblot). Release of mitochondrial cytochrome C to the cytosol is a critical step in the mechanism of TNF- α induced apoptotic cell death. Figure 4-6C shows a dramatic increase in cytosolic cytochrome C levels in TNF- α treated myocytes, an effect that was prevented by addition of DEX.

4.3.7 Consequence of AMPK inhibition on Bad phosphorylation and TNF- α induced caspase-3 activation

To confirm if DEX induced AMPK activation influences Bad phosphorylation, we used Compound C to inhibit AMPK phosphorylation. Pre-incubation of cardiomyocytes with Compound C abolished the DEX induced activation of AMPK (Figure 4-7A). Compound C had no effect on the DEX induced augmentation of total AMPK protein (Figure 4-7A, immunoblot). Interestingly, this decrease in AMPK phosphorylation led to a substantial reduction in Bad (Ser112) phosphorylation (Figure 4-7B). To evaluate the effects of AMPK inhibition on TNF- α mediated caspase-3 activation, cells were treated with TNF- α , DEX and Compound C. Addition of Compound C to cells treated with DEX + TNF- α reduced phosphorylation of AMPK (Figure 4-7C) and Bad (Figure 4-7C, immunoblot), increased the association between Bad and Bcl-xL (Figure 4-7D) and provoked caspase-3 activation (Figure 4-7E).

4.3.8 Cardioprotective effects of MET against TNF- α induced caspase-3 activation

Metformin time dependently stimulated AMPK phosphorylation without changing total AMPK protein (see supplementary, Figure 4-S3A). In the presence of TNF- α , metformin like dexamethasone: a) increased Bad phosphorylation (see supplementary, Figure 4-S3B, inset), b) reduced the association between Bad and Bcl-xL (see supplementary,

Figure 4-S3B), c) decreased cytochrome c release (see supplementary material online, Figure 4-S3C), and d) significantly lowered caspase-3 activation (see supplementary, Figure 4-S3D). Pre-incubation of cardiomyocytes with Compound C prevented all of these effects (see supplementary, Figure 4-S4A-E). Collectively, our results imply that once AMPK is activated by DEX or MET, similar mechanisms are turned on to protect against TNF- α induced cell death.

4.4 DISCUSSION

TNF- α has been reported to induce apoptosis in numerous cell types through its activation of a variety of signaling pathways. In cardiac myocytes, these include increased expression of iNOS (40), production of ceramides (22), and activation of the mitogen activated protein kinase (MAPK) pathway (24). Limited information is available that documents signaling mechanisms that protect myocytes against TNF- α induced apoptosis. Our data suggests that activation of AMPK using DEX or MET protects adult cardiomyocytes against TNF- α induced apoptosis by phosphorylating Bad, thereby preventing cytochrome c release and attenuating caspase-3 activation.

In cardiac cells, AMPK is the switch that regulates cellular energy during metabolic stress (26). Activation of AMPK can occur as a consequence of a rise in the AMP/ATP ratio (when ATP is depleted) or through its regulation by upstream kinases like LKB1 and CaMKK β (27). Glucocorticoids such as DEX, which are potent anti-inflammatory drugs used for the treatment of a number of human diseases, are believed to act via both non-genomic (rapid) and genomic pathways (41). In the present study, DEX treatment of cardiomyocytes led to an early (within 1 hr) increase in AMPK phosphorylation that was sustained upto 8 hr after DEX. Although this early increase in AMPK phosphorylation may well be a product of the rapid action of glucocorticoids to compromise ATP production, that highlights its actions as an immunosuppressant to reduce inflammatory processes (42) this is unlikely to occur in the heart that is fundamentally dependant on this nucleotide for its normal functioning. In the absence of this mechanism, a possible candidate to explain the early activation of AMPK is calcium. Elevation of intracellular calcium activates CaMKK β , which directly phosphorylates CaMKI (Thr177), an

upstream regulator of AMPK (38; 39; 43). Glucocorticoids transiently via non-genomic pathway increases Ca^{2+} in many cell types including brain synaptosomes (44) and cultured hippocampal (44) cells. In the heart, DEX treatment improves the reduced myocardial function and metabolism in acute myocardial infarction by its influence on intracellular Ca^{2+} levels (45). In rat neonatal cardiomyocytes, DEX augments intracellular calcium levels by increasing the activity of L-type calcium channels (46). Given this established role of DEX in influencing cellular calcium levels, we measured and document a rapid and transient increase in intracellular calcium followed by a rise in CaMKI on *in vitro* exposure of cardiomyocytes to this glucocorticoid. As STO-609 (a selective cell-permeable inhibitor of CaMKK), and not RU486 (a glucocorticoid receptor antagonist), inhibited the activities of CaMKI and AMPK, our data suggest that early activation of AMPK by DEX is independent of receptor stimulation and likely mediated through a calcium/CaMKI pathway. Interestingly, AMPK activation by DEX was maintained upto 8 hr, even though intracellular calcium declined, and CaMKI phosphorylation returned to near normal levels. As glucocorticoids act predominantly through genomic mechanisms that include binding to a cytosolic receptor, relocation into the nucleus, and an increase or decrease in gene expression (47) we measured AMPK protein and gene expression, and report an increase only after 8 hr of DEX. Given that RU486 and not STO-609 prevented the DEX induced increases in AMPK protein and gene expression and phosphorylation at this time, our data imply that activation of AMPK at 8 hr is receptor mediated and genomic in nature.

Cardiac failure induced by $\text{TNF-}\alpha$ is either a consequence of direct reduction in contractility (48) or stimulation of myocyte apoptosis (49). In this study, appreciable

activation of caspase-3 and evidence of apoptosis in rat cardiomyocytes occurred at a concentration of 10 ng/ml TNF- α and within 8 hr of incubation. Using different cell types, other studies have also reported similar concentration and time dependant effects of TNF- α on this mode of cell death (50). To evaluate the influence of AMPK activation on protecting cardiomyocytes against TNF- α mediated apoptosis, we used DEX or MET. Interestingly, when compared to MET, AMPK phosphorylation in myocytes treated with DEX was approximately two-fold higher, and probably was a reflection of both the non-genomic and genomic actions of DEX. Activation of AMPK with DEX or MET was associated with a robust reduction in TNF- α induced caspase-3 activation and apoptotic cell death. As these effects were apparent even with a disparate activation of AMPK, our data suggests that a threshold for AMPK activation likely exists to suppress the action of TNF- α on apoptosis. In support of these findings, other studies have also documented beneficial effects of AMPK activation against other initiators of cell death. For example, in H9c2 cardiac cells, AMPK activation has been shown to protect against reactive oxygen species mediated cell death (30). In osteoblasts, AICAR by activating AMPK, has been shown to inhibit palmitate induced apoptosis (51). In adult cardiomyocytes, we have reported that activation of AMPK by MET protects against palmitate induced cell death (33). Other studies have also reported that MET confers cardioprotection against myocardial infraction and heart failure by activating AMPK (52; 53). Overall, our data suggest that although these drugs are used as anti-inflammatory agents (DEX) or insulin sensitizers (MET), their common property to phosphorylate AMPK confers protection against cytokine induced cardiac cell death.

The function of Bad, a pro-apoptotic protein, is tightly regulated by phosphorylation. Bad phosphorylation facilitates its association with 14:3:3 proteins and prevents its translocation to the mitochondria. This event limits its interaction with the anti-apoptotic protein Bcl-xL, allowing the latter protein to promote cell survival (24). Maintenance of Bad phosphorylation has been reported to prevent apoptosis of rat hepatic sinusoidal endothelial cells (54). In failing hearts, a significant decrease in phosphorylated Bad (Ser112) has been reported to initiate apoptosis (55). TNF- α is known to decrease Bad phosphorylation, augment its association with Bcl-xL and promote cytochrome c release and caspase-3 activation (56), effects that were duplicated in the present study. DEX treatment of cardiomyocytes led to a rapid and sustained increase in the phosphorylation of Bad, an effect that was comparable to its influence on AMPK phosphorylation. As compound C prevented the DEX induced activation of AMPK and phosphorylation of Bad, our data suggest that AMPK is an upstream regulator of Bad. More importantly, the effect of DEX on Bad phosphorylation reduced the TNF- α mediated association between Bad and Bcl-xL, and prevented the release of cytochrome c (Figure. 4-6 and 4-8). As compound C abrogated all of these effects, our data suggest that in addition to its previously reported modulation of cardiac metabolism, AMPK can promote cardiomyocyte cell survival through its regulation of Bad and the mitochondrial apoptotic mechanism.

In summary, irrespective of the mechanism by which AMPK is phosphorylated, its activation is crucial for imparting protection to the cardiomyocyte against TNF- α induced cytotoxicity. As the production of TNF- α is widely reported to increase during obesity,

diabetes (57) and ischemia reperfusion (58) activation of AMPK in these conditions may protect against this specific cytokine induced cardiac injury.

4.5 FIGURES

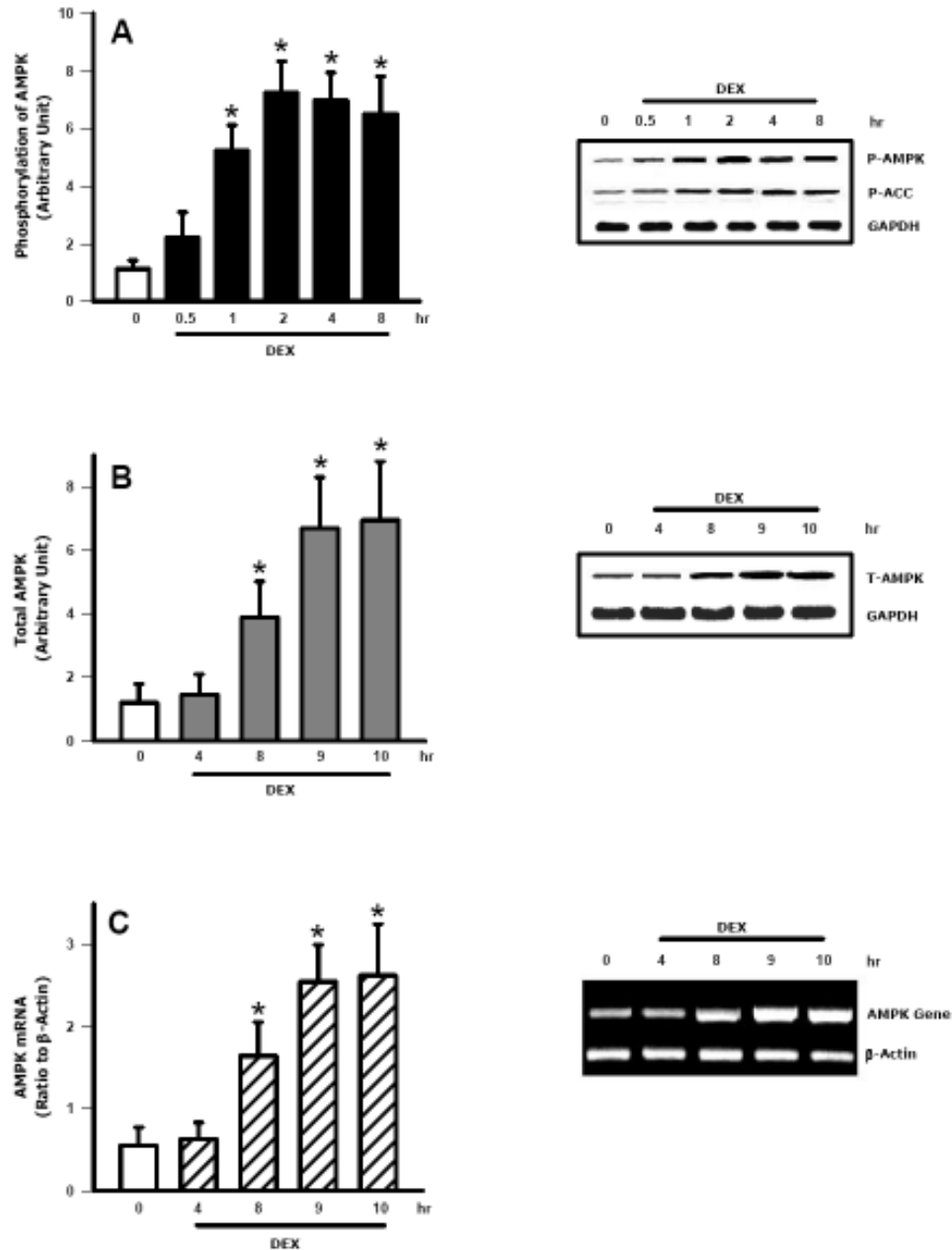


Fig. 4-1 Time dependant changes in AMPK in control and DEX treated cardiomyocytes. Cardiomyocytes were plated on laminin-coated culture plates. Cells were maintained using Medium 199 and incubated at 37°C under an atmosphere of 95% O₂–5% CO₂ for 16 hr. Subsequently, DEX (100 nM) was added to the culture medium. At the indicated times, cells were scraped and protein extracted to determine phosphorylated AMPK (A) and ACC (A, immunoblot), and total AMPK (B) using Western blotting. AMPK gene expression was evaluated using RT-PCR (C). Results are mean \pm SE of 5 myocyte preparations in each group. *Significantly different from untreated control (0 min), $P < 0.05$. DEX, dexamethasone; P, phosphorylated.

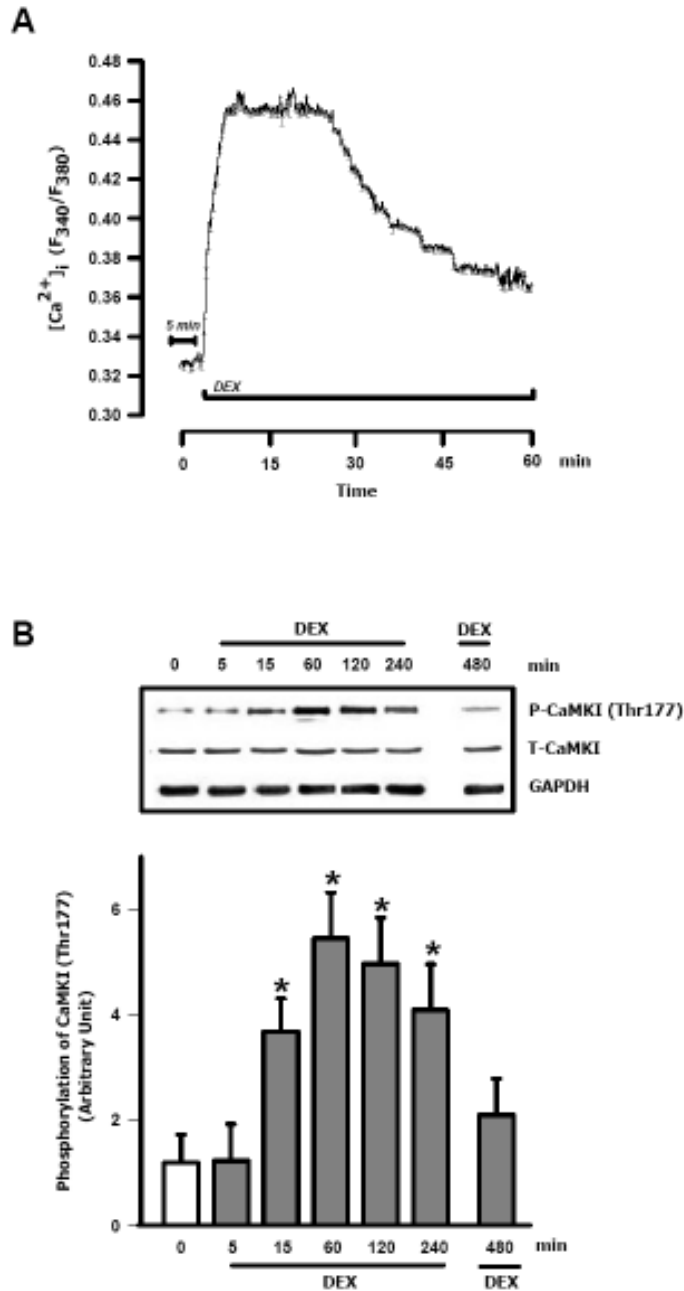


Fig. 4-2 Effects of DEX on cardiomyocyte intracellular Ca^{2+} and CAMKI phosphorylation. In cardiomyocytes exposed to DEX (100 nM), changes in cytosolic Ca^{2+} over time were measured using Fura 2 (A). Horizontal bars indicate an initial baseline period of 5 min followed by DEX treatment for 1 hr. The panel indicates an average response of 15-25 cardiac cells of 4 separate myocyte preparations. To evaluate the effects of DEX on CAMKI phosphorylation, laminin plated cardiomyocytes were exposed to DEX (100 nM). At the indicated times (0-480 min), protein was extracted to determine phosphorylation of CaMKI (Thr177) (B) and total CaMKI (B, immunoblot). Results are means \pm SE of 5 myocyte preparations in each group. *Significantly different from untreated control (0 min), $P < 0.05$. DEX, dexamethasone.

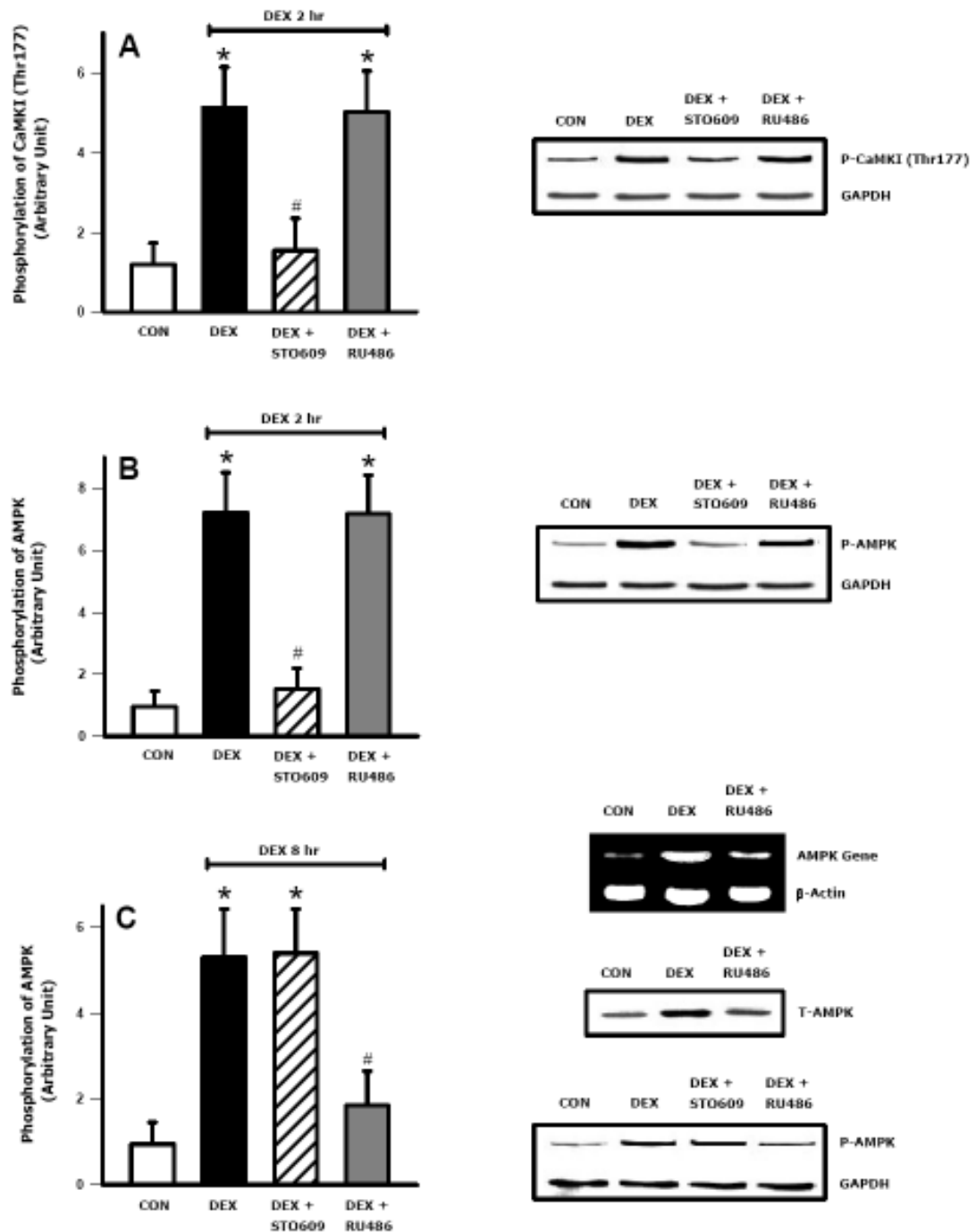


Fig. 4-3 Inhibition of AMPK activation induced by DEX. Laminin plated cardiomyocytes were incubated with 100 nM DEX for 2 (A and B) or 8 (C) hr. Where indicated, cells were pre-incubated for 45 mins with STO609 (2 μ M) or RU486 (10 μ M) prior to addition of DEX. Total protein and RNA were extracted to determine phosphorylation of CAMKI (Thr177) (A) and AMPK (B and C), total AMPK (C, immunoblot) and AMPK gene expression (C, immunoblot). Results are means \pm SE of 5 myocyte preparations in each group. *Significantly different from untreated control (CON), #Significantly different from DEX, $P < 0.05$. DEX, dexamethasone; P, phosphorylated.

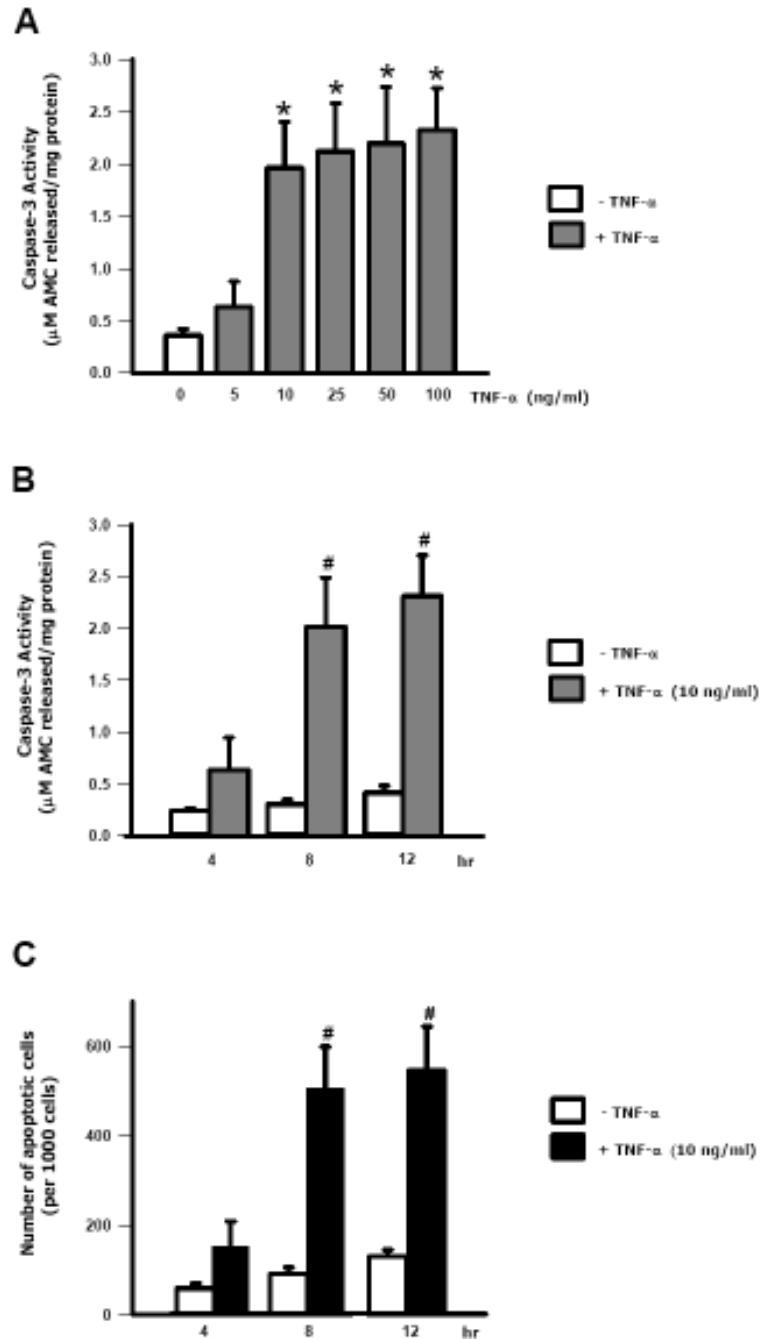


Fig. 4-4 TNF- α induced cardiomyocyte apoptosis. (A) Ventricular cardiomyocytes were exposed to various concentrations of TNF- α (0-100 ng/ml) for 8 hr and caspase-3 activity measured. To evaluate time dependant effects, cardiomyocytes were incubated with 10 ng/ml TNF- α for 4, 8 and 12 hr and caspase-3 activity (B) and evidence of apoptosis using the fluorescent DNA-binding dye Hoechst 33342 (C) were determined. Results are means \pm SE of 4-5 myocyte preparations in each group. *Significantly different from untreated control (0 min), #Significantly different from 4 hr TNF- α treated, $P < 0.05$.

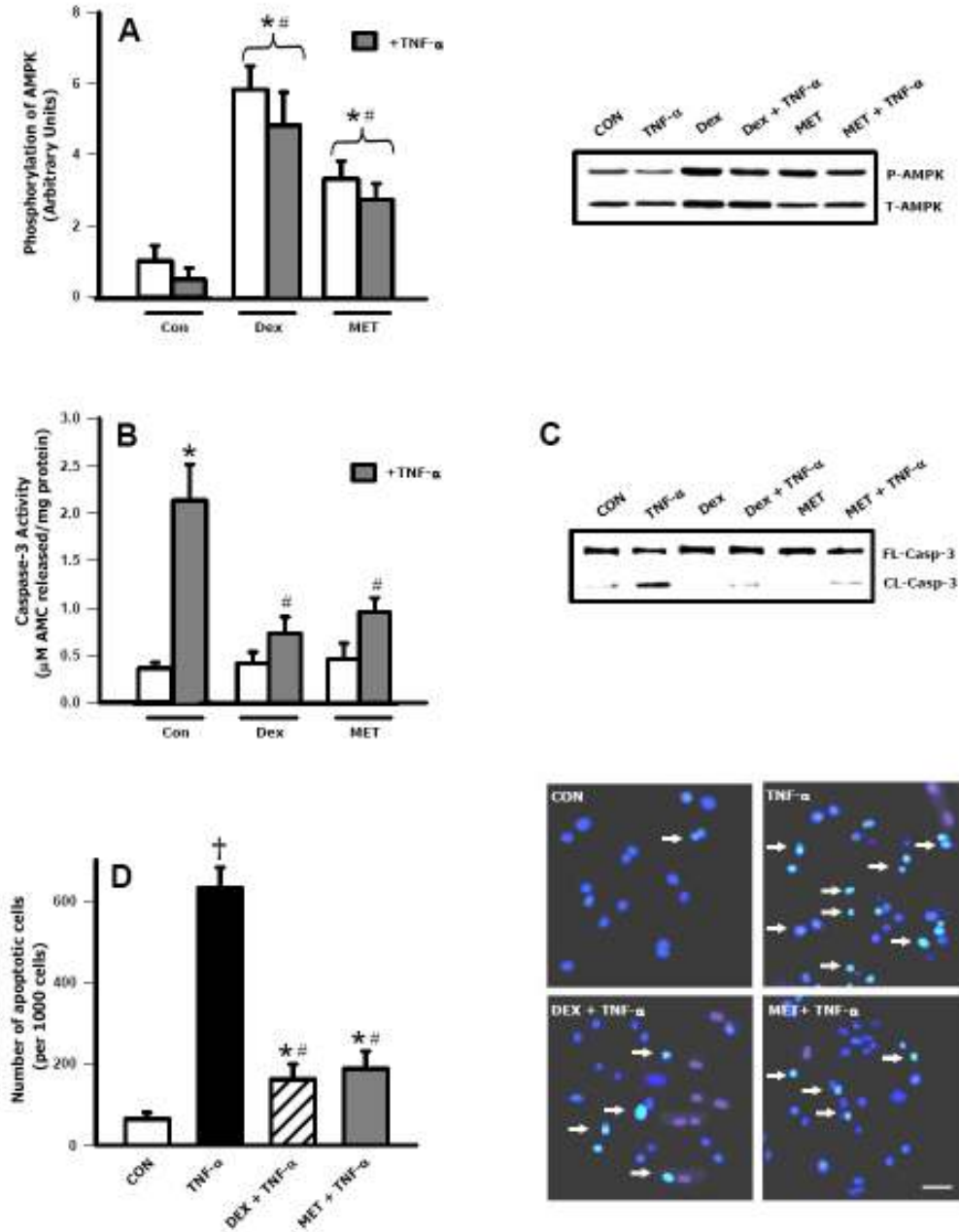


Fig. 4-5 Effects of AMPK activation on TNF- α induced apoptosis. Cardiomyocytes were incubated with DEX (100 nM) or metformin (2 mmol/L) in the presence or absence of 10 ng/ml TNF- α . Following 8 hr of incubation, cells were scraped and protein extracted to determine phosphorylated AMPK (A) and total AMPK (A, immunoblot). Caspase-3 activity (B) and cleavage (C) were measured using a fluorometric assay kit or Western blotting. Cells were also examined for morphological evidence of apoptosis using the fluorescent DNA-binding dye Hoechst 33342 (D). Results are means \pm SE of 5 myocyte preparations in each group. Bar = 25 μ m. *Significantly different from control (CON), #Significantly different from TNF- α (without DEX or MET), \dagger Significantly different from all other groups, $P < 0.05$. DEX, dexamethasone; MET, metformin; P, phosphorylated; T, total; FL, full length; CL, cleaved.

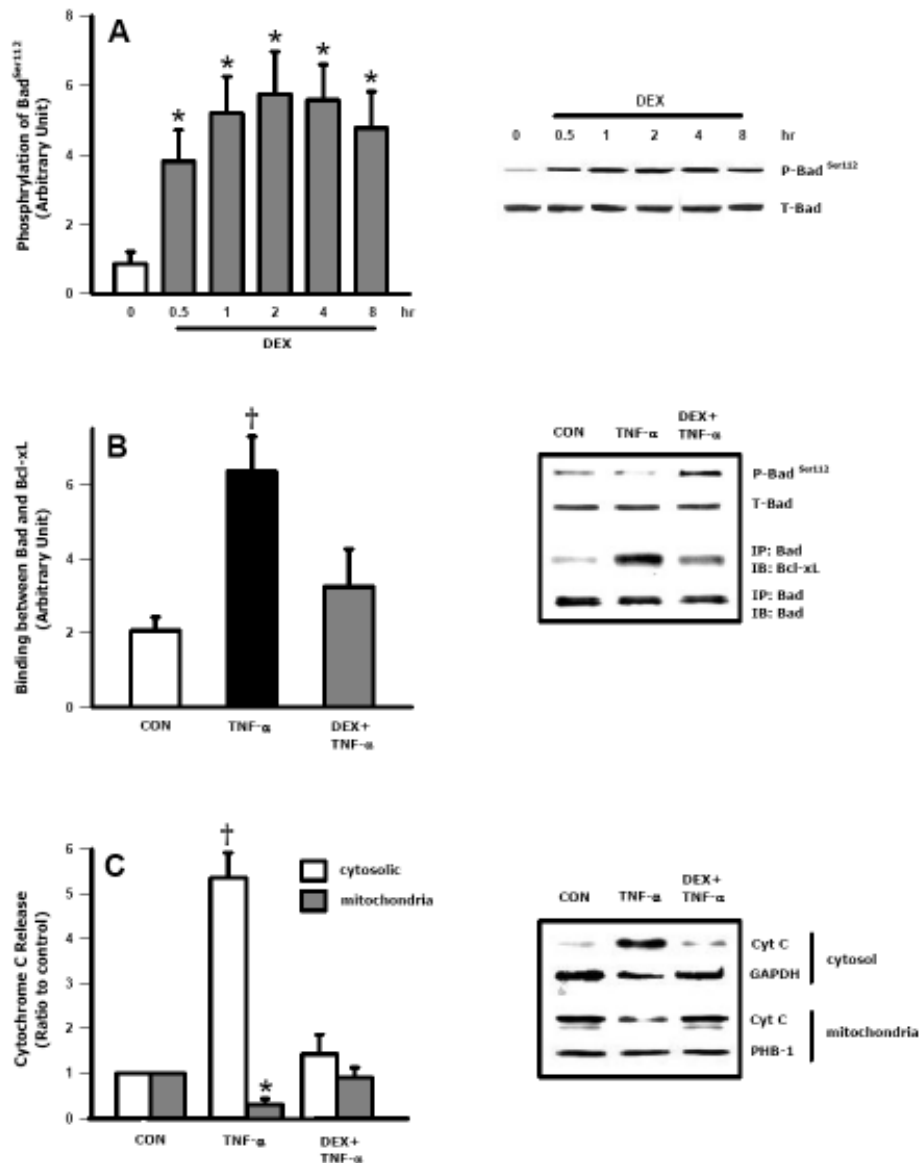


Fig. 4-6 DEX induced regulation of Bad phosphorylation and its association with BCL-xL. In cardiomyocytes treated with DEX (100 nM), time dependant changes in Bad phosphorylation (Ser112) (A) and total Bad (A, immunoblot) were determined using Western blotting. To determine the effects of DEX on TNF- α induced changes in total and phosphorylated Bad (Ser112), ventricular cardiomyocytes were incubated with 10 ng/ml TNF- α for 8 hr, in the presence or absence of DEX (100 nM) (B, immunoblot). To examine the association between Bad and Bcl-xL in these cells, Bad was immunoprecipitated (IP) using a Bad antibody and immunoblotted (IB) with anti-Bcl-xL (B). Cytochrome c release was also determined in these cells by preparing cytosolic and mitochondrial extracts as described in methods. The samples were then subjected to Western blot analysis for cytochrome c (C). Prohibitin-1 (PHB 1) was immunoblotted as a mitochondrial marker (C, immunoblot). Results are means \pm SE of 4 myocyte preparations in each group. *Significantly different from control (CON), [†]Significantly different from all other groups, $P < 0.05$. DEX, dexamethasone; P, phosphorylated; T, total.

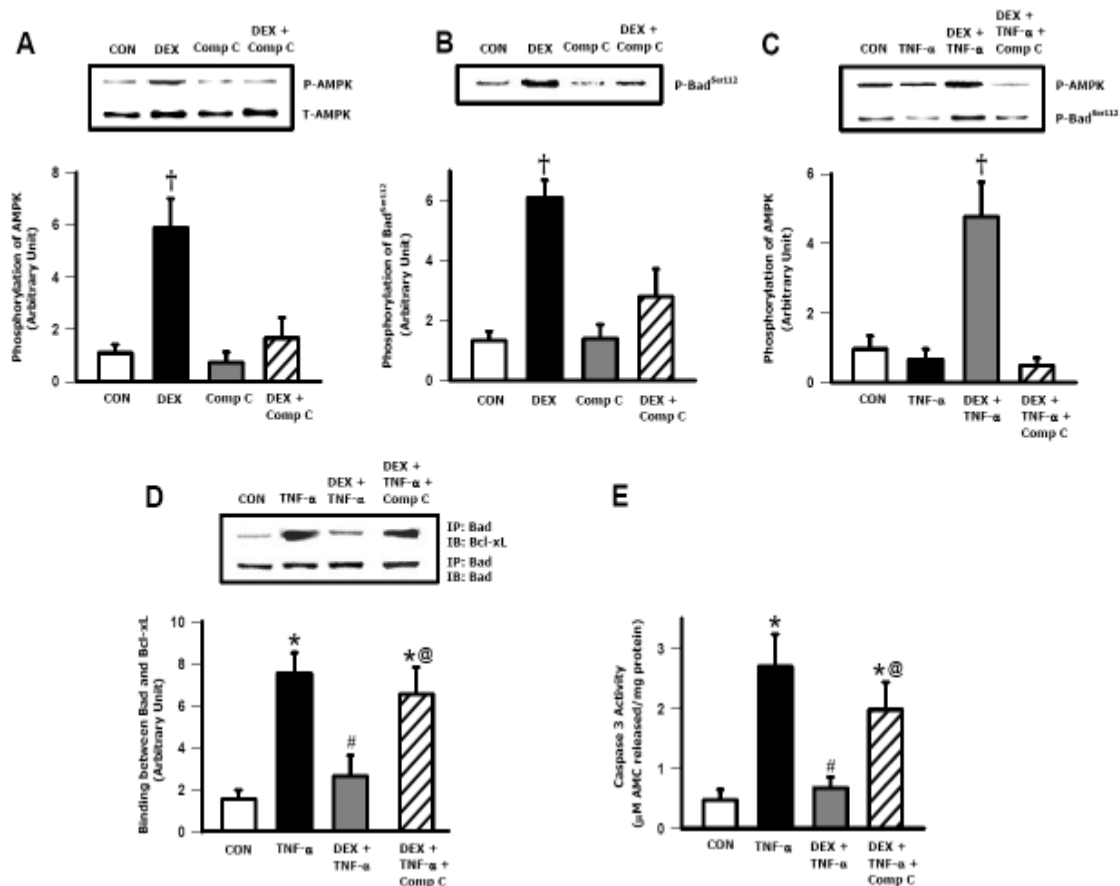


Fig. 4-7 Consequence of AMPK inhibition on TNF- α induced Bad phosphorylation and caspase-3 activity. Cardiomyocytes were pre-incubated with Compound C (40 μ M) for 45 min, prior to DEX (100 nM) treatment for 8 hr. Cells were scraped and protein extracted to determine total (A, immunoblot) and phosphorylated (A) AMPK, and phosphorylated Bad (Ser112) (B). To evaluate the effects of AMPK inhibition on TNF- α mediated effects on cardiomyocytes, cells were exposed to TNF- α (10 ng/ml) or DEX (100 nM), or their combination for 8 hr. Where indicated, one group was subjected to a 45 minute pre-exposure to Compound C followed by incubation with DEX and TNF- α for 8 hr. Cells were scraped and protein extracted to determine the phosphorylation of AMPK (C) and Bad (Ser112) (C, immunoblot). Cell lysates from the above groups were also used to evaluate the interaction between Bad and Bcl-xL using immunoprecipitation (D). Caspase-3 activity was measured using a fluorometric assay kit (E). Results are means \pm SE of 4 myocyte preparations in each group. *Significantly different from control (CON), #Significantly different from TNF- α , @Significantly different from DEX + TNF- α , †Significantly different from all other groups, $P < 0.05$. DEX, dexamethasone; P, phosphorylated; T, total; IP, immunoprecipitated; IB, immunoblot.

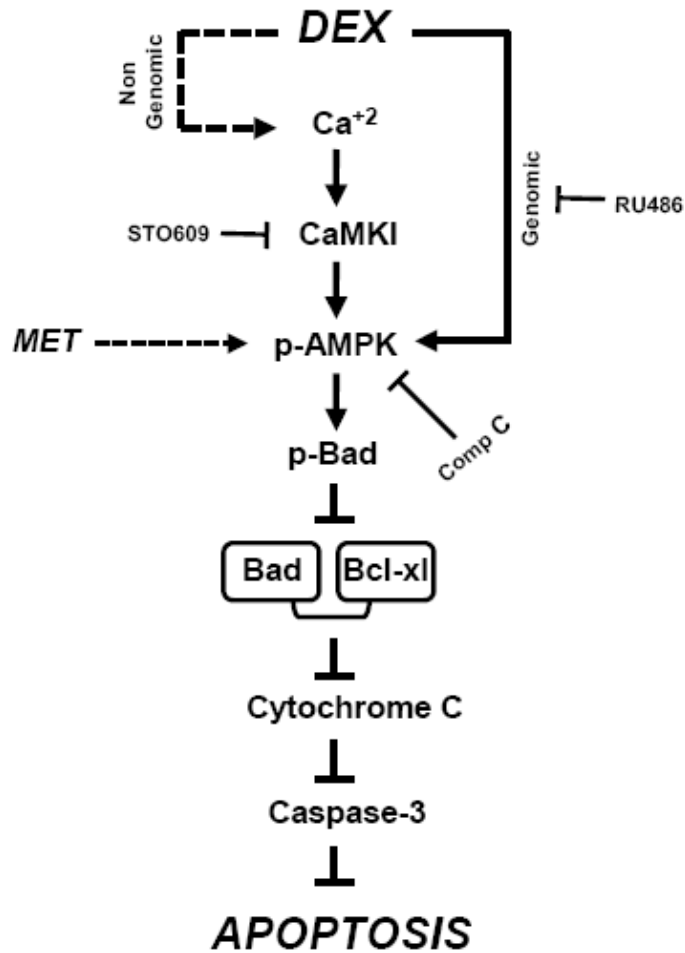


Fig. 4-8 Graphic representation of the proposed mechanism mediating the protective effect of AMPK activation on TNF- α induced apoptosis in adult rat ventricular cardiomyocytes. DEX (or MET), by activating AMPK, either through a Ca²⁺/CaMKI/AMPK pathway and receptor mediated increase in gene expression, phosphorylates and inactivates Bad, prevents cytochrome c release, inhibits activation of the caspase cascade and apoptotic cell death.

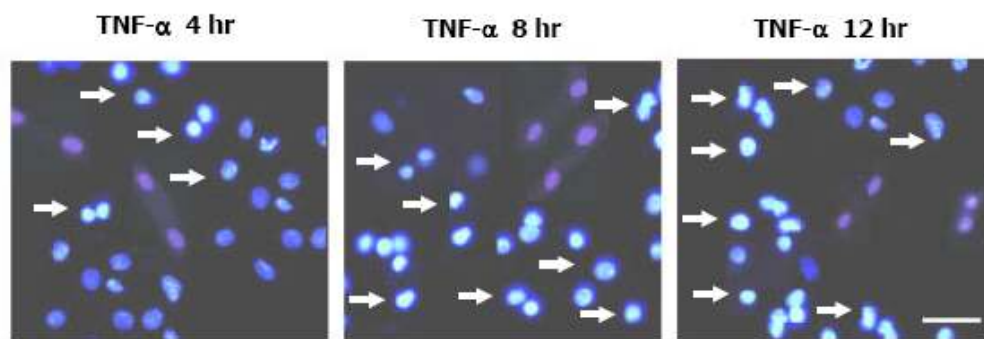


Fig. 4-S1 TNF-alpha induced cardiomyocyte apoptosis. Ventricular cardiomyocytes were exposed to TNF- α (10 ng/ml) for 4, 8 and 12 hr and morphological evidence of apoptosis using the fluorescent DNA-binding dye Hoechst 33342 were determined. Cells were scored as apoptotic (arrow) if they exhibited unequivocal nuclear chromatin condensation and/or fragmentation. Bar = 25 μ m

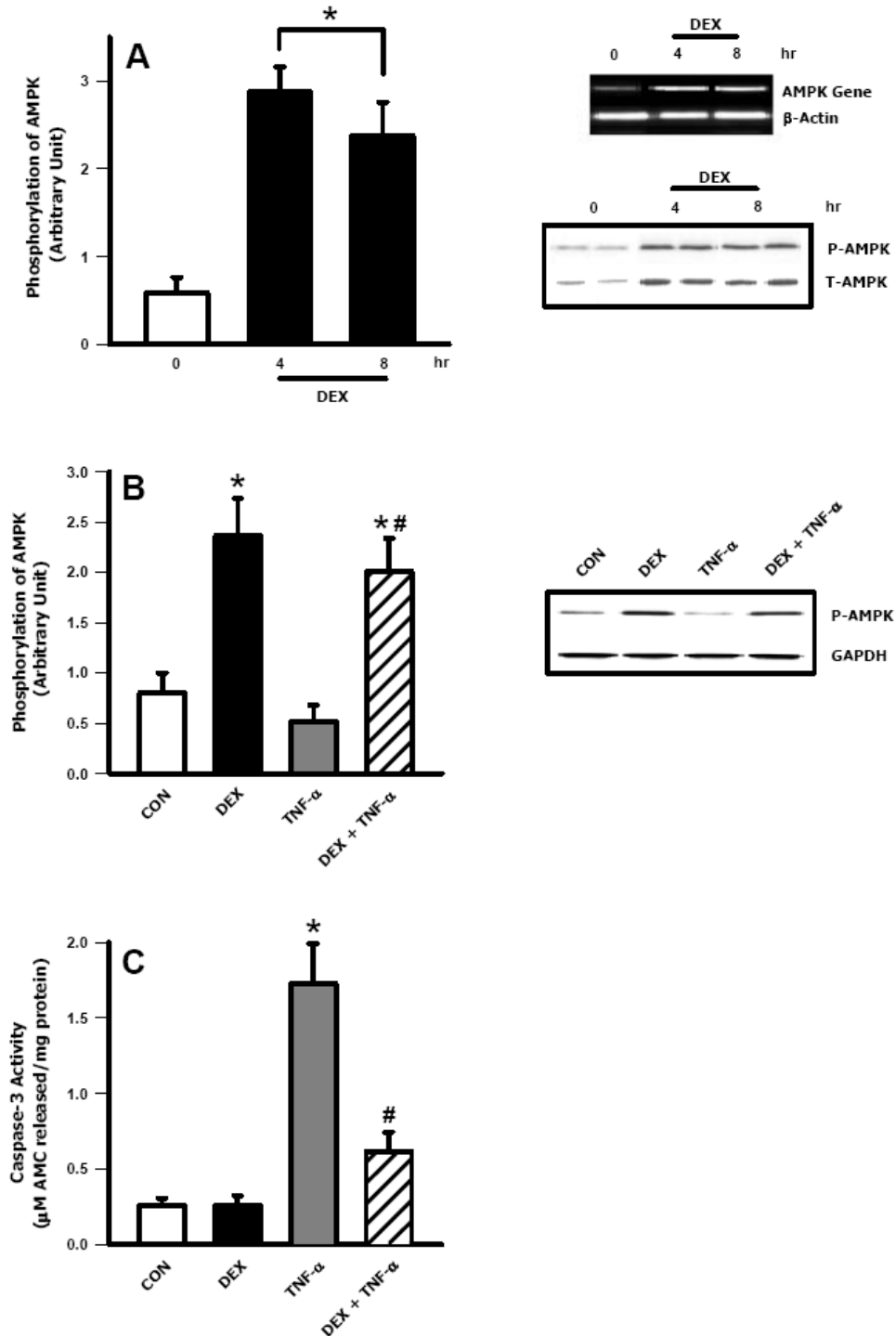


Fig. 4-S2 In vivo effects of DEX administration in on TNF- α induced cell death *in vitro*. DEX (1 mg/kg) was administered i.p and the animals killed 4 hr later. Hearts removed were used either for determination of whole heart AMPK or preparation of cardiomyocytes. Cells were plated for 8 hr in the presence or absence of TNF- α . Results are means \pm SE of 4 myocyte preparations in each group. *Significantly different from control (CON), #Significantly different from TNF- α . $P < 0.05$.

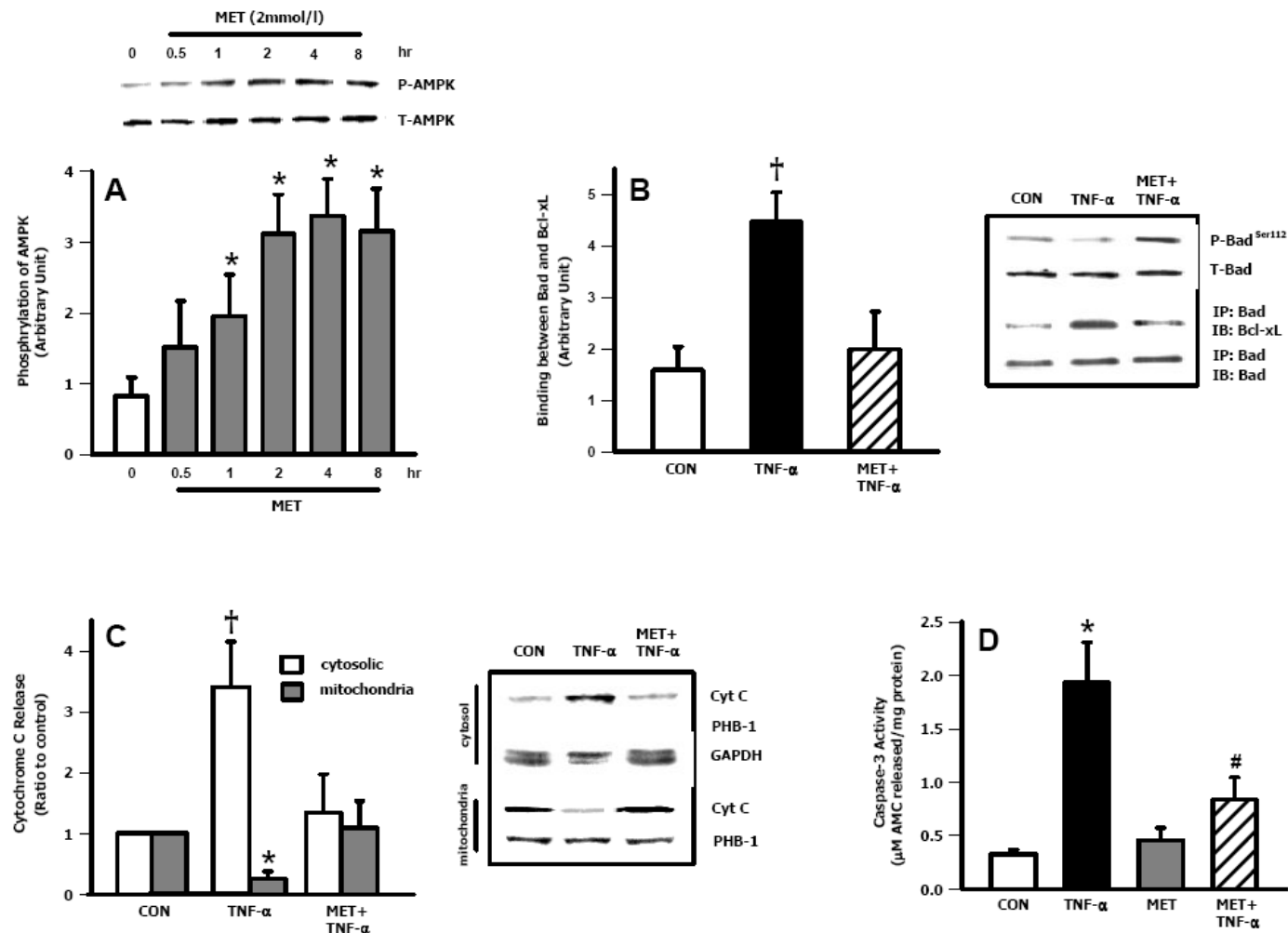


Fig. 4-S3 Metformin induced regulation of Bad phosphorylation, its association with BCL-xL and its influence on caspase-3 activity. Control cardiomyocytes were incubated with TNF- α (8 hr) in the presence or absence of MET (2 mmol/l, 8 hr). Results are means \pm SE of 4 myocyte preparations in each group. *Significantly different from control (CON), [†]Significantly different from all other groups, [#]Significantly different from TNF- α , $P < 0.05$. MET, metformin; P, phosphorylated; T, total.

4.6 BIBLIOGRAPHY

1. Levine SJ. Molecular mechanisms of soluble cytokine receptor generation. *J Biol Chem* 2008;283:14177-14181.
2. Kirkegaard T, Pedersen G, Saermark T, Brynskov J. Tumour necrosis factor-alpha converting enzyme (TACE) activity in human colonic epithelial cells. *Clin Exp Immunol* 2004;135:146-153.
3. Marques LJ, Zheng L, Poulakis N, Guzman J, Costabel U. Pentoxifylline inhibits TNF-alpha production from human alveolar macrophages. *Am J Respir Crit Care Med* 1999;159:508-511.
4. Torrado E, Adusumilli S, Fraga AG, Small PL, Castro AG, Pedrosa J. Mycolactone-mediated inhibition of tumor necrosis factor production by macrophages infected with *Mycobacterium ulcerans* has implications for the control of infection. *Infect Immun* 2007;75:3979-3988.
5. Ryffel B, Brockhaus M, Durmuller U, Gudat F. Tumor necrosis factor receptors in lymphoid tissues and lymphomas. Source and site of action of tumor necrosis factor alpha. *Am J Pathol* 1991;139:7-15.
6. Ranta V, Orpana A, Carpen O, Turpeinen U, Ylikorkala O, Viinikka L. Human vascular endothelial cells produce tumor necrosis factor-alpha in response to proinflammatory cytokine stimulation. *Crit Care Med* 1999;27:2184-2187.
7. McLachlan JB, Hart JP, Pizzo SV, Shelburne CP, Staats HF, Gunn MD et al. Mast cell-derived tumor necrosis factor induces hypertrophy of draining lymph nodes during infection. *Nat Immunol* 2003;4:1199-1205.

8. Hotamisligil GS, Shargill NS, Spiegelman BM. Adipose expression of tumor necrosis factor-alpha: direct role in obesity-linked insulin resistance. *Science* 1993;259:87-91.
9. Saliba E, Henrot A. Inflammatory mediators and neonatal brain damage. *Biol Neonate* 2001;79:224-227.
10. Benderdour M, Hess K, Dzondo-Gadet M, Nabet P, Belleville F, Dousset B. Boron modulates extracellular matrix and TNF alpha synthesis in human fibroblasts. *Biochem Biophys Res Commun* 1998;246:746-751.
11. Grandel U, Fink L, Blum A, Heep M, Buerke M, Kraemer HJ et al. Endotoxin-induced myocardial tumor necrosis factor-alpha synthesis depresses contractility of isolated rat hearts: evidence for a role of sphingosine and cyclooxygenase-2-derived thromboxane production. *Circulation* 2000;102:2758-2764.
12. Liu ZG, Han J. Cellular responses to tumor necrosis factor. *Curr Issues Mol Biol* 2001;3:79-90.
13. Micheau O, Tschopp J. Induction of TNF receptor I-mediated apoptosis via two sequential signaling complexes. *Cell* 2003;114:181-190.
14. Scaffidi C, Fulda S, Srinivasan A, Friesen C, Li F, Tomaselli KJ et al. Two CD95 (APO-1/Fas) signaling pathways. *Embo J* 1998;17:1675-1687.
15. Aikawa R, Nitta-Komatsubara Y, Kudoh S, Takano H, Nagai T, Yazaki Y et al. Reactive oxygen species induce cardiomyocyte apoptosis partly through TNF-alpha. *Cytokine* 2002;18:179-183.
16. Kubota T, McTiernan CF, Frye CS, Slawson SE, Lemster BH, Koretsky AP et al. Dilated cardiomyopathy in transgenic mice with cardiac-specific overexpression of tumor necrosis factor-alpha. *Circ Res* 1997;81:627-635.

17. Engel D, Peshock R, Armstrong RC, Sivasubramanian N, Mann DL. Cardiac myocyte apoptosis provokes adverse cardiac remodeling in transgenic mice with targeted TNF overexpression. *Am J Physiol Heart Circ Physiol* 2004;287:H1303-1311.
18. Zhang L, Peppel K, Sivashanmugam P, Orman ES, Brian L, Exum ST et al. Expression of tumor necrosis factor receptor-1 in arterial wall cells promotes atherosclerosis. *Arterioscler Thromb Vasc Biol* 2007;27:1087-1094.
19. Hotchkiss RS, Karl IE. The pathophysiology and treatment of sepsis. *N Engl J Med* 2003;348:138-150.
20. Schulz R, Aker S, Belosjorow S, Heusch G. TNFalpha in ischemia/reperfusion injury and heart failure. *Basic Res Cardiol* 2004;99:8-11.
21. Arbustini E, Grasso M, Diegoli M, Bramerio M, Foglieni AS, Albertario M et al. Expression of tumor necrosis factor in human acute cardiac rejection. An immunohistochemical and immunoblotting study. *Am J Pathol* 1991;139:709-715.
22. Krown KA, Page MT, Nguyen C, Zechner D, Gutierrez V, Comstock KL et al. Tumor necrosis factor alpha-induced apoptosis in cardiac myocytes. Involvement of the sphingolipid signaling cascade in cardiac cell death. *J Clin Invest* 1996;98:2854-2865.
23. Song W, Lu X, Feng Q. Tumor necrosis factor-alpha induces apoptosis via inducible nitric oxide synthase in neonatal mouse cardiomyocytes. *Cardiovasc Res* 2000;45:595-602.
24. Grethe S, Porn-Ares MI. p38 MAPK regulates phosphorylation of Bad via PP2A-dependent suppression of the MEK1/2-ERK1/2 survival pathway in TNF-alpha induced endothelial apoptosis. *Cell Signal* 2006;18:531-540.

25. van Empel VP, Bertrand AT, Hofstra L, Crijns HJ, Doevendans PA, De Windt LJ. Myocyte apoptosis in heart failure. *Cardiovasc Res* 2005;67:21-29.
26. Hardie DG, Hawley SA. AMP-activated protein kinase: the energy charge hypothesis revisited. *Bioessays* 2001;23:1112-1119.
27. Hurley RL, Anderson KA, Franzone JM, Kemp BE, Means AR, Witters LA. The Ca²⁺/calmodulin-dependent protein kinase kinases are AMP-activated protein kinase kinases. *J Biol Chem* 2005;280:29060-29066.
28. Blazquez C, Geelen MJ, Velasco G, Guzman M. The AMP-activated protein kinase prevents ceramide synthesis de novo and apoptosis in astrocytes. *FEBS Lett* 2001;489:149-153.
29. Ido Y, Carling D, Ruderman N. Hyperglycemia-induced apoptosis in human umbilical vein endothelial cells: inhibition by the AMP-activated protein kinase activation. *Diabetes* 2002;51:159-167.
30. Hwang JT, Kwon DY, Park OJ, Kim MS. Resveratrol protects ROS-induced cell death by activating AMPK in H9c2 cardiac muscle cells. *Genes Nutr* 2008;2:323-326.
31. Rodrigues B, Cam MC, Jian K, Lim F, Sambandam N, Shepherd G. Differential effects of streptozotocin-induced diabetes on cardiac lipoprotein lipase activity. *Diabetes* 1997;46:1346-1353.
32. Kewalramani G, Puthanveetil P, Kim MS, Wang F, Lee V, Hau N et al. Acute dexamethasone-induced increase in cardiac lipoprotein lipase requires activation of both Akt and stress kinases. *Am J Physiol Endocrinol Metab* 2008;295:E137-147.

33. An D, Kewalramani G, Chan JK, Qi D, Ghosh S, Pulinilkunnil T et al. Metformin influences cardiomyocyte cell death by pathways that are dependent and independent of caspase-3. *Diabetologia* 2006;49:2174-2184.
34. Xu YJ, Shao Q, Dhalla NS. Fura-2 fluorescent technique for the assessment of Ca²⁺ homeostasis in cardiomyocytes. *Mol Cell Biochem* 1997;172:149-157.
35. An D, Pulinilkunnil T, Qi D, Ghosh S, Abrahani A, Rodrigues B. The metabolic "switch" AMPK regulates cardiac heparin-releasable lipoprotein lipase. *Am J Physiol Endocrinol Metab* 2005;288:E246-253.
36. Qi D, Pulinilkunnil T, An D, Ghosh S, Abrahani A, Pospisilik JA et al. Single-dose dexamethasone induces whole-body insulin resistance and alters both cardiac fatty acid and carbohydrate metabolism. *Diabetes* 2004;53:1790-1797.
37. Qi D, An D, Kewalramani G, Qi Y, Pulinilkunnil T, Abrahani A et al. Altered cardiac fatty acid composition and utilization following dexamethasone-induced insulin resistance. *Am J Physiol Endocrinol Metab* 2006;291:E420-427.
38. Jensen TE, Rose AJ, Jorgensen SB, Brandt N, Schjerling P, Wojtaszewski JF et al. Possible CaMKK-dependent regulation of AMPK phosphorylation and glucose uptake at the onset of mild tetanic skeletal muscle contraction. *Am J Physiol Endocrinol Metab* 2007;292:E1308-1317.
39. Kim A, Li Ji, Hu J, Edelman AM, Young LH. Ca²⁺/Calmodulin-dependant kinase kinase beta (CaMKK β) contributes to AMPK activation in the heart during hypoxia. *Circulation* 2007;116:II 34 (Abstract).
40. Lee SM, Yune TY, Kim SJ, Kim YC, Oh YJ, Markelonis GJ et al. Minocycline inhibits apoptotic cell death via attenuation of TNF-alpha expression following iNOS/NO

induction by lipopolysaccharide in neuron/glia co-cultures. *J Neurochem* 2004;91:568-578.

41. Stahn C, Buttgerit F. Genomic and nongenomic effects of glucocorticoids. *Nat Clin Pract Rheumatol* 2008;4:525-533.

42. Song IH, Buttgerit F. Non-genomic glucocorticoid effects to provide the basis for new drug developments. *Mol Cell Endocrinol* 2006;246:142-146.

43. Stahmann N, Woods A, Carling D, Heller R. Thrombin activates AMP-activated protein kinase in endothelial cells via a pathway involving Ca²⁺/calmodulin-dependent protein kinase kinase beta. *Mol Cell Biol* 2006;26:5933-5945.

44. Haller J, Mikics E, Makara GB. The effects of non-genomic glucocorticoid mechanisms on bodily functions and the central neural system. A critical evaluation of findings. *Front Neuroendocrinol* 2008;29:273-291.

45. Ito Y, Matsuura H, Ueba Y, Fukuzaki H. The effects of large doses of dexamethasone on myocardial contractility and calcium metabolism in experimental myocardial infarction. *Adv Myocardiol* 1980;2:457-464.

46. Whitehurst RM, Jr., Zhang M, Bhattacharjee A, Li M. Dexamethasone-induced hypertrophy in rat neonatal cardiac myocytes involves an elevated L-type Ca²⁺ current. *J Mol Cell Cardiol* 1999;31:1551-1558.

47. Buttgerit F, Scheffold A. Rapid glucocorticoid effects on immune cells. *Steroids* 2002;67:529-534.

48. Krown KA, Yasui K, Brooker MJ, Dubin AE, Nguyen C, Harris GL et al. TNF alpha receptor expression in rat cardiac myocytes: TNF alpha inhibition of L-type Ca²⁺ current and Ca²⁺ transients. *FEBS Lett* 1995;376:24-30.

49. Bajaj G, Sharma RK. TNF-alpha-mediated cardiomyocyte apoptosis involves caspase-12 and calpain. *Biochem Biophys Res Commun* 2006;345:1558-1564.
50. Zhao X, Bausano B, Pike BR, Newcomb-Fernandez JK, Wang KK, Shohami E et al. TNF-alpha stimulates caspase-3 activation and apoptotic cell death in primary septo-hippocampal cultures. *J Neurosci Res* 2001;64:121-131.
51. Kim JE, Ahn MW, Baek SH, Lee IK, Kim YW, Kim JY et al. AMPK activator, AICAR, inhibits palmitate-induced apoptosis in osteoblast. *Bone* 2008;43:394-404.
52. Calvert JW, Gundewar S, Jha S, Greer JJ, Bestermann WH, Tian R, Lefer DJ. Acute metformin therapy confers cardioprotection against myocardial infarction via AMPK-eNOS-mediated signaling. *Diabetes* 2008;57:696-705.
53. Gundewar S, Calvert JW, Jha S, Toedt-Pingel I, Ji SY, Nunez D et al. Activation of AMP-activated protein kinase by metformin improves left ventricular function and survival in heart failure. *Circ Res* 2009;104:403-411.
54. Ohi N, Nishikawa Y, Tokairin T, Yamamoto Y, Doi Y, Omori Y et al. Maintenance of Bad phosphorylation prevents apoptosis of rat hepatic sinusoidal endothelial cells in vitro and in vivo. *Am J Pathol* 2006;168:1097-1106.
55. Steenbergen C, Afshari CA, Petranka JG, Collins J, Martin K, Bennett L et al. Alterations in apoptotic signaling in human idiopathic cardiomyopathic hearts in failure. *Am J Physiol Heart Circ Physiol* 2003;284:H268-276.
56. Ray RM, Bhattacharya S, Johnson LR. Protein phosphatase 2A regulates apoptosis in intestinal epithelial cells. *J Biol Chem* 2005;280:31091-31100.
57. Schreyer SA, Chua SC, Jr., LeBoeuf RC. Obesity and diabetes in TNF-alpha receptor- deficient mice. *J Clin Invest* 1998;102:402-411.

58. Schulz R. TNFalpha in myocardial ischemia/reperfusion: damage vs. protection. J Mol Cell Cardiol 2008;45:712-714.

5. CONCLUSIONS AND FUTURE DIRECTIONS

Ours is the first report to identify that AMPK, but not PPAR- α , controls FA oxidation in acute 4-day STZ diabetic heart. As cardiac glucose oxidation is altered during diabetes, AMPK stimulation in these hearts phosphorylates ACC to guarantee adequate cardiac energy supply. The precise mechanism that causes AMPK activation under these conditions is unclear. Elevated insulin levels by stimulating the PI3K/PKB pathway have shown to inhibit AMPK function. Given that, Type 1 diabetes exhibits a considerable reduction in plasma insulin levels, insulin deficit could be a likely mechanism that triggers AMPK activation. In chronic diabetes, reduced plasma insulin levels were complemented by a massive increase of both plasma and cardiac lipids. A direct up-regulation of PPAR- α and its downstream targets during this condition were likely providing the heart with excess FA. Accumulation of excess FA following chronic diabetes potentially prevented myocardial AMPK activation seen after acute hypoinsulinemia. Although the mechanisms responsible for this event remain unresolved, a recent study has demonstrated that long chain acyl-CoA esters prevent AMPK phosphorylation by the upstream AMPKK. In another study using ob/ob mice or ZDF rats, decreased cardiac AMPK phosphorylation was found to be associated with augmented lipid oversupply and over-expression of PP2C, which is known to dephosphorylate and inactivate AMPK. Thus in summary, in hyperglycemia and hypoinsulinemia, without any changes in plasma or cardiac FA, AMPK is activated and controls cardiac FA oxidation. In chronic diabetes, the additional drop in insulin initiates changes in both carbohydrate and lipids. With the addition of augmented plasma and

heart lipids, AMPK activation is prevented, and control of FA oxidation is likely through PPAR- α .

In addition to its role in FA utilization, AMPK has been implicated to control FA delivery through its regulation of the FA transporter, CD36. Given that LPL derived FA is the principal source of energy during insulin resistance, it is possible that cardiac AMPK could regulate LPL translocation to the vascular lumen to increase the exogenous FA pool. Using DEX as an acute model of insulin resistance, our study demonstrates that, following a single dose of DEX, although genomic mechanisms are activated, a rapid nongenomic phosphorylation of stress kinases (AMPK, p38 MAPK, HSP25) together with insulin facilitate cytoskeleton rearrangement and promote LPL translocation to the myocyte cell surface. Thus during insulin resistance, AMPK mediated deployment of LPL from its major storage site, the cardiomyocyte, to the coronary lumen could represent an instant compensatory response by the heart to ensure FA supply.

Finally, using established AMPK activators like DEX or MET, we document that AMPK activation prevents TNF- α -induced apoptosis in adult rat ventricular cardiomyocytes. Our data demonstrated that both DEX and MET by activating AMPK promote Bad phosphorylation, maintain the anti-apoptotic property of Bcl-xL and prevent cytochrome c release and apoptosis. The early activation of AMPK by DEX was due to a non-genomic response of this glucocorticoid to elevate cytosolic calcium that induced the rapid phosphorylation of CaMKI, an upstream regulator of AMPK. As glucocorticoids also act through genomic mechanisms, we believe that activation of AMPK over time was also receptor mediated and genomic in nature. The mechanism responsible for MET

induced activation of cardiac AMPK in our study is currently unknown. Taken together, my findings suggest that although DEX and MET are used as anti-inflammatory agents or insulin sensitizers, their common property to phosphorylate AMPK promotes cardiomyocyte survival through its regulation of Bad and the mitochondrial apoptotic mechanism. It should be noted that this study was performed *in vitro* in isolated rat adult cardiomyocytes. Whether cardioprotective effects of AMPK against TNF- α -induced cytotoxicity persist *in vivo* is currently unknown.

Overall, evidence gathered from my studies indicates that the effects of AMPK on cardiac tissue are beneficial and its activation during acute hypoinsulinemia and insulin resistance ensures the much-needed energy generation within the myocardium. However, excess FA accumulation in the cardiac tissue over-time can deactivate AMPK and could likely disrupt its cardioprotective effects. In addition, as the production of TNF- α is widely reported to increase during obesity, diabetes and ischemia reperfusion activation of AMPK in these conditions may protect against this specific cytokine induced cardiac injury.

Future directions:

- 1 Although AMPK activation was seen in acute STZ hearts, the precise mechanism responsible for its inactivation during chronic conditions is unknown and should be explored further. Given that decreased cardiac AMPK phosphorylation has been associated with augmented lipid oversupply and over-expression of phosphatases, future studies should focus on determining whether phosphatases influence cardiac AMPK activation during chronic hypoinsulinemia.

- 2 Although my data demonstrated that DEX via a rapid nongenomic phosphorylation of stress kinases, together with insulin, facilitates LPL translocation to the myocyte cell surface, the mechanisms governing the transfer of LPL from the myocyte cell surface to the coronary lumen following DEX remain unclear and could be investigated.
- 3 In isolated cardiomyocytes, both DEX and MET by activating AMPK confer protection against TNF- α induced cytotoxicity. Whether the same modification also occurs *in vivo* is unknown and can be investigated. In addition, whether activation of AMPK by DEX or MET protects cardiomyocytes from other death-inducing stimuli or oxidative stress could also be determined.

APPENDIX



THE UNIVERSITY OF BRITISH COLUMBIA

ANIMAL CARE CERTIFICATE

Application Number: A08-0627

Investigator or Course Director: [Brian B. Rodrigues](#)

Department: Pharmaceutical Sciences

Animals:

Rats Wistar 420

Start Date: July 1, 2008

Approval Date: October 22, 2008

Funding Sources:

Funding Agency: Canadian Diabetes Association

Funding Title: Metabolic basis for diabetic heart disease: role of cardiac lipoprotein lipase

Unfunded title: N/A

The Animal Care Committee has examined and approved the use of animals for the above experimental project.

This certificate is valid for one year from the above start or approval date (whichever is later) provided there is no change in the experimental procedures. Annual review is required by the CCAC and some granting agencies.

A copy of this certificate must be displayed in your animal facility.

Office of Research Services and Administration
102, 6190 Agronomy Road, Vancouver, BC V6T 1Z3
Phone: 604-827-5111 Fax: 604-822-5093